# 5 INTERFERENCE MEASUREMENTS ON A FIXED GROUND-BASED METEOROLOGICAL RADAR

## 5.1 Introduction

The key objective of the work described in this section was to establish the maximum interference level that a representative meteorological radar, deployed on a worldwide basis, could withstand before its forecasting capability was compromised; the interference being based on typical communication signal modulations. Based upon the radar's technical specifications, mathematical models were developed for its key outputs, or 'products' (called base reflectivity, mean radial velocity, and spectrum width), that indicate what these expected levels should be. In order to physically validate this analysis, a test and data analysis methodology was defined through which data were collected and analyzed.

The data analysis supported the calculated value required for protection of the reflectivity measurements. Limitations in the radar calibration and noise removal process performed by the system's low-level data processor at the time the tests were run tended to limit the measurement accuracy of the necessary protection criteria for the spectrum width measurements. However, correction of the data for the limitations of this processing did result in values that supported the calculated protection values.

Field tests were run on the meteorological radar to determine the appropriate criteria necessary for protection from CW and CDMA signals in the 2700-2900 MHz band. The tests were performed by injecting a CW signal and six different CDMA modulation schemes into the radar receiver while it was scanning the atmosphere. Low-level (called base) meteorological products (base reflectivity, mean radial velocity, and spectrum width) were recorded while conducting a series of radar antenna rotations at a single antenna elevation. Interference signals were injected with *I/N* levels ranging from -15 dB to +6 dB.

## 5.2 Theoretical Calculation of Necessary Protection Criteria

The radar generated three base products that are used by the signal processing system to derive meteorological products. These base products are:

- Volume reflectivity, Z, in $mm^6/m^3$, which for rain is a measure of total water in the radar sample volume;
- Mean radial velocity, V, in m/s, which is the power-weighted mean radial motion of the targets in the sample volume;
- Spectrum width, W, in m/s, which is a measure of the radial velocity dispersion of the targets in the sample volume.

### 5.2.1 Minimum Signal Level

Radar signal processing normally removes the radar system noise effects from the reflectivity and spectrum width products so that the system can provide these products when the signal level

is below the receiver noise level. The signal to noise ratio (SNR) threshold, i.e., the lowest level for which the return signal is processed, is selectable by the radar operator between the limits of -12 dB SNR and +6 dB SNR. With the present version of signal processing, the lower values are generally not used due to limitations with noise removal but the system does provide useful products down to -3 dB SNR. The interference level that compromises the system is related to the minimum signal level of -3 dB SNR and the product characteristics themselves, as described below. Excessive interference will adversely impact data quality, degrade the meteorological products, and compromise the system's ability to accomplish its mission of providing data necessary for public weather forecasting, severe weather warning, and rainfall measurement for flash flood prediction and water management.

### 5.2.2 Reflectivity

Reflectivity is used in multiple applications; the most important of these is rainfall rate estimation. Reflectivity is calculated from a linear average of return power and is subject to contamination by interference as an unknown increase in the measured reflectivity. Reflectivity is seriously contaminated if the bias exceeds 1 dB. A 1-dB bias is twice the radar calibration accuracy and equal to the standard deviation of the reflectivity estimate specified in the radar technical requirements. Bias in terms of interference to signal ratio is given by [21]:

$$dBbias = 10\log\left(\frac{S+I}{S}\right), \tag{17}$$

and a 1-dB bias occurs at:

$$I/S = 0.26$$

$$10 \log I/S = -6 \text{ dB}.$$

Therefore, reflectivity is biased 1 dB at an interference level 6 dB below the signal. Since the minimum signal level has an SNR of -3 dB and the maximum I/S level for the reflectivity product is -6 dB, the maximum *I/N* is:

$$(-3 \text{ dB}) + (-6 \text{ dB}) = -9 \text{ dB } I/N.$$

### 5.2.3 Mean Radial Velocity

Mean radial velocity is calculated from the argument of the single lag complex covariance. The complex covariance argument provides an estimate of the Doppler signal vector angular displacement from pulse to pulse. The displacement divided by the time interval between the pulses is the Doppler vector angular velocity.

If it has the characteristics of broadband noise, an interference signal vector has uniform probability over the complex plane and thus does not introduce a systematic rotation nor a bias in

the estimate. However, the randomness of the composite signals plus interference vector due to the interference increases the variance of the Doppler signal estimate.

The Doppler frequency variance, retaining all terms except those inversely proportional to the number of samples squared can be calculated as [21]:

$$\mathrm{var}\left(\hat{f}\right) = \frac{2\pi^{3/2}WT}{8\pi^2 M\beta^2(T)T^2} + \frac{\left(\frac{N}{S}\right)^2 + 2\left(\frac{N}{S}\right)\left[1-\beta(2T)\right]}{8\pi^2 M\beta^2(T)T^2}, \quad (18)$$

where:

$\hat{f}$ = frequency estimate, Hz;
$W$ = standard deviation of frequency spectrum, Hz;
$W$ = 4 m/s for NTR benchmark = 80 Hz at $f_c$ = 2995 MHz;
$T$ = sampling interval, sec;
$T$ = $10^{-3}$ sec for NTR benchmark;
$M$ = number of samples in estimate;
$N$ = noise power;
$S$ = signal power;
$\beta$ = signal correlation at lag T;
$\beta$ = exp [$-2\pi^2 W^2 T^2$ ] for the assumed Gaussian spectra.

The first term is the variance contribution due to the signal characteristics and the second term is the variance contribution due to the noise.

The frequency variances are severely compromised if the interference increases the variance by more than 50%. The uncertainty in the data degrades all velocity based products and the velocity shear measurements in particular. (Velocity shear is a velocity difference over some distance.) A 50% increase in variance increases the reliably detected shear value approximately 25% above the severe weather event formative stage value.

An expression for the interference to noise ratio resulting in a 50% variance increase of the technical requirements benchmark parameters and SNR = -3 dB is given by [21]:

$$2\pi^{3/2}WT + \left(\frac{I+N}{S}\right)^2 + 2\left(\frac{I+N}{S}\right)\left[1-\beta(2T)\right] = \frac{3}{2}\left(2\pi^{3/2}WT\right) + \frac{3}{2}\left(\frac{N}{S}\right)^2 + \frac{3}{2}(2)\left(\frac{N}{S}\right)\left[1-\beta(2T)\right], \quad (19)$$

where:

$W$ = 80 Hz;
$T$ = $10^{-3}$ sec;
$2\pi^{3/2}WT$ = 0.89;
$[1 - \beta(2T)]$ = 0.4;
$S$ = 0.5 $N$.

Substituting and solving for $I/N$ yields the quadratic expression:

$$(I/N)^2 + 2(I/N) - 1.21 = 0$$
$$I/N = 0.49 .$$

Therefore, the interference must not exceed the minimum signal value.

### 5.2.4 Spectrum Width

The spectrum width is calculated from the single lag correlation assuming a Gaussian spectral density. The algorithm is expressed as [21]:

$$W = \frac{Va}{\pi}\left|\ln\frac{R^2}{S^2}\right|^{1/2}, \tag{20}$$

where:

$W$ = Spectrum width (standard deviation);
$Va$ = Nyquist velocity, 25m/s from the radar technical requirements document;
$R$ = single lag covariance power;
$S$ = signal power.

Interference causes both a bias and a variance increase in spectrum width estimation but the bias is more detrimental. Spectrum width is compromised when the interference-induced bias exceeds the radar technical requirement width accuracy of 1 m/s. The interference to noise ratio at which this bias level occurs can be calculated by solving for the covariance at 4 m/s and signal power of *N/2*, then solving for the *(S+I)* level producing a 5 m/s spectrum width. 4 m/s is the base value given in the radar technical requirements document. To calculate *I/N*, the equation above is solved for the 4 m/s and 5 m/s cases.

| For $W$ = 4 m/s: | | For $W$ = 5 m/s: | |
|---|---|---|---|
| $25 / \pi \left\| \ln (R^2/S^2) \right\|^{(1/2)} = 4$ | | $25 / \pi \left\| \ln (R^2 / (S + I)^2) \right\|^{(1/2)} = 5$ | |
| $ln\ (R^2/S^2)$ | = -0.25 | $ln\ ( R^2 / (S + I)^2 )$ | = -0.39 |
| $R/S$ | = 0.88 | $R/(S+I)$ | = 0.82 |
| $R$ | = 0.88 S | | |

$$R = 0.88(N/2)$$

Substitute: $R = 0.88(N/2)$, $S = N/2$:

$$[0.88\ (N/2)] / [(N/2) + I] = 0.82$$
$$0.82\ [(N/2) + I] = 0.88\ (N/2)$$
$$I/N = 0.0366$$
$$10\log(I/N) = -14.4 \text{ dB}.$$

So in this example, an *I/N* ratio of -14.4 dB will cause a spectrum width error of 1 m/s.

## 5.3 System Operation, Output Products, and Interference Sensitivity

### 5.3.1 System Operational Mode for Testing

The radar that was used for the tests and measurements has multiple modes of operation that utilize different antenna rotation rates, antenna elevations and prfs. The operational mode selected for the tests was one that is commonly used, and is optimized for system sensitivity, leading to high susceptibility of interference. Table 8 provides the characteristics of the radar mode used in testing.

Table 8. Technical Characteristics of the Meteorological Radar

| Parameter | Value |
|---|---|
| Frequency | 2995 MHz |
| Pulse power (peak) | 750 kW |
| Pulse width | 4.7 μs |
| Pulse repetition frequency | 322 Hz (first cut)<br>446 Hz (second cut) |
| Maximum coverage range | 290 mi. |
| RF bandwidth (at 3-dB points) | 13 MHz |
| IF bandwidth (at 3-dB points) | 630 kHz |
| System noise figure | 4.9 dB |
| System noise floor (in receiver bandwidth of 630 kHz) | -111 dBm |
| Main beam antenna gain | [45 dBi] |
| Antenna pattern type | pencil |
| Antenna scan interval (scan period) | 0.84 rpm (71.4 sec) |
| Antenna height above ground | 30 m |
| Antenna beamwidth (vertical and horizontal) | 0.90 deg |
| Polarization | linear horizontal |

In the mode used, the antenna rotation starts at an elevation of 0.5 deg., the radar transmits a 4.7-μs pulse every 3.1 ms for the first rotation, and then transmits a pulse every 2.24 ms for the second rotation. These correspond to prfs of 322 Hz and 446 Hz, respectively. Each revolution covers 360 deg. in azimuth. In normal operation, the radar also performs antenna rotations at several higher elevation angles before returning to 0.5 deg. For the purposes of this test, the two elevation cuts at the single antenna elevation provided sufficient data for analysis and the cuts at higher elevations were not performed. The first antenna rotation is used to measure reflectivity and the second rotation is used to measure mean radial velocity and spectrum width (see below). For each location in the atmosphere, multiple pulses are transmitted and received. Due to the duration of the transmit pulses compared to the time between pulses, the system is in receive mode more than 99.5% of the time. The magnitude of the received pulses is approximately

200 dB lower than the transmitted pulses because the pulses are scattered by small airborne objects (on the order of millimeters in diameter or smaller) at distances up to hundreds of kilometers from the radar. The received signal is downconverted from 2,995 MHz to the IF frequency of 57 MHz where it is then applied to a synchronous detector. The detected *I-Q* baseband signals are digitized to a 16-bit level for use in the processing subsystems.

### 5.3.2 Output Products

The returned pulses from each location are used by the processing subsystems to derive the three meteorological base moments of base reflectivity, mean radial velocity, and spectrum width. The base moments are displayed as products to users and are used to develop other meteorological products representing rainfall accumulation, tornadoes, wind shear, etc. Reflectivity is derived from the amplitude (or power) of the received signal. Mean radial velocity is the mean radial speed and is derived from the differences in the I and Q vectors caused by the Doppler shift. Spectrum width is the variance between pulses of the velocities received from the same location.

### 5.3.3 Interference Sensitivity

Base products are affected by interference in two different ways. First, values can be biased which decreases the accuracy of the system, and second, the variance of the outputs can be affected. In the presence of interference, reflectivity is sensitive to bias, mean radial velocity is sensitive to variance errors, and spectrum width is affected by both bias and variance errors. For spectrum width, the errors due to biasing are more significant than the errors due to variance because the bias, or offset, represents a velocity measurement error while the variance represents the uncertainty of the velocities measured. Table 9 shows which interference-induced errors, bias and variance affect the base products.

Table 9. Sensitivity of Meteorological Products to Interference Induced Error

| | **Interference Induced Errors** | |
|---|---|---|
| **Meteorological Product** | **Bias** | **Variance** |
| Reflectivity | X | |
| Velocity | | X |
| Spectrum Width | X | X |

To calibrate the test set-up for a known interference level at the radar receiver input, the receiver noise floor was measured, without interference, at the 57.55 MHz IF output of the receiver. When the noise floor was recorded at the IF output, the interference signal was activated and its level was increased until the radar IF output noise floor increased by 3 dB. The point at which the noise increased by 3 dB corresponded to the interference level within the radar passband being equal to the radar receiver noise within the passband, and an *I/N* ratio of 0 dB. The signal source output was recorded for the 0-dB *I/N* ratio and the actual level being injected into the radar

receive path was also measured and recorded. Knowing the signal source setting for the 0 dB *I/N*, the signal source could be set for any other desired *I/N* by adjusting the signal source output level. Testing was conducted at interference level points corresponding to the following *I/N* levels: -15 dB, -12 dB, -10 dB, -6 dB, -3 dB, 0 dB, +3 dB and +6 dB. Figure 12 shows an example result of the receiver noise level measurement with and without the presence of interference for the W-CDMA signal testing; Figures B-6 and B-7 show spectra of CDMA interference signals used for this testing.

The radar was set to scan the atmosphere (hereafter called a "volume scan") at one antenna elevation without interference followed by a volume scan with interference. For each volume scan, with or without interference, the antenna made two complete rotations allowing elevation cuts at the same elevation using two different prfs. The prf used on the first rotation was a low value optimized for collecting the base reflectivity product. The prf used on the second rotation was a high value and was used for collecting the mean radial velocity and spectrum width data. This alternating pattern of volume scans, with and without interference, was continued for interference levels ranging from -15 dB to +6 dB. This test approach provided a volume scan immediately before and after each interference volume scan that could be used as baseline references for determining the statistical effects of the interference. During the entire test, base product radar data was recorded for analysis.

Figure 33 shows the test setup, which consisted of a signal generator feeding an RF coupler where the interference signal is combined with the received radar return signal at input to the receiver. The receiver amplified and downconverted the signal to IF where it was monitored on a spectrum analyzer. The I and Q outputs were digitized and processed to provide the meteorological base products of base reflectivity, mean velocity and spectrum width. The base products were recorded for statistical analysis. Testing with each of the CDMA signal types, at all data rates and modulation schemes, was not feasible due to the large number of available permutations. Representative modulations (CDMA and TDMA, for example) and a representative range of data rates were used instead.

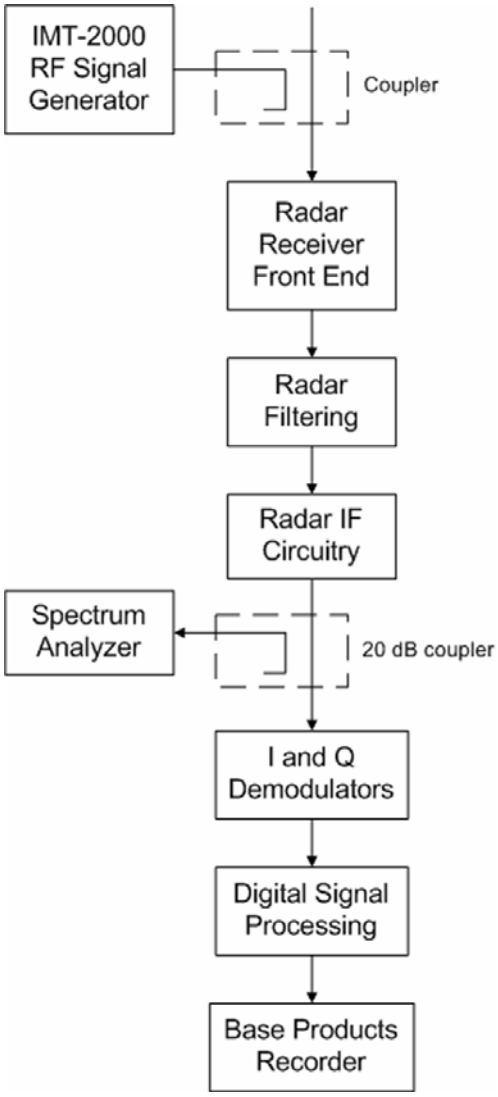


Figure 33. Meteorological radar test set-up block diagram.

### 5.4 Data Analysis Methodology and Results

Radar tests described in other sections of this report concern systems that locate and track discrete, point targets. Meteorological radars, in contrast, collect a completely different type of data, namely on extended, diffuse phenomena. Meteorological radars such those addressed in this section perform volume scans of the atmosphere and present data on the atmosphere for a full 360 degrees in azimuth and through elevations as high as about 60 degrees.

For discrete-target radars, analysis of the effects of interference on the probability of detection are usually sufficient, and interference effects in those types of systems will tend to mask desired targets and/or created false targets.

In meteorological radars, where data are collected and analyzed for a volume of the atmosphere, the system performance is not characterized with the use of probability of detection. Although visual inspection of the radar display can show some effects due to interference, such inspection does not provide a scientific analysis of the results on the meteorological products generated such as rain fall estimates, wind speed measurement or shear detection. The data analysis for meteorological radar outputs must take a much different approach in order to provide meaningful results, and it has been determined that in fact an extensive statistical analysis must be performed on the low level meteorological data for each range gate response that is received.

### 5.4.1 Assumptions

- As stated above, the test procedure used to inject interference signals into the radar receiver called for injecting a known interference level at the radar receiver's input.
- The minimum usable signal, with current technology, is 3 dB below the noise floor.
- The required maximum *I/N* ratio is equal to the interference level below the signal that resulted in a 1-dB bias plus the minimum signal level that needed to be retrieved.

The system used processing to remove the effects of noise, allowing the radar to process signals below the noise floor. In a system that would contain no residual effects, one would expect the interference that was injected at the receiver input to linearly track the interference level that was detected through the data analysis. Figure 34 compares the relative levels of the interference that was injected at the receiver input to the interference level that was detected through the data analysis. A divergence can be seen at -6 dB.

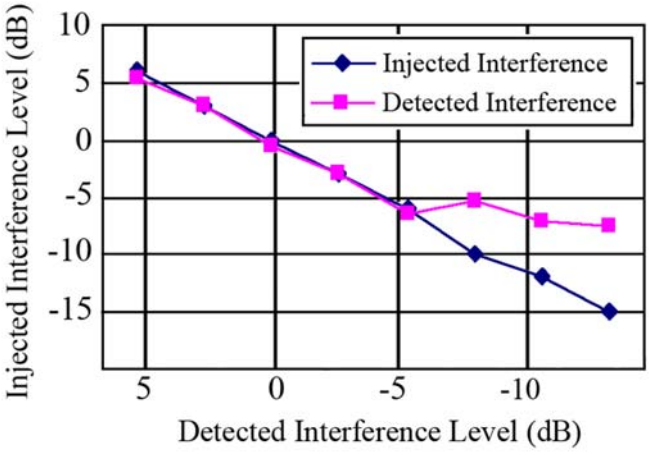


Figure 34. Injected versus detected interference level in the meteorological radar receiver.

This residual effect impacts the analysis in the following way:

- Reflectivity: No effect as the graphical technique that was used to determine the level at which a 1-dB bias in the reflectivity occurs is relative and is not impacted by this residual effect.
- Spectrum width: Residual noise (be it present because it is an artifact of the radar's calibration, inherent to the radar's performance, or as a result of graphical analysis errors) impacts the analysts' ability to graphically determine the level at which the spectrum width difference exceeds 1 m/s.

This residual effect can be characterized, and the data analysis can be compensated accordingly, using the curve shown in Figure 35. These data were used to compensate for analysis errors that were introduced by using an absolute graphical technique to determine the level at which the spectrum width difference is 1 m/s. The data were not required for the reflectivity analysis. Additional variability that adds to the data analysis errors comes into play as a function of graphically estimating the mean and associated data points. An analysis follows, based on the topics of reflectivity and spectrum width.

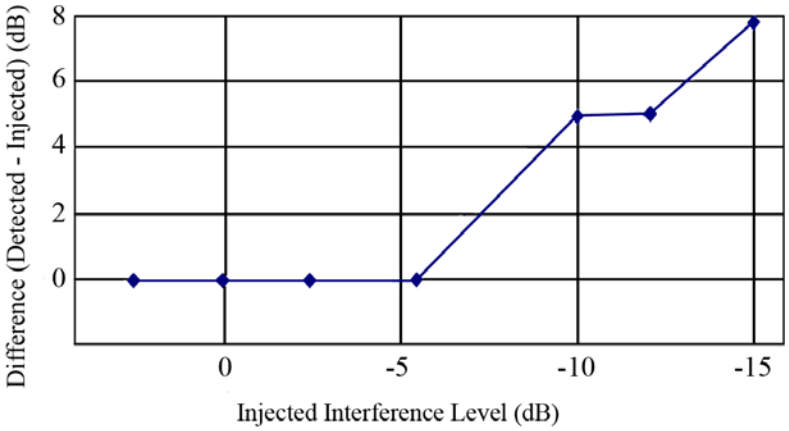


Figure 35. Detected minus injected interference levels as a function of injected level.

### 5.4.2 Reflectivity Analysis Methodology

Figure 36 represents the regression of the (interference+signal) level to the signal level for the TDMA-GMSK interference signal. This regression analysis has been used to graphically derive an interference level relative to the received signal level that results in a 1-dB bias in the reflectivity measurement. The interference level that results in a 1-dB bias is set equal to the difference between SNR (without interference) corresponding to the 3-dB and 1-dB SNR difference points. Adding this number to the -3-dB SNR level that was derived above results in the true *I/N* level. As an example, an average has been drawn on the data in Figure 36. The 1-dB and 3-dB points are noted on the y-axis and horizontal lines have been drawn to intersect the average. At the points of intersection, vertical lines have been drawn to intersect the x-axis (SNR without interference). The difference between these points of intersection represents the interference level below the signal level that results in a 1-dB bias.

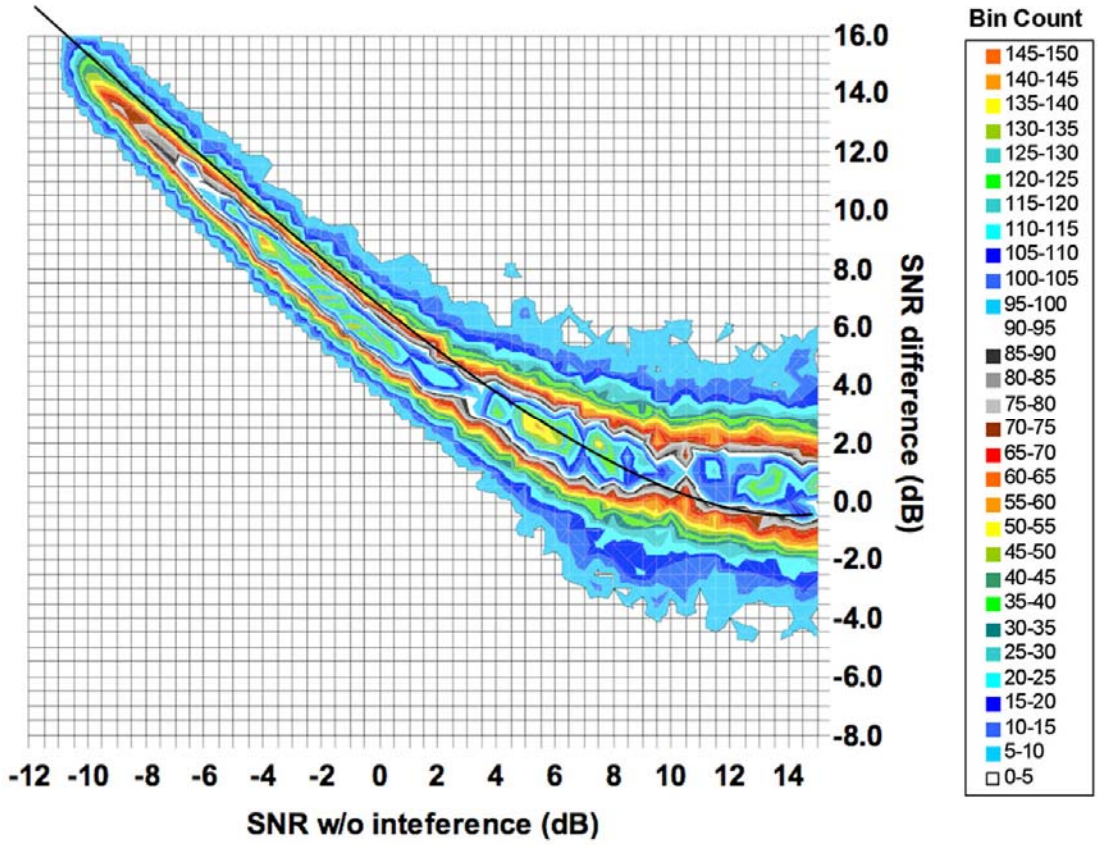


Figure 36. Reflectivity regression for interference in the meteorological radar.

For this example analysis, the *I/N* calculation yields the following results:

> *I/N* = (The interference level below the signal that results in a 1 dB bias) + (The minimum signal level that needs to be retrieved).

Table 10 illustrates the results of this analysis for one test case. The results presented in this table are consistent with the expected values as derived in Section 5.3.2.

### 5.4.3 Spectrum Width Analysis Methodology

A similar analysis approach was taken for determining the level at which a 1m/s bias occurred in the spectrum width product. In this case the regression that was used for graphically determining this value is shown in Figure 37.

Table 10. Reflectivity Results for Example Analysis

| **Interference Level Relative to Signal (dB)** | ***I/N* Level at which 1-dB Bias Occurs (dB)** |
|---|---|
| +6 | -9.5 |
| +3 | -9.5 |
| 0 | -9.5 |
| -3 | -10 |
| -6 | -7.5 |
| -10 | -9 |
| -12 | -7.5 |
| -15 | -8 |
| | |
| Mean | -8.9 |
| Standard Deviation | 0.93 |

### 5.4.4 Spectrum Width Regression

The process for analysis of spectrum width regression is very similar to the method used to determine the level at which a 1-dB bias occurred in the reflectivity data. An absolute level is derived from the reflectivity plot at a SNR difference level of 3 dB. A visual estimate of the mean is drawn onto the spectrum width plot and a spectrum width difference of 1 m/s is identified on the y-axis. A horizontal line is drawn to intersect the mean, and the SNR without interference level at which the spectrum width difference equals 1 m/s second is identified on the x-axis. To compensate for the residual effect that was described earlier, the values from Table 11 need to be algebraically added to this number. The results of using this technique at *I/N* level of -3 dB are shown in Table 12. The data set supports the theoretical analysis results in Section 5.2.4.

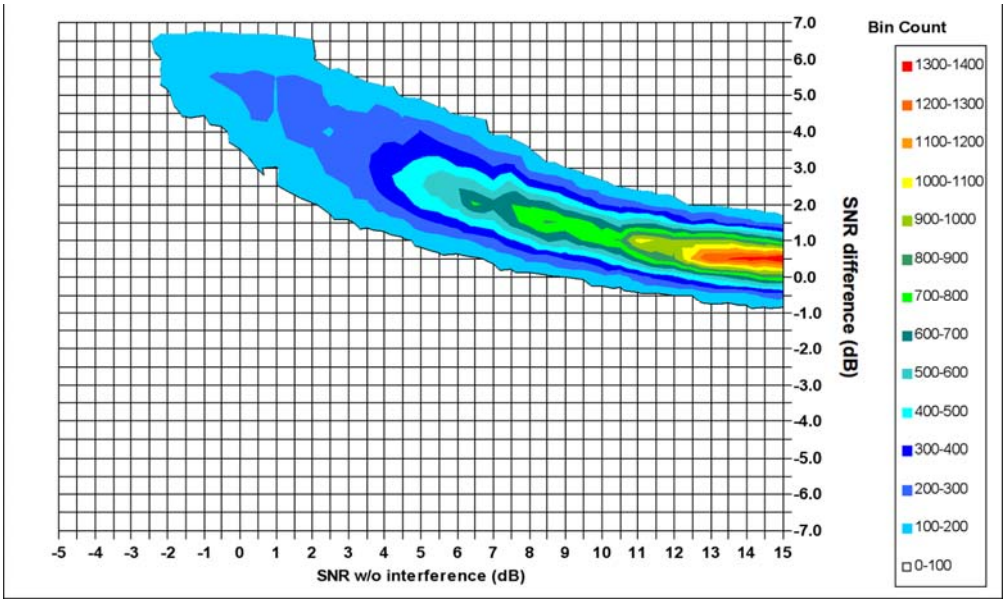


Figure 37. Spectrum width regression for the meteorological radar.

Table 11. Error Reduction Values

| Interference Level Relative to Signal (dB) | SNR w/o Interference (dB) | SNR – IL (dB) |
|---|---|---|
| 6 | 5.5 | -.5 |
| 3 | 2.5 | -.5 |
| 0 | -.5 | -.5 |
| -3 | -3.5 | -.5 |
| -6 | -3.75 | 2.25 |
| -10 | -5.25 | 4.75 |
| -12 | -7 | 5 |
| -15 | -7.6 | 7.4 |

Table 12. Spectrum Width Results for Example Analysis

| Interference Level Relative to Signal (dB) | *I/N* Level at which a 1 m/s difference occurs (dB) |
|---|---|
| 6 | 14 |
| 3 | 11.5 |
| 0 | 7 |
| -3 | 5.5 |

## 5.5 Summary of Measurement Results

The interference test results are summarized in Table 13.

Table 13. Measured *I/N* Thresholds Necessary for Protection of the Meteorological Radar

| Interference Signal | | Reflectivity Bias | Spectrum Width Bias |
|---|---|---|---|
| CW | | -7.5 dB | -11.5 dB |
| W-CDMA | 4.096 MS/sec | -9.5 dB | -10.75 dB |
| CDMA-2000-3X (fwd link) | 3.686 MS/sec | -7.0 dB | -13.5 dB |
| CDMA-2000-3X (rev link) | 3.686 MS/sec | -9.5 dB | -13.75 dB |
| TDMA-GMSK | 384 kS/sec | -8.75 dB | -14.0 dB |
| TDMA–8PSK | 384 kS/sec | -8.75 dB | -11.75 dB |

These results support the calculated value required for protection of the reflectivity measurements. As noted above, the measurements and analysis of the mean velocity were difficult to perform because the mean radial velocity is the least sensitive to interference, and those results do not necessarily indicate the overall interference levels that the radar can tolerate. As discussed above, current limitations in the radar calibration and noise removal process performed by the low level data processor limit the measurement of the necessary protection criteria for the spectrum width measurements. However, correction of the data for the limitations of the radar processing do result in values that support the calculated protection values presented in Section 5.2.4. Improvements to the radar receiver and processor are currently underway which will allow the system to approach or exceed its originally intended design criteria. This lower value will become meaningful when those improvements are made. Section 5.6 addresses those improvements in more detail.

## 5.6 Meteorological Radar Improvements

The weather radar system that was used for testing is one that has been operating in the United States for approximately eleven years. Upgrades to these systems that incorporate advances in signal-processing systems are currently underway. These upgrades will enable signal detection 10 dB below the current level.

The need for these improvements is driven by several requirements: 1) improved measurement performance above the planetary boundary layer; 2) detection of small water drops and fine mist precipitation that can result in aircraft icing; and 3) with the event of dual polarization measurements, improved monitoring of meteorological growth processes. All of these requirements call for a detection performance that is about 10 dB better than what is achievable today with current weather radar systems. To meet these requirements the radar's performance can be improved by increasing the transmitter power, reducing the receiver's noise floor, or increasing the radar's computational power for better signal processing capabilities.

Among these possibilities, increasing the transmitter power is not cost effective. The alternative of noise floor reduction could be accomplished by extending the pulse width, because extension of the pulse width reduces the required bandwidth of the matched filter and thereby reduces the noise power within the receiver IF. Increasing the pulse width by a factor of 2 increases the sample volume by a factor of 3 dB. Matching the receiver bandwidth results in a reduction of the receiver noise by 3 dB. This would lead to an overall detection improvement of 6 dB. Unfortunately, design limitations on the transmitter duty cycle will not allow extension of the pulse width for the system used in these tests. The receiver noise temperature could also be reduced but a reduction of 1 to 2 dB in noise is all that can be achieved with technology that will be available in the foreseeable future.

Ultimately, the most cost-effective way to achieve these improvements is through enhanced signal processing. Increasing the radar processing power with upgraded hardware will enable implementation of data processing algorithms that were not previously available. This additional processing will utilize coherent integration and frequency domain detection. The radar currently collects all the parameters necessary for performing these functions, but limited processing power has prevented implementation. The planned improvements that are currently under way will eliminate the processing power limitation.

Coherent integration, as implemented on this radar, has demonstrated a 10 dB improvement in detection. Frequency domain detection, the upgrade that is presently underway, will provide about 10 dB of improved performance. With frequency domain detection, the spectrum is broken into discrete coefficients, where the actual number of coefficients is determined by antenna rotation rate and operating mode. In the present storm modes the number of samples ranges from 41 to 111. Processing in the frequency (spectral density calculation) domain results in the desired signal being confined to a few spectral coefficients while the noise is spread over all the coefficients at a much lower level. Although about 20 dB of improvement is anticipated through the use of these two technologies, 10 dB of degradation is expected due to other engineering changes, including a new feature in which transmitter power will be divided between two polarizations. The net change, however, is [(20 dB) - (10 dB)]=10 dB.

The improvements to the radar performance enabled by greater processing power do not reduce the actual noise floor of the receiver, but the effect is a reduction in the effective noise floor by providing the ability to recover signals of interest at much lower signal levels. The difference between the actual noise floor and the effective noise floor is the processing detection improvement. Ultimately, improvements to the radar performance will also cause the radar to be adversely affected by interference at even lower levels.

### 5.7 Summary of Interference Effects on a Weather Radar

Weather radars, designed to track particles in the atmosphere and hydrometeors of submillimeter size, utilize extensive processing to extract signals from received noise. Tests conducted on one radar type used worldwide have characterized this processing gain as on the order of 6 to 9 dB. In addition, meteorological radars detect more than just the presence of return pulse energy; the processing derives data on return pulse characteristics to determine factors such as wind velocity, wind shear, turbulence, and precipitation type. This processing makes them very vulnerable to interference.

The test results demonstrate that depending on the radar base product considered, the necessary protection criteria vary. Since all three products are necessary for proper operation of the radar, the most stringent values are applicable to ensuring the radar does not experience harmful interference. Though testing was conducted on a single type of meteorological radar, most modern meteorological radar systems employ equally complex processing systems that are as susceptible to interference.

The test results suggest a requirement for a protection value of -9 dB *I/N* for the base reflectivity data. The results also show that while the theory predicts a necessary protection value of -14 dB *I/N* for spectrum width, the radar is presently sensitive to interference down to an *I/N* of approximately -6 dB for that parameter. Introduction of the radar improvements discussed in Section 5.6 will provide a net improvement of about 10 dB through improved processing power, resulting in a reduction in the effective noise floor by a value equivalent to the detection improvement. The end result is that the point where the radar's actual sensitivity to interference deviates from the theoretical curve in Figure 38 will decrease by the amount equal to the processing power. Figure 38 shows the divergence between test results and theory at *I/N*= -6 dB. Near-term improvements will provide 10 dB of processing power.

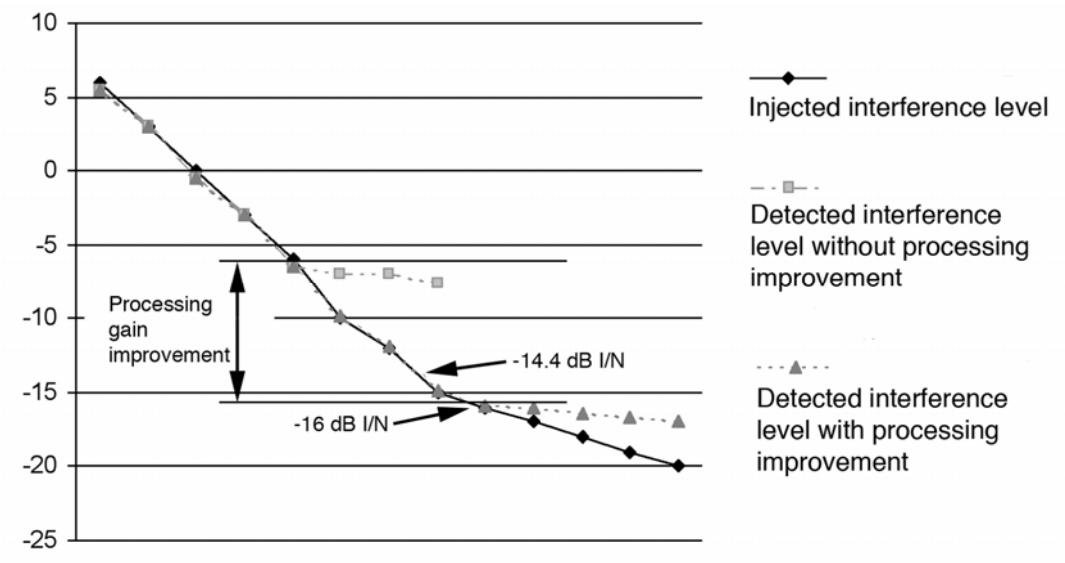


Figure 38. Impact of near-term processing improvements on the weather radar interference threshold, which is expected to ultimately be about *I/N*=-14.4 dB.

# 6 INTERFERENCE MEASUREMENTS ON MARITIME RADIONAVIGATION RADARS

## 6.1 Introduction

Maritime radionavigation radars may fail to meet their performance requirements if undesired signals inflict excessive amounts of various types of interference degradation. Dependent upon the specific interacting systems and the operational scenarios, those types of degradation may include:

- diffuse effects, e.g. desensitization or reduction of detection range, target drop-outs and reduction of update rate;
- discrete effects, e.g. detected interference, increase of false alarm rate.

Associated with these varieties of degradation, interference protection criteria may consist of threshold values of parameters, e.g., for a collision avoidance system:

- tolerable reduction of detection range and associated desensitization;
- tolerable missed-scan rate;
- tolerable maximum false-alarm rate;
- tolerable loss of real targets.

These protection criteria and the thresholds used to derive them for shipborne radionavigation systems need to be developed further. The operational requirement for maritime radars is a function of the operational scenario. This is related to the distance from shore and sea obstacles. In simplistic terms this can be described as oceanic, coastal or harbor/port scenarios.

There is as yet no international agreement on the protection criteria required for radars installed on ships for the scenarios identified above. The International Maritime Organization (IMO) is developing a revision to the operational performance standards for maritime radar that takes account of ITU-R requirements for limits on unwanted emissions from radio services. The IMO revision, for the first time, gives recognition to the possibility of interference from other radio services. Most importantly, the IMO has stated without reservation in its recent update of the IMO Safety of Life at Sea (SOLAS) Convention that *radar remains a primary sensor for the avoidance of collisions*. This statement should be viewed in the context of the mandatory fitting of Automatic Identification Systems (AIS) to some classes of ships.

AIS technology relies upon external references (e.g., GPS) for the verification of relative position indication in terms of collision avoidance scenarios. However, AIS cannot take account of many maritime objects (e.g., icebergs, floating debris, small vessels, and wrecks) that are not fitted with AIS. These objects may potentially cause collisions at sea, and must be detectable by maritime radars. Radar will therefore remain the primary system for oceanic collision avoidance for the foreseeable future.

Intensive discussion with maritime authorities, including users, has not yet created any quantitative consensus regarding the minimum required $P_d$ level for any scenarios. Rather, the instinctive reaction by such authorities is that during any maritime voyage *no interference that can be controlled by regulation is acceptable*. In the absence of additional guidance, a $P_d$ value of 0.9 for maritime targets (within a single scan) has been used as a nominal minimum in electromagnetic compatibility studies submitted to the ITU-R.

Tests were performed to assess the effects of pulsed emissions and emissions from digital-signal communication systems on three maritime radionavigation radars that operate with a primary allocation in the 2900-3100 MHz band and three radars that operate with primary allocation in the 9200-9500 MHz band. The systems that were tested are IMO category maritime radionavigation radars that employ scan rates, pulse widths, prfs, IF bandwidths, noise figure, and antenna beamwidths typical of those identified in a pertinent ITU-R Recommendation [22]. These radars are representative of the types being used by the United States Coast Guard (USCG) for shipboard navigation, by the commercial shipping industry, and recreational boaters as well. The radars operating in the 2900-3100 MHz band are identified as maritime radionavigation Radars A, B, and C and the 9200-9500 MHz radars are identified as maritime radionavigation Radars D, E, and F. Tests on radar F concentrated on the effects of pulsed interference.

Radars such as those identified in [22] and used in the NTIA tests typically employ interference mitigation techniques and processing methods identified in another ITU-R Recommendation [18] to allow them to operate in the presence of other radionavigation and radiolocation radars. Techniques of that kind are effective in reducing or eliminating low duty-cycle asynchronous pulsed interference between radars. All of the radars that were tested have some type of interference rejection circuitry/processing, which by default was enabled during testing.

These tests investigated the effectiveness of each of the radar's interference suppression circuitry and software to reduce or eliminate interference due to the emissions from a communication systems employing digital modulation schemes. Additional tests were also performed using low duty-cycle pulsed emissions as an interference source. The tests were performed with the assistance of the radar manufacturers and experienced mariners. Their guidance was used to properly set up and to operate the radars. This section describes the results of those studies to date.

### 6.1.1 Objectives

The objectives of the maritime radar testing were to:

- quantify the capability of each of the six maritime radionavigation radar's interference-rejection processing to mitigate unwanted emissions from digital communication systems as a function of their power level;
- develop *I*/*N* protection criteria that would mitigate interference from digital communication systems emissions in maritime radionavigation radars;
- observe and quantify the effectiveness of each of the maritime radionavigation radar's IR techniques to reduce the number of false targets, radial streaks (strobes), and background noise or "speckle."

## 6.2 Description of Maritime Radars Tested

### 6.2.1 Maritime Radionavigation Radar A

Maritime radionavigation Radar A, which was introduced circa 2000 and is still being refined, is designed for commercial applications and is an IMO category radar that operates in the 2900-3100 MHz band. Nominal values for the principal parameters of this radar were obtained from regulatory type-approval documents, sales brochures and technical manuals. These are presented in Table 14.

Table 14. Technical Characteristics of Maritime Radionavigation Radar A.

| Parameter | Value | | | |
|---|---|---|---|---|
| Frequency (MHz) | 3050 (+/-30) MHz | | | |
| Pulse power (peak) into antenna | 30 kW | | | |
| Range | 0.375-1.5 nmi | 3-6 nmi | 12 nmi | 24-96 nmi |
| Pulse width | 0.08 μs | 0.30 μs | 0.60 μs | 1.2 μs |
| Pulse repetition frequency | 2.2 kHz | | 1.028 kHz | 600 Hz |
| IF bandwidth | 28 MHz | 3 MHz | 3 MHz | 3 MHz |
| Spurious response rejection | 60 dB | | | |
| System noise figure | 4 dB | | | |
| Receiver noise in given bandwidth | -96 dBm | -105 dBm | -105 dBm | -105 dBm |
| Antenna mainbeam gain | [xx] | | | |
| RF bandwidth | Unknown | | | |
| Antenna scan rate (scan period) | 26 rpm (2.3 sec/rev) | | | |
| Antenna horizontal beamwidth | 1.9 degrees | | | |
| Antenna vertical beamwidth | 22 degrees | | | |
| Polarization | Linear horizontal | | | |

The radar uses a multistage logarithmic IF amplifier/detector. This type of receiver design is very common in marine radionavigation radars since they have to detect targets that have very small and large returns. A logarithmic amplifier increases the range of target returns that can be handled by the radar receiver without it becoming saturated.

The noise figure of the radar was measured and was found to be 5.3 dB, which was consistent with the nominal value of 4 dB. The 3-dB IF bandwidth is about 3 MHz for the range scale used for the tests. Using those parameters the noise power of the radar receiver is calculated to be about -104 dBm.

Radar A has extensive signal processing and target tracking capabilities, including an adaptive local CFAR feature and a scan-to-scan correlation feature. The local CFAR (acting within a small fraction of one range sweep) is known as an ordered-statistic CFAR, which is a type that permits the desensitizing effect of interfering pulses to be lessened or avoided. This is done by discarding a selectable number of background signal samples that would otherwise be used in establishing the detection threshold. The process discards the samples having the greatest amplitude. As more samples are discarded which contain the higher amplitude interfering pulses, the less influence they are likely to have on the sensitivity of valid target detection.

Radar A can also perform a scan-to-scan correlation process that provides an additional means for discriminating between signals that are present consistently, such as a valid target, and signals that appear at random times, such as asynchronous pulsed interference.

### 6.2.2 Radars B and D

Radars B and D are maritime radionavigation IMO category type of radars produced by the same manufacturer and are designed for commercial applications. Radar B operates in the 2900-3100 MHz band while Radar D operates in the 9200-9500 MHz band. Radars B and D locate their transmitter/receiver below deck and use waveguides to send/receive signals from the antenna. They use different antennas and receiver front-ends, but have a common display along with common receiver elements, including the interference rejection processing and IF circuitry. The radars use a multistage logarithmic IF amplifier and a separate video detector. Radars B and D also use pulse jitter. The transmitted pulse prf can be jittered to prevent second time around echoes and also to reduce the interference from other transmitters in the vicinity. This function is automatically set in the transceiver and provides up to ±25μs jitter about the nominal value. Nominal values for the principal parameters of these radars were obtained from regulatory type-approval documents, sales brochures and technical manuals. They are presented in Table 15.

Table 15. Technical Characteristics of Maritime Radionavigation Radars B and D

| Parameter | Value | | | |
|---|---|---|---|---|
| Frequency | 3050 (± 10) MHz | 9410 (± 30) MHz | | |
| Pulse power (peak) into antenna | 30 kW | | | |
| Range | 0.125-1.5 nmi | 3-24 nmi | 48 nmi | 96 nmi |
| Pulse width | 0.070 μs | 0.175 μs | 0.85 μs | 1.0 μs |
| Pulse repetition frequency | 3.1 kHz | 1.55 kHz | 775 Hz | 390 Hz |
| IF bandwidth | 22 MHz | 22 MHz | 6 MHz | 6 MHz |
| Spurious response rejection | Unknown | | | |
| System noise figure | 5.5 dB | | | |
| Receiver noise in given bandwidth | -95 dBm | -95 dBm | -101 dBm | -101 dBm |
| RF bandwidth | Unknown | | | |
| Antenna mainbeam gain | [xx] | | | |
| Antenna scan rate (scan period) | 24/48 rpm (2.5/1.25 sec/rev) | | | |
| Antenna horizontal beamwidth | 2.8 degrees | 1.2 degrees | | |
| Antenna vertical beamwidth | 28 degrees | 25 degrees | | |
| Polarization | Linear horizontal | | | |

The values of pulse width and prf in Table 15 are the default settings for that particular range. The operator can, for some ranges, select pulse widths and prfs that differ from the default values.

Pulse-to-pulse and scan-to-scan correlators are used by Radars B and D to mitigate interference from other radars. For pulse-to-pulse correlation, returns from successive pulses are compared to reduce interference; a target is displayed only if it is present for consecutive pulses. This IR function is most effective if the transceiver has been set to provide prf jitter. Scan-to-scan correlation will only display targets if they are present in consecutive scans. These radars do not have CFAR processing. More discussion of these radar interference mitigation techniques can be found in Section 1 and Appendix A of this report, as well as in an ITU-R Recommendation [18].

### 6.2.3 Maritime Radionavigation Radars C and E

Radars C and E are maritime radionavigation IMO category type of radars produced by the same manufacturer and were designed for commercial applications. Radar C operates in the 2900-3100 MHz band while Radar E operates in the 9200-9500 MHz band. Radars C and E are a topmast design. The receiver/transmitter (R/T) is encapsulated in a metal housing located directly below the rotating antenna. The video from the R/T unit is sent to the PPI located below deck via cables. They use different antennas and receiver front-ends, but have a common display along

with common receiver elements including the interference rejection processing and IF circuitry. Both of the radars use an eight-stage successive approximation logarithmic IF amplifier/detector.

Nominal values for the principal parameters of these radars were obtained from regulatory type-approval documents, sales documentation, and technical manuals. They are presented in Table 16. The values of pulse width and prf in the table are the default settings for that particular range. The operator can, for some ranges, select pulse widths and prfs that differ from the default values.

Radars C and E use pulse-to-pulse and scan-to-scan correlators to mitigate interference from other radars, as described above. These radars do not have CFAR processing.

Table 16. Technical Characteristics of Maritime Radionavigation Radars C and E

| Parameter | Value | | |
|---|---|---|---|
| Frequency | 3050 (+/-10) MHz | 9410 (+/-30) MHz | |
| Pulse power into antenna | 30 kW | | |
| Range | 0.125-3 nmi | 6-24 nmi | 48-96 nmi |
| Pulse width | 0.050 μs | 0.25 μs | 0.80 μs |
| PRF (Hz) | 1.8 kHz | 785 Hz | |
| IF bandwidth | 20 MHz | 20 MHz | 3 MHz |
| Spurious response rejection | Unknown | | |
| System noise figure | 4 dB | | |
| Receiver noise in given bandwidth | -97 dBm | -97 dBm | -105 dBm |
| RF bandwidth | Unknown | | |
| Antenna mainbeam gain | 30 dBi | | |
| Antenna scan rate (scan period) | 25/48 rpm (2.4/1.25 sec/rev) | | |
| Antenna horizontal beamwidth | 2.0 degrees | 1 degree | |
| Antenna vertical beamwidth | 30 degrees | 15 degrees | |
| Polarization | Linear horizontal | | |

### 6.2.4 Maritime Radionavigation Radar F

Maritime radionavigation Radar F is nearly identical to Radar A, except that its RF front end operates in the 9200-9500 MHz band. Nominal technical characteristics of this radar are presented in Table 17. The radar uses a summing multistage logarithmic amplifier with the IF bandwidths given in Table 17 for each pulse width and associated range. A test point was provided that is located at the output of the third IF amplifier. A CW signal was swept in frequency to determine the response of the receiver and measure the IF bandwidth. The result is shown in Figure C-5. The 3 dB IF bandwidth of the radar when set to short pulse mode 1, which

uses a pulse width of 200 ns for a maximum range of 3 nautical miles, was measured to be about 6.5 MHz. This mode was used for all of the tests.

Table 17. Technical Characteristics of Maritime Radionavigation Radar F

| Parameter | Value | | | | |
|---|---|---|---|---|---|
| Frequency | 9410 (+/-30) MHz | | | | |
| Pulse mode | Short pulse 1 | Short pulse 2 | Medium pulse 1 | Medium pulse 2 | Long pulse |
| Pulse width | 80 ns | 200 ns | 400 ns | 700 ns | 1.2 μs |
| Range mode | 0.125-1.5 nm | 0.5-3 nm | 1.5- 6 nm | 3-24 nm | 6-72 nm |
| Pulse repetition rate | 2.2 kHz | | 1 kHz | | 600 Hz |
| IF bandwidth | 27 MHz | 4.5 MHz | 3 MHz | | |
| Spurious response rejection | 60 dB | | | | |
| System noise figure | 4 dB | | | | |
| Receiver noise in given bandwidth | -96 dBm | | | | |
| Antenna mainbeam gain | 31 dBi | | | | |
| RF bandwidth | Unknown | | | | |
| Antenna scan rate (scan period) | 24 rpm (2.5 sec/rev) | | | | |
| Antenna horizontal beamwidth | 1.5 degrees | | | | |
| Antenna vertical beamwidth | 22 degrees | | | | |
| Polarization | Linear horizontal | | | | |

### 6.2.5 Radar Video Displays

Radars A and F use the same video display unit. Their enhanced signal processing capabilities can display various types of targets in different combinations. The radars could display amorphous, raw-video "blips" (known as the image display), synthetic targets that appeared as "o" symbols, and/or tracked targets that appeared as "x" symbols. The brightness of the video image targets roughly corresponded to the power of the target echoes. Figure 39 shows an example of synthetic and raw video targets on the same PPI display.

Synthetic targets require about 2-3 dB of additional desired power compared to raw-video targets to obtain the same $P_d$ when operating at minimum detectable signal (MDS) level but do not

change their brightness in correspondence with echo strength. That is, if the target power for the 0.9 $P_d$ for blip display was -90 dBm, then the power level to achieve the 0.9 $P_d$ for the synthetic targets would be about -88 dBm. Adding signal power did not change the intensity of the display of the synthetic targets. For synthetic targets the radar has a built-in target counter that shows the number of targets per scan and displays that value on the PPI display.

Radars B and D (from the same manufacturer) use a color CRT to display targets and radar information to the user, including prf, pulse width, range rings, and other parameters. These radars do not show synthetic targets and only display raw-video blips. Likewise, Radars C and E (from another manufacturer) only display raw-video blips. However, the displays used with radars C and E are monochromatic raster scan types. Besides targets, these displays also indicate various radar parameters. Like Radar A, for these radars the raw-video blips are brighter for targets that have stronger return echoes.

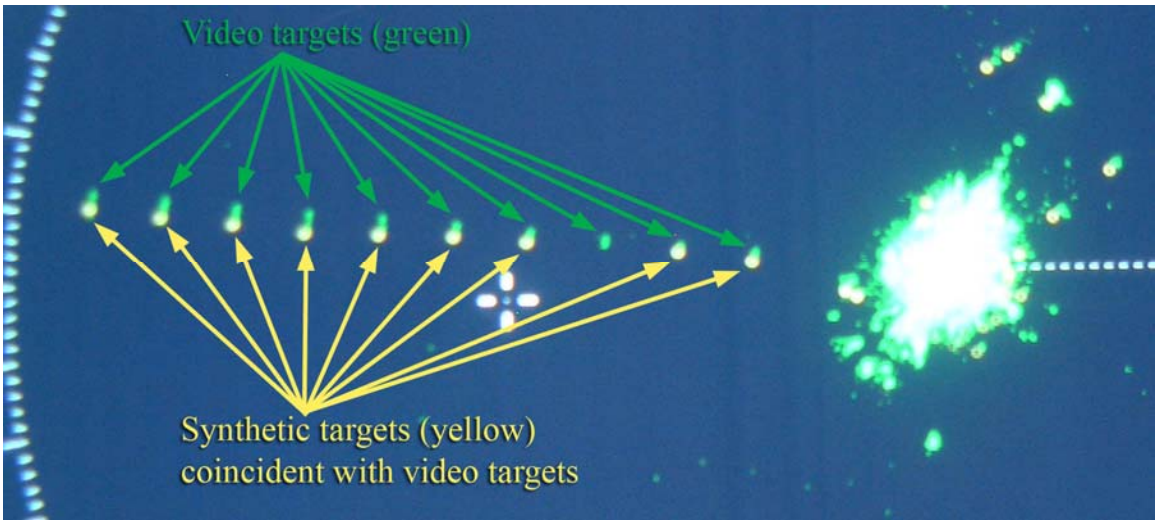

Figure 39. Example of synthetic and raw video targets on a PPI display.

## 6.3 Interference Signal Characteristics

### 6.3.1 Interference Generation for Radars A Through E

Radar A was tested with a 2 MBit/s QPSK waveform as an interference source. Radars B and C were tested with 64 quadrature amplitude modulation (QAM), 16 QAM, CDMA-2000, and W-CDMA signals as interference sources. Radars D and E were only tested with the CDMA-2000 and W-CDMA signals. All interfering signals were on-tune (co-channel) with the radars. The QPSK signal injected into Radar A was continuous, occurring for a full 360 degrees.

The unwanted CDMA signals that were injected into Radars B, C, D and E were gated to occur at the same time of the target generation within the same azimuth. The gate time was equal to the length of time that a stationary interference source would be within the radar's antenna 3-dB horizontal beamwidth as it rotates. The QAM signals were not gated. A measured emission spectrum of the continuous QPSK signal is shown in Figure B-5.

Communication test sets were used to generate the DVB-T 16 QAM, DVB-T 64 QAM, CDMA 2000 and WCDMA signals. Spectrum shots of each of the unwanted signals are shown in Figures B-8 and B-9. The CDMA-2000 signal was for the reverse link (mobile-to-base) standard according to interim standard 95 (IS-95) format for cellular mobile telephones. The W-CDMA signal was for the uplink standard according to the 3GPP 3.5 format. The 16 and 64 DVB-T QAM signals in Figure B-8 represent the type of modulation scheme that is television camera crews for electronic news gathering outdoor broadcast (ENG-OB) purposes.

### 6.3.2 Interference Generation for Radar F

Tests on Radar F concentrated on the effects of pulsed interference from radiolocation radars. In a departure from most of the work described in this report, and for reasons that will become clear, effects of pulsed interference were explored up to +40 dB *I/N* levels. In fact, at one point during the testing, an attenuator setting was inadvertently set to a lower value than was intended. As a result, *I/N* levels as high as +60 dB were injected. At these levels, the LNA at the radar RF front end was gain-compressed and radar performance was seriously compromised as a result. The tests were performed with radiolocation waveforms that are representative of the radar systems that operate in the 9000-9200 MHz and 9300-9500 MHz bands.

Three types of radiolocation waveforms were used for the tests. They are chirped, phase coded, and unmodulated (simple pulsed) waveforms. The waveforms were gated on for the duration of the mainbeam dwell time for the radionavigation receiver as if it were scanning past a stationary object. They were also on-tuned (co-channel) with the radar.

#### *6.3.2.1 Linear Chirped-Pulse Interference Waveform*

Table 18 shows the parameters of the chirped interference. They were developed based on the characteristics of existing 9-GHz radars. The number of pulses per beam dwell is dependent on the type of radiolocation system being simulated.

Table 18. Chirped-Pulse Interference Waveform Characteristics

| Waveform | Pulse width | Prf | Pri | Duty cycle | Chirp | Chirp rate |
|---|---|---|---|---|---|---|
| Chirp 1 | 10 μs | 750 Hz | 1.3 ms | 0.8% | 10 MHz | 1 μs/MHz |
| Chirp 2 | 10 μs | 750 Hz | 1.3 ms | 0.8% | 50 MHz | 5 μs/MHz |
| Chirp 3 | 13.6/1.65 μs | 5 kHz | 0.20 ms | 0.8% | 660/80 MHz | 48.5 μs/MHz |
| Chirp 4 | 10 μs | 2 kHz | 0.5 ms | 0.4% | 400/80 MHz | 40 MHz/μs |
| Chirp 5 | 80 μs | 4.5 kHz | 0.22 ms | 7.2% | 400/80 MHz | 5 MHz/μs |
| Chirp 6 | 10 μs | 515 Hz | 1.94 ms | 0.91% | 45/80 MHz | 4.5 MHz/μs |
| Chirp 7 | 10 μs | 5.15 kHz | 1.94 ms | 0.88% | 460/80 MHz | 46 MHz/μs |

Radar F was tested with linear chirped pulsed interference waveforms. These waveforms primarily use a chirped modulation scheme as shown in Table 18. The duty cycles are calculated from the scaled pulse widths.

In some cases, the frequency sweep range of the chirp-pulse generation system used in these tests was limited by hardware to less than the full chirp range of the corresponding radar emission being modeled. In such cases, the tests were still performed to fully and accurately replicate the response of radar receivers to the specified chirp parameters. To accomplish this goal, the chirped pulses used in the tests were swept across at least twice the -20-dB frequency response range of the Radar F receiver, at the same rate as the sometimes wider-bandwidth chirp pulses from potentially interfering sources.

For example in Table 18, the 660-MHz chirp in a 13.6 μs pulse ($R_c$ = (660 MHz/13.6 μs) = 48.5 MHz/us) was not possible to generate with available test equipment. But an equivalent interference effect was generated with an 80-MHz chirp pulse in an interval of 1.65 μs ($R_c$ = (80 MHz/1.65 μs) = 48.5 MHz/μs), provided that the -20-dB radar IF pass-band of the Radar F victim receiver is less than 50 MHz wide.

In these tests, the value of $R_c$ was always preserved and the Radar F receiver always saw the chirped interference across its full receiver IF passband in exactly the same way as it would have if the chirped interference had been generated across wider bandwidths. That was the key element in accessing the effects of the interference.

For Radar F, the interference signals were injected into the radar at the same azimuth as the targets for a duration time equal to the antenna beam sweeping across a stationary object. The receiver's noise power measured at the IF test point using a spectrum analyzer in zero span mode without any targets, radiolocation, or linear chirped pulsed waveforms present in the bandwidth was about -57 dBm. This indicated a nominal gain of about 40-42 dB in the receiver. The gain compression point[23] using an on-tune CW signal was found to be -25 dBm on the generator panel display, or -43 dBm at the LNA input. The radar receiver interference suppression circuitry and software *cannot* mitigate the effects of receiver saturation.

The Radar F receiver IF output response (amplitude and pulse width) to interference from chirped pulses is a function of the rate at which the chirped frequency sweeps through the victim radar receiver pass-band. This rate, called chirp rate ($R_c$), is given by: $R_c = (B_c/\tau)$, where $R_c$ is the sweep rate in megahertz per microsecond, $B_c$ is the chirp frequency range in megahertz and $\tau$ is the pulse duration in microseconds. Victim radar receivers should not respond to interference on frequencies outside the -20-dB pass-band of their IF circuitry, assuming that the interference is below the RF front-end overload threshold.

### *6.3.2.2 Phase Coded Pulsed Interference Waveform*

Table 19 shows the parameters of the phase coded pulsed interference waveform, based on a 13-bit Barker code sequence.

[23] The gain compression point is the value where the LNA is saturated by the input signal and will no longer give a linear relationship between the input and output signals.

Table 19. Phase Coded Pulsed Interference Waveform Characteristics

| Waveform | Pulse width | Prf | Sub-pulse width |
|---|---|---|---|
| Phase 1 | 0.64 μs | 1.6 kHz | 0.049 μs |
| Phase 2 | 20 μs | 1.6 kHz | 1.54 μs |

*6.3.2.3 Unmodulated Pulsed Interference Waveform*

Table 20 shows the parameters of the unmodulated pulsed interference waveforms. They are based on the characteristics of existing radars along with higher duty cycles that may be used in future systems. The starred (*) waveforms did not replicate particular radar signals; they were used determine the effectiveness of radar signal processing at high duty cycles.

Table 20. Unmodulated Pulsed Interference Waveform Characteristics

| Waveform | Pulse width | Prf | Pri | Duty Cycle |
|---|---|---|---|---|
| Unmod 1 | 1 μs | 8 kHz | 125 μs | 0.8% |
| Unmod 2 | 1 μs | 19 kHz | 52.63 μs | 1.9% |
| Unmod 3 | 1 μs | 35 kHz | 28.57 μs | 3.5% |
| Unmod 4* | 1 μs | 50 kHz | 20.0 μs | 5.0% |
| Unmod 5* | 1 μs | 75 kHz | 13.3 μs | 7.5% |
| Unmod 6* | 1 μs | 100 kHz | 10 μs | 10% |
| Unmod 7* | 1 μs | 200 kHz | 5 μs | 20% |

*6.3.2.4 OFDM/BPSK Interference Waveforms*

In addition to the radiolocation waveforms, Radar F was subjected to an on-tune orthogonal frequency division multiplexing (OFDM/BPSK) waveform. It was used to demonstrate the radar response to interference of a continuous nature (non-pulsed). These signals were gated for the duration of the mainbeam dwell time. The OFDM/BPSK waveforms, although not specific to any type of communication system in the 9-GHz band, are a typical modulation of those types of waveforms used by communications systems in other bands for broadband, high data rate applications. It was used to show the contrast in interference suppression capabilities between the effects of pulsed interference in the radar receiver and a digital modulation that appears noise-like.

## 6.4 Target Generation

### 6.4.1 Target Generation for Maritime Radars A Through E

Ten simulated, equally-spaced, equi-amplitude targets were generated along a radial using RF signal generators, AWGs, and other miscellaneous equipment (combiners, attenuators, etc.) for each of the radars out to a 3-nmi range as shown in Figure 40. The target generation system provided groups of RF pulses with the width and timing to appear as ten individual targets on the radar's PPI display. The targets had identical signal power in the radar receiver, simulating RCS that increased with distance. The number of pulses needed to generate each target depended on the radar's characteristics.

The train of transmitter trigger pulses (A) was used to trigger the simulated-target generator. A free-running pulse generator was used to produce gate pulses (B) representing the amplitude modulating effect on target return due to the antenna beam. Those pulses gated the train of transmitter triggers in an AND gate circuit, producing bursts (C) of trigger pulses containing from 6 to 23 pulses each. Each trigger pulse was applied to an arbitrary waveform generator, which delayed the trigger appropriately and generated a burst of ten pulses (D), each having the width of one of the radar's short pulses. All ten of these occurred within one "sweep" of the radar, i.e., within the displayed fraction of one pulse repetition interval or PRI. Each of those pulses in turn modulated an RF signal generator set to a frequency near 3050 or 9410 MHz to produce a simulated-target-return pulse train. The specific RF signal generator frequency was adjusted to maximize the radar's response.

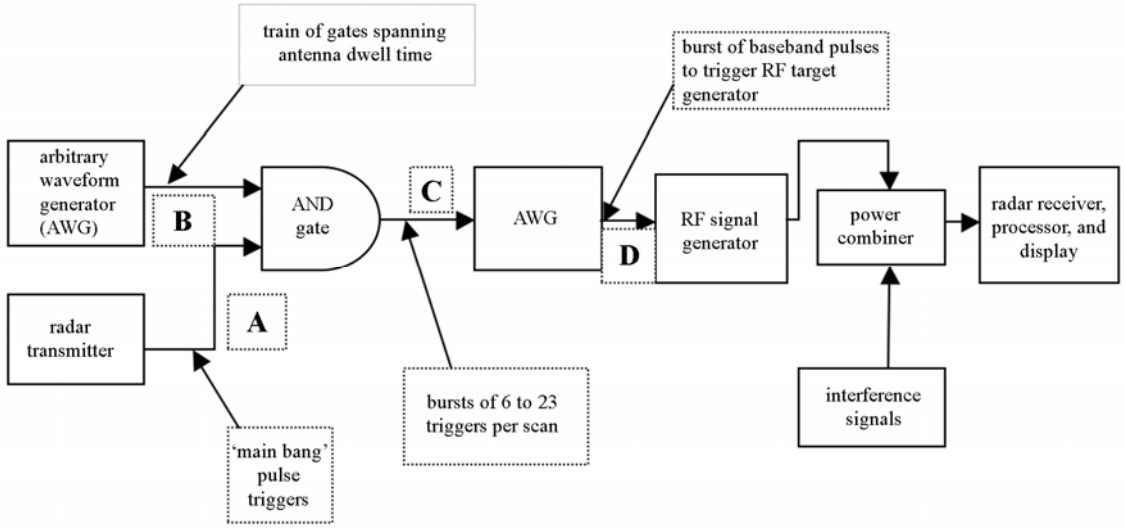


Figure 40. Target generator instrumentation for maritime radionavigation radar tests.

### 6.4.2 Non-Fluctuating Target Generation for Radar F

The targets for these tests were generated using the same basic hardware as for the other maritime radars, with ten equally spaced targets generated on a radial and the farthest target

being located at the maximum range of 3-nmi. Each target was comprised of 18-19 pulses with the characteristics of the short pulse 2 mode setting in Table 17. Each target on the radial had the same power level in the radar receiver.

The ten target pulses triggered by each radar trigger all occur within the return time of one of the radar's short range scales, i.e., one "sweep". Consequently, the pulses simulate ten targets along a radial, i.e., a single bearing. For adjustment of the display settings, the RF power of the target generator was set to a level so that all ten targets were visible along the radial on the PPI display with the radar's video controls set to positions representative of normal operation. The pulse repetition rate of the target generator (waveform B) was adjusted so the targets would appear at the same azimuth on consecutive scans of the PPI. The target generator timing diagram is shown in Figure 41.

A number of trials were performed to determine the target signal power that would result in a $P_d$ of 90 percent *without* the interference radiolocation or linear chirped pulse waveforms being present. This value was found to be about -70 dBm at the panel display of the target generator. With RF losses, the target power supplied to the LNA input of the radar receiver was -88 dBm. The noise figure was measured to be about 9 dB. This results in a calculated noise power of about -97 dBm in the (approximately) 6-MHz IF bandwidth of the radar receiver. Therefore, the signal-to-noise value to achieve the $P_d$ of 90 percent was about 8-10 dB. Note that the accuracy of this measurement is probably within ±2 dB.

While the Radar F antenna was not used for the tests, appropriate signals from the antenna positioner circuitry were supplied to the radar receiver to mimic the antenna's normal rotation.

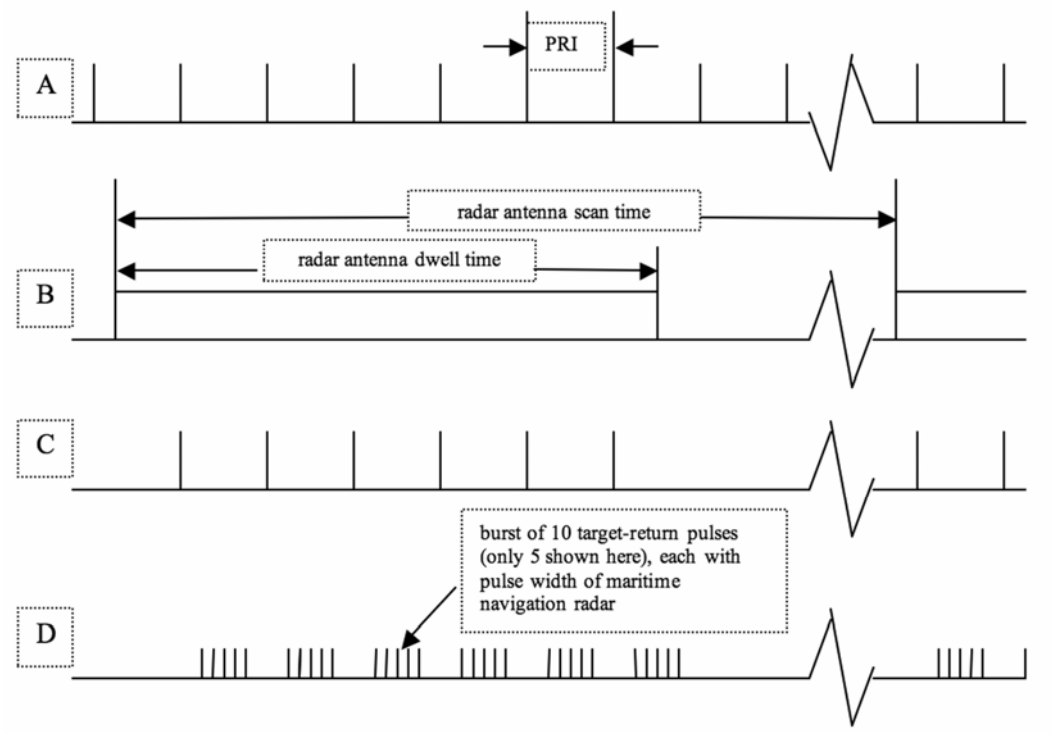


Figure 41. Target generator timing diagram for maritime radionavigation radar tests.

### 6.4.3 Fluctuating Target Generation for Radar F

For maritime Radar F, tests were also performed with fluctuating-power targets that changed their power levels on a scan-by-scan basis according to Swerling case 1 statistics[24] (see Section 2.3 of this report). All ten targets on the PPI radial were varied by the same amount; each Swerling level was held constant for all ten targets for a total of twenty scans, then the next Swerling level was used for all ten targets for the next twenty scans, and so forth. Thus each data point represented the counting of (10 targets per scan x 20 scans per level)=200 injected targets at each Swerling level. A total of twenty Swerling levels were used, and were programmed to run in a random order from one level to the next. The Swerling power levels were applied relative to the nominal value of RF power that gave $P_d$=0.9 without interference; their order and values are shown in Table 21. For example, the $P_d$=0.9 nominal target power value was -88 dBm and on the first scan the power was adjusted by +2.1 dB to be -85.9 dBm, on the second scan the power was -86.5 dBm, and so on.

For the tests, the signal levels of all targets were adjusted to produce stationary target detections consistent with a fixed $P_d$ of about 0.9. This $P_d$ value was chosen to reflect the case that the $P_d$ can never be 100 percent due to propagation effects, interference and other factors. As of the time that this report was written, the IMO has not specified a minimum $P_d$ for marine radionavigation radars. The IMO performance standard[25] does specify target types, RCS, and the minimum ranges to detect them. The IMO is developing a minimum $P_d$ for these types of radars and should publish this value in the near future.

The target power level output was controlled by a computer and sequenced through the twenty Swerling values of Table 21 without interruption to accurately reproduce the true effect of a scan-to-scan scenario. Note that in other interference tests the radar was allowed about five scans to 'settle' between each data point. A number of baseline runs through the sequence were performed without interference, versus with the OFDM signal being injected. Effects of fluctuating levels on target $P_d$ *without* any interference are noted in Table 21.

[24] Swerling case 1 target levels were generated by summing the squares of pairs of Gaussian-distributed real numbers.

[25] Extracts from IMO Resolutions A222(VII), A278(VIII), A477(XII) for radar equipment required by Regulation 12, Chapter 5 of the IMO-SOLAS Convention.

Table 21. Swerling Case 1 Target Power Levels (Relative to Nominal Value of -88 dBm)

| **Signal levels in dB Relative to Median Power Level and Effect on Target $P_d$ Without Interference** | | | | | |
|---|---|---|---|---|---|
| Scan number | dB | Effect | Scan number | dB | Effect |
| Scan 1 | +2.1 | $P_d$ 100% | Scan 11 | +2.7 | $P_d$ 100% |
| Scan 2 | +1.5 | Near 100% | Scan 12 | +0.90 | $P_d$ higher |
| Scan 3 | +3.3 | $P_d$ 100% | Scan 13 | -5.6 | No targets |
| Scan 4 | +0.3 | Baseline | Scan 14 | +7.3 | $P_d$ 100% |
| Scan 5 | +4.5 | $P_d$ 100% | Scan 15 | -0.3 | Reduced $P_d$ |
| Scan 6 | -7.2 | No targets | Scan 16 | -2.5 | No targets |
| Scan 7 | -1.7 | Few targets | Scan 17 | -3.3 | No targets |
| Scan 8 | -14.4 | No targets | Scan 18 | -9.5 | No targets |
| Scan 9 | +4.0 | $P_d$ 100% | Scan 19 | -4.3 | No targets |
| Scan 10 | +5.7 | $P_d$ 100% | Scan 20 | -1.0 | Reduced $P_d$ |

## 6.5 Maritime Radar Test Conditions

The tests were performed with the following parameters set on the maritime radionavigation radars as shown in Table 22.

For all of the radars, the STC and FTC features could be activated at the operator's discretion. As noted in Sections 1.10.1 and 1.10.2, STC suppresses sea-clutter returns by attenuating strong echoes at short ranges, while FTC suppresses rain clutter by differentiating echo returns after envelope detection.

For each of the radars that were tested, baseline values for the software functions that controlled the target and background brilliance, hue, and contrast settings were found through experimentation by test personnel and with the assistance of the manufacturers and with professional mariners that were experienced with operating these types of radars on ships of various sizes. Once these values were determined, they were used throughout the test program for that radar.

Table 22. Maritime Radar Test Control Settings

| **Parameter** | **Value** |
|---|---|
| Sensitivity time control (STC) | Disabled |
| Fast time constant (FTC) | Disabled (default) |
| Interference rejection (IR) | On (default) |
| Automatic gain control | On (default) |
| Radars A and F image selected | Raw video ("image") and/or synthetic targets |
| Radars B, C, D, E | Raw video |
| Range scale | 3 nmi |

### 6.5.1 Interference Suppression Features in Radars A and F

In addition to conventional STC and FTC features for clutter reduction, Radars A and F deserve special mention of the following capabilities to minimize clutter and RF interference: ordered statistic CFAR, spike suppression, clutter mapping, and scan-to-scan correlation. As shown in Table 22, STC and FTC were disabled for the tests, since they are used to discriminate sea clutter returns from target returns and to offset the effects of rain, respectively. Obviously, sea clutter and rain did not affect these measurements as they were performed on a test bench. A brief description of the other interference mitigation features follows.

The spike suppression circuitry provides a means of instantaneously filtering interference from other transmitters by detecting and eliminating spikes that occur at a given range over three adjacent sweeps based on a maximum rise and fall criteria. The circuit substitutes the spike value with the average of the amplitudes on the previous and subsequent sweeps.

The CFAR uses an ordered statistic (OS) technique. This adaptive technique minimizes clutter breakthrough in large homogeneous clutter areas. It permits target returns near or above the peak noise plus clutter level to be detected while eliminating the bulk of the noise and clutter. The OS CFAR operates by automatically adjusting the detection threshold based on an instantaneously derived estimate of the predominant noise plus clutter level in the vicinity of the test cell. A programmable guard cell region allows the OS CFAR to accommodate targets of extended range run length, such as supertankers, without loss of sensitivity while still discriminating against clutter.

The clutter mapping compensates for unique spatially distributed clutter situations, such as ones that might be caused by multi-path, grazing angle versus sea state, or a combination of such conditions. The radar operator is provided a means of biasing the OS CFAR derived threshold on an area-by-area basis through the use of a threshold bias map (TBM). The threshold offset stored in the TBM for a particular area is added to the OS CFAR computed threshold for all detections occurring in that area. There are sixteen TBM areas centered around the radar's position which permit the specification of an annulus clutter filter area, and which may be used to counter effects that are range dependent but bearing independent. The TBM area may be defined to negatively bias the OS CFAR generated threshold to increase sensitivity or completely mask returns such as those from land mass. The TBM is organized as a table of 1024 range cells by 1024 azimuth cells.

The scan-to-scan correlator takes advantage of the fact that sea clutter is correlated on a pulse-by-pulse basis, but de-correlated on a scan-by-scan basis. Clutter that is permitted to pass through all previous clutter suppression stages is processed through a temporal-spatial de-correlation filter, the retrospective processor. This processor performs scan-to-scan correlation, maintaining as many as nine scans of data.

### 6.6 Maritime Radar Test Procedures (Non-Fluctuating Targets)

For each radar that was tested, the RF power output of the target generator system was adjusted so that the target $P_d$ was about 90 per cent without unwanted signals being present, with the baseline PPI target and background display settings. Table 22 lists the target power at each radar's RF input that was required to obtain a $P_d$ of 0.90. Once these values were determined, they were used throughout the tests.

Table 23. Target Power Levels (Non-Fluctuating) Required to Achieve a $P_d$ of 0.90

| Radar | Target power at RF input for a $P_d$ of 0.90 |
|---|---|
| A | -90 dBm |
| B | -89 dBm |
| C | -77 dBm |
| D | -89 dBm |
| E | -86 dBm |
| F | -88 dBm |

For Radars A, C and E, the appropriate levels of unwanted signal powers that were required to produce the *I*/*N* levels within the radar receivers was determined using the calculated receiver noise power calibrated to the receiver's waveguide input. The receiver noise power was calculated using the IF bandwidth and noise figure. Any differences in bandwidths between the radar receiver and the test signals were accounted for in setting the *I*/*N* levels.

The appropriate levels of unwanted signal powers that were required to produce the *I*/*N* levels within radar receivers B and D were determined by monitoring the output of the IF circuitry at a test point located at the detector input with the spectrum analyzer. The spectrum analyzer was set to zero-span mode and the value of the radar receiver noise power at the IF test point, without any unwanted signal being present, was measured and recorded. The unwanted signal was then injected into the radar RF front-end and the noise power at the IF test point was monitored for a 3-dB increase as the power level of the unwanted signal was also increased. A 3-dB increase in the receiver noise power is equal to an *I*/*N* of 0 dB. Once the value of the unwanted signal that generated the *I*/*N* of 0 dB was found, the unwanted signal power levels that generated the other *I*/*N* values were easily determined. The power levels of the unwanted signals were controlled using step attenuators or the test set panel display.

For Radars B and D, the number of targets on each radial was counted for 50 simulated rotations of the antenna for each *I*/*N* level for each type of unwanted signal. The $P_d$ was calculated by dividing the number of counted targets by the total number of targets that were generated.

For Radars A, C and E, observations of the relative strength or brightness of the targets displayed on the PPI were performed and documented at the various *I*/*N* levels. The nature of the effect of the interference on Radars A, C, and E target displays prevented performing an actual "count" of the targets because all of the targets tended to "fade" at the same rate. These effects included a

"dimming" of the targets, an increase in the number of false targets, radial streaks ("strobes"), and an increase in background "speckle" or noise.

## 6.7 Test Results for Maritime Radionavigation Radars

### 6.7.1 Radar A (3 GHz)

Figure 42 shows a digital photograph of Radar A's PPI baseline operating state (no interference injected). Note that the raw-video targets appear along a radial at about 320 degrees. Local clutter returns from buildings and slight speckling are also visible on the radar display.

Observations of video image targets on the radar's PPI display were made with emissions from the QPSK generator applied to its receiver. The power level of the QPSK emission was adjusted until the appearance of the radar's PPI was in a baseline condition. The power level of the QPSK waveform was adjusted within a range of values to find the level where the QPSK emissions did not adversely affect the performance of the radar in displaying video targets. Figures 43 and 44 are photographs of the radar's PPI that show the effects of the QPSK waveform at power levels of -112 and -102 dBm (measured within a 3-MHz bandwidth), respectively. The radar's receiver noise power was approximately -104 dBm. The resulting $I/N$ ratios were -8 dB and +2 dB.

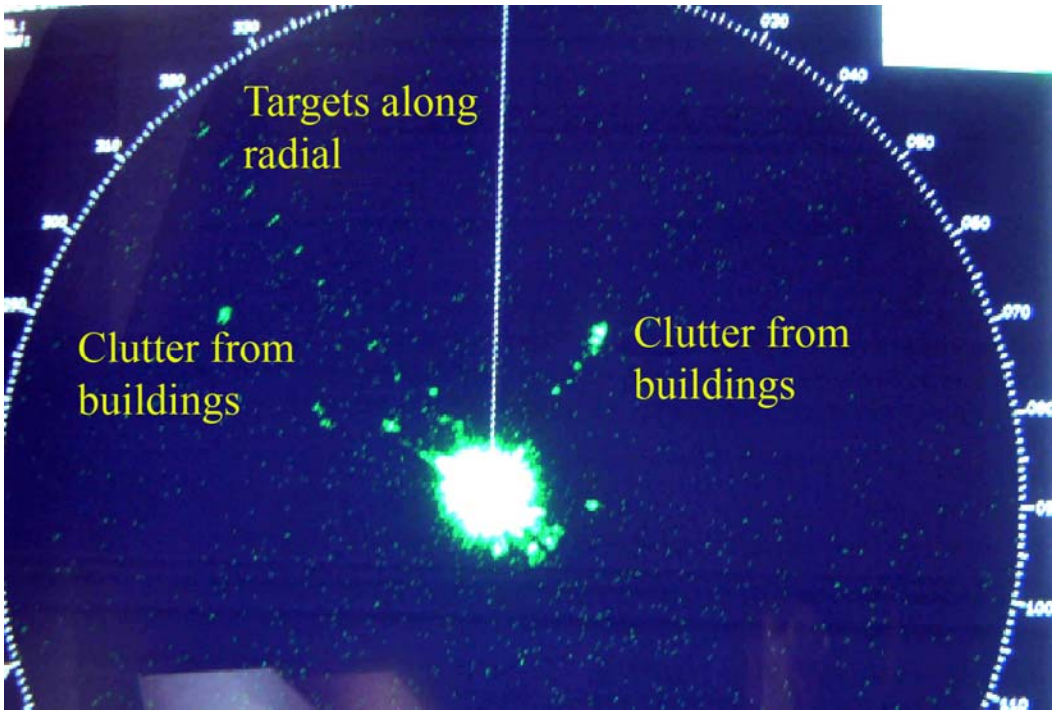

Figure 42. Radar A baseline state (no interference) with video targets.

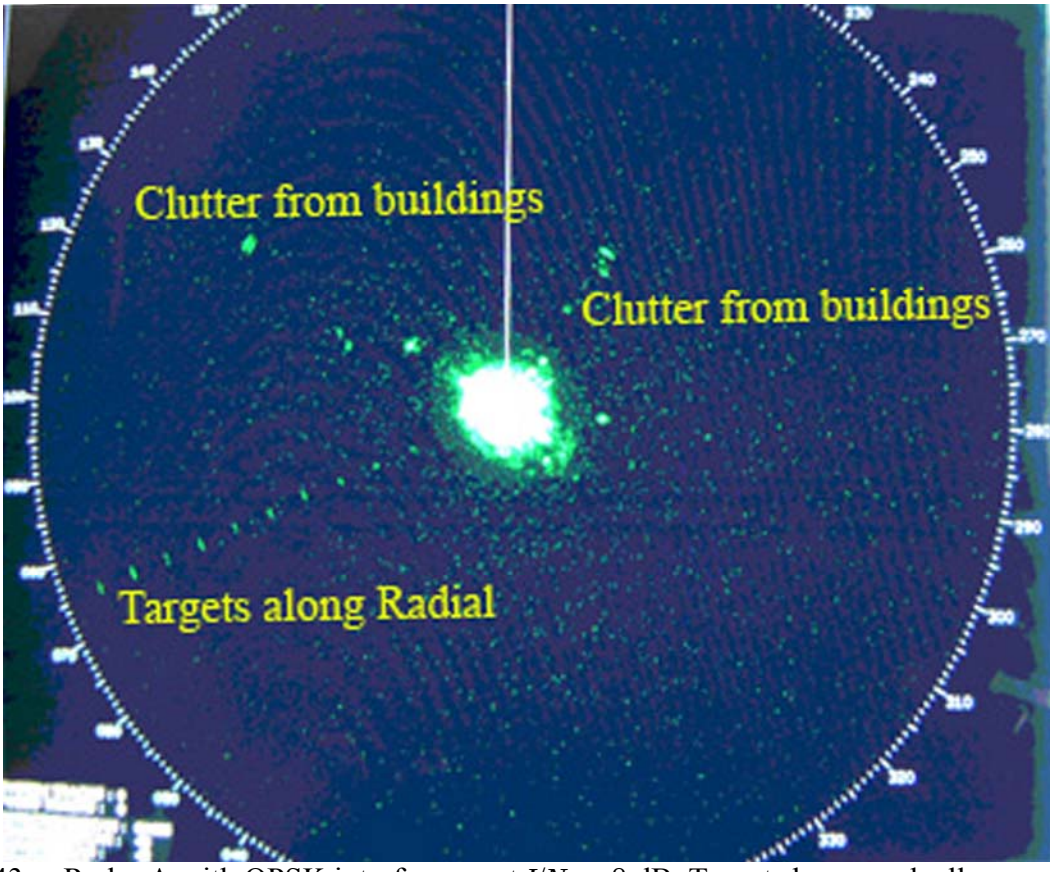

Figure 43. Radar A with QPSK interference at $I/N$ = -8 dB. Targets have gradually precessed on the display since the time that the picture of Figure 42 was taken.

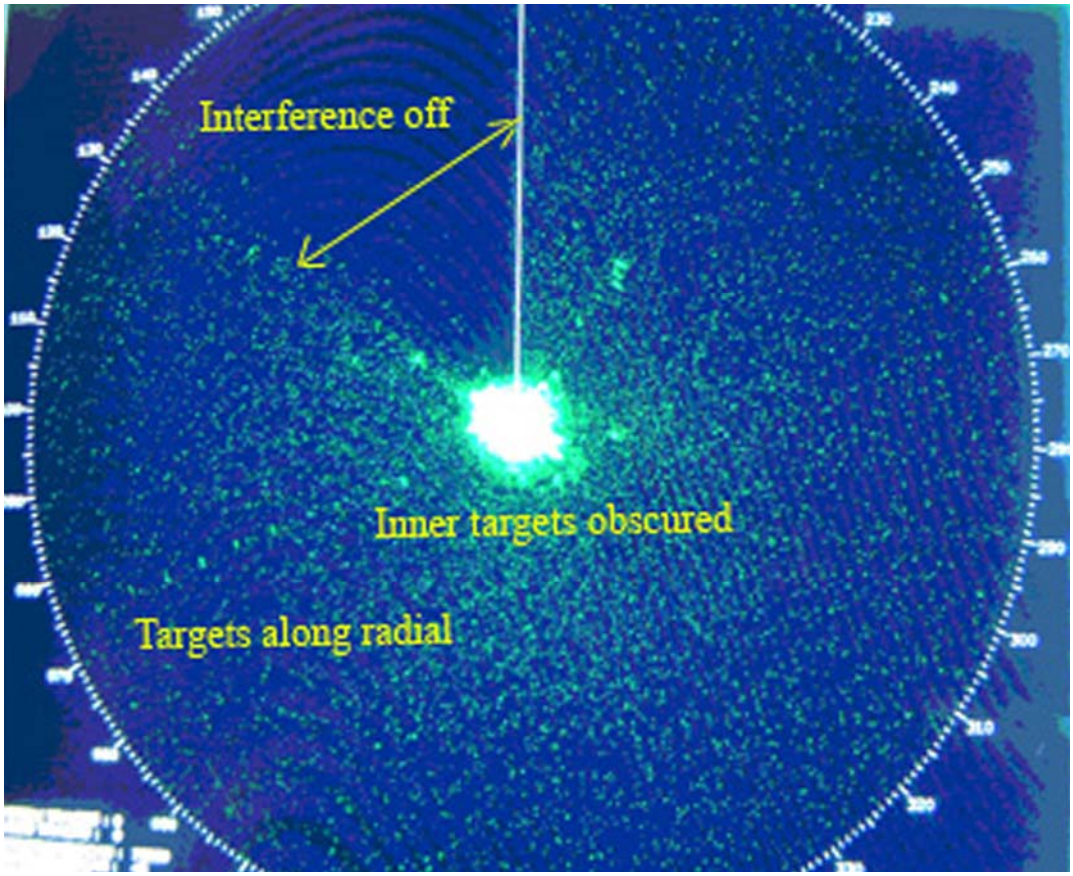


Figure 44. Radar A with QPSK interference at *I*/*N* = +2 dB. Targets are on same radial as in Figure 43. Interference was turned off during the indicated segment of the scan at upper left. The black lines (Moiré pattern) in that sector were not present on the radar screen; they are an artifact of the reproduction of this image.

Table 24 summarizes the results for Radar A. The images show that the QPSK emissions caused an increase in the background noise or speckle. In comparing Figure 41, which is the radar baseline state without interference, to Figure 42 (which has an *I*/*N* of -8 dB) the background speckle has increased but the targets are still detected and displayed. In Figure 44 the *I*/*N* is +2 dB and the QPSK emissions have increased the background noise to the extent that the targets are becoming indistinguishable from the speckle.

Table 24. Radar A Responses to QPSK Interference

| ***I*/*N* Ratio of Interference** | **Effect** |
|---|---|
| -8 dB | Slight increase in background speckle; targets distinguishable |
| -7 dB | More increase in background speckle; targets distinguishable |
| -6 dB | Target visibility degraded due to increasing speckle effect |
| +2 dB | Targets becoming indistinguishable from background speckle |

The power level of the QPSK emissions was adjusted to find the point where the video targets were still clearly visible and the background speckle was similar to the baseline level. That power level was found to be about -111 dBm at the receiver input, for an *I*/*N* ratio of about -7 dB.

It is important to note that the test targets on the radial are more visible than "real world" targets that would be distributed anywhere on the radar's PPI. Therefore, care needs to be taken in interpreting radar presentations in the presence of noise. The *I*/*N* values were not based on one specific photograph *per se*. The photographs in this report are representative of the interference condition. Some of the radar's scans might show a worse state (denser speckle/false targets) while others might show a better state (clearer PPI) at the same *I*/*N* level. Approximately 20 scans were observed at each *I*/*N* level in choosing the *I*/*N* values represented in Figures 42 through 44.

### 6.7.2 Radar B (3 GHz)

For Radar B it was possible to observe the effect that the unwanted signals had on individual targets. For each unwanted signal, it was possible to count the decrease in the number of targets that were visible on the PPI as the *I*/*N* level was increased. Target counts were made at each *I*/*N* level for each type of interference. A baseline target $P_d$ count was performed before the beginning of each test. The results of the tests on Radar B are shown in Figure 45, which shows the target $P_d$ versus the *I*/*N* level for each type of interference. The baseline $P_d$ in Figure 45 is 0.93 with the 1-sigma error bars 0.016 above and below that value. Note that each point in Figure 45 represents a total of 500 desired targets.

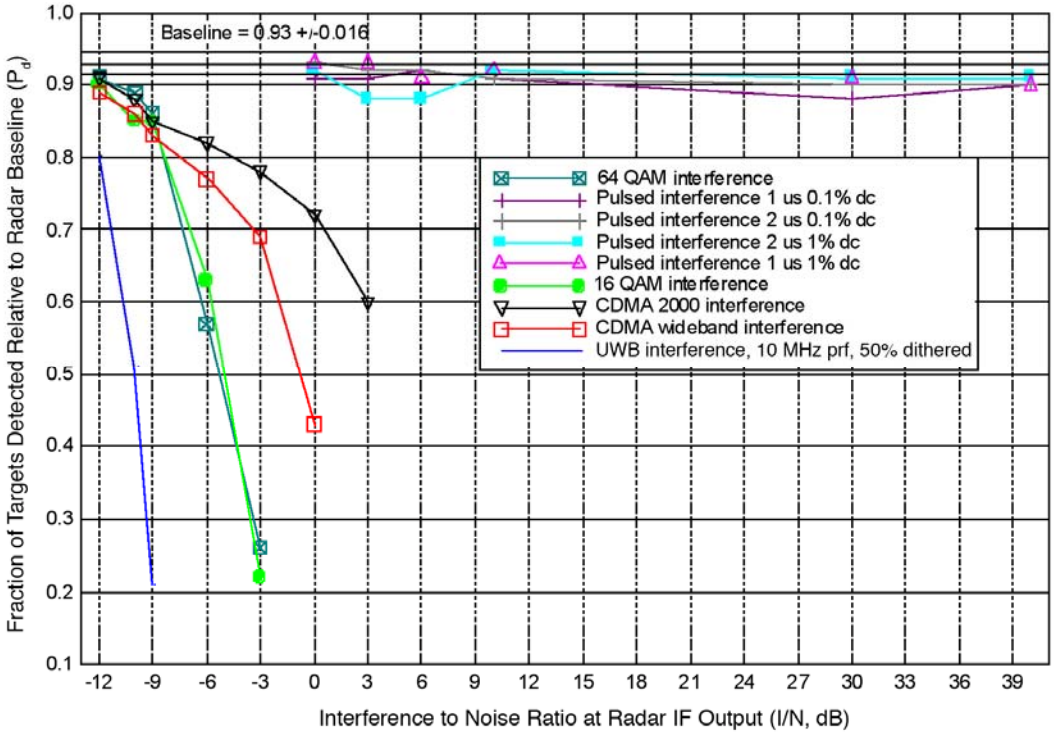


Figure 45. Radar B $P_d$ curves.

Figure 45 shows that, except for the case of the pulsed interference, the target $P_d$ was reduced below the baseline $P_d$ used in these tests minus the standard deviation for *I*/*N* values above -12 dB for all of the unwanted signals that used a digital modulation. The QAM interference caused the quickest drop in the $P_d$ as the *I*/*N* was increased. Data was not taken for higher *I*/*N* values above of -3 dB for QAM because all of the targets were gone on the PPI above that level. The CDMA 2000 had the least effect on the target $P_d$, but it was still causing a drop in the target $P_d$ at *I*/*N* values above -12 dB.

The performance of Radar B was highly robust against in the presence of pulsed interference up to *I/N* levels of +39 dB. The low duty cycle of the pulsed interference allowed the radar's interference rejection mechanism (which relies on non-coherence between the desired and the undesired pulse repetition sequences) to work effectively.

### 6.7.3 Radar C (3 GHz)

For Radar C it was difficult to count the decrease in target $P_d$ as the interference was injected into the radar's receiver. The interference caused all of the targets to fade at the same rate no matter where they were located in the string of targets. It was not possible to make individual targets "disappear" as the interference power was increased, and count the number of lost targets in order to calculate the $P_d$. Therefore, the data taken for Radar E reflects whether or not the appearance of all the targets was affected at each *I*/*N* level for each type of interference. The data for Radar C are summarized in Tables 25 and 26.

Table 25. Radar C Responses to Continuous QAM Interference

| ***I*/*N* Ratio** | **64 QAM** | **16 QAM** |
|---|---|---|
| -12 dB | No effect | No effect |
| -10 dB | No effect | No effect |
| -9 dB | Targets slightly dimmed | Targets slightly dimmed |
| -6 dB | Targets dimmed | Targets dimmed |
| -3 dB | Targets not visible | Targets not visible |
| 0 dB | Targets not visible | Targets not visible |
| +3 dB | Targets not visible | Targets not visible |
| +6 dB | Targets not visible | Targets not visible |

The data in Table 25 show that the unwanted QAM signals affected the visibility of the targets for Radar C on its PPI at an *I*/*N* level of -9 dB. At that level the brightness of the targets on the PPI was slightly dimmed from their baseline state. At *I*/*N* levels of -6 dB they were dimmed more and for *I*/*N* levels above -3 dB the targets had dimmed so much that they were no longer visible on the PPI display.

The data in Table 26 show that the unwanted CDMA signals affected the visibility of the targets for Radar C on its PPI at an *I*/*N* level of -6 dB. At that level the brightness of the targets on the

PPI was noticeably dimmed from their baseline state. At *I*/*N* levels of -3 dB and above, the targets had dimmed so much that they were no longer visible on the PPI.

For Radar C, the gated 2.0 and 1.0 μs pulsed interference with duty cycles of 0.1 and 1.0 percent did not affect the visibility of the targets on the PPI at the highest *I*/*N* level, which was 40 dB.

Table 26. Radar C Responses to Gated CDMA Interference

| ***I*/*N* Ratio** | **W-CDMA** | **CDMA-2000** |
|---|---|---|
| -12 dB | No effect | No effect |
| -10 dB | No effect | No effect |
| -9 dB | No effect | No effect |
| -6 dB | Targets dimmed | Targets dimmed |
| -3 dB | Targets not visible | Targets not visible |
| 0 dB | Targets not visible | Targets not visible |
| +3 dB | Targets not visible | Targets not visible |
| +6 dB | Targets not visible | Targets not visible |

### 6.7.4 Radar D (9 GHz)

For Radar D it was possible to observe the effect that the unwanted signals had on individual targets. For each unwanted signal, it was possible to count the decrease in the number of targets as the *I*/*N* level was increased. Target counts were made at each *I*/*N* level for each type of interference. A baseline target $P_d$ count was performed before the beginning of each test. The results of the tests on Radar D are shown below in Figure 46 with the target $P_d$ versus the *I*/*N* level for each type of interference. The baseline is shown at a $P_d$ of 0.92 with the 1-sigma error bars 0.016 above and below. Note that each point in Figure 46 represents a total of 500 desired targets.

The performance of Radar D was highly robust against in the presence of pulsed interference up to *I/N* levels of +39 dB. The low duty cycle of the pulsed interference allowed the radar's interference rejection mechanism (which relies on non-coherence between the desired and the undesired pulse repetition sequences) to work effectively.

The data in Figure 46 show that, except for the case of the pulsed interference, the target $P_d$ was reduced below the baseline $P_d$ used in these tests minus the standard deviation for *I*/*N* values above -12 dB for the unwanted CDMA signal.

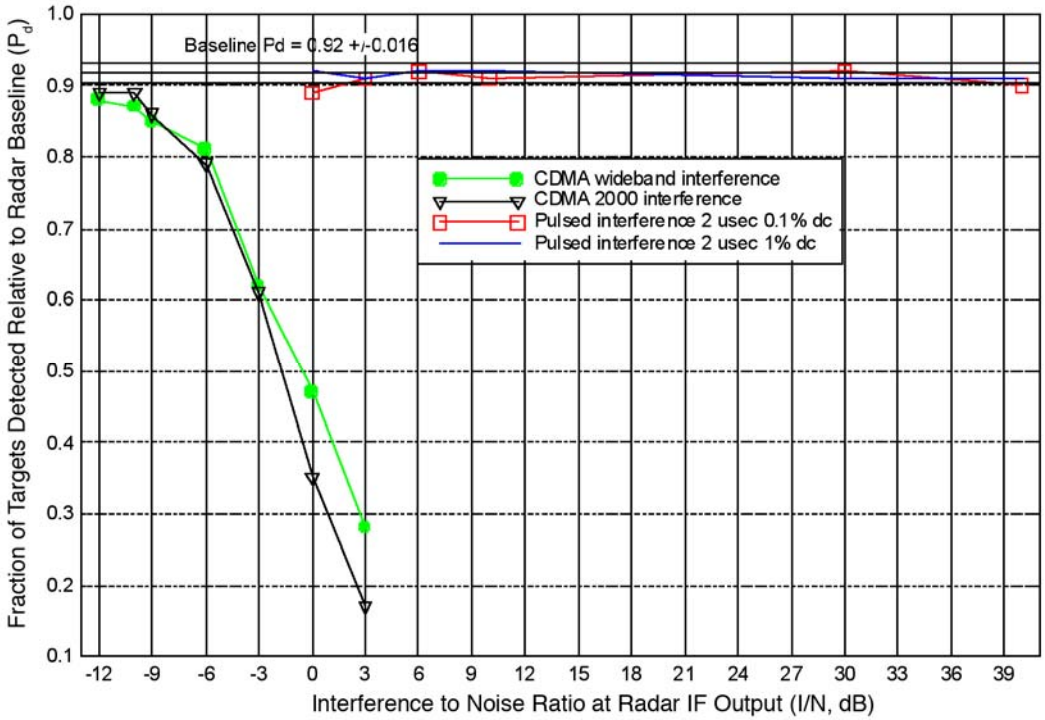


Figure 46. Radar D $P_d$ curves.

### 6.7.5 Radar E (9 GHz)

As in the case of Radar C, for Radar E it was difficult to count the decrease in target $P_d$ as the interference was injected into the radar's receiver. The interference caused all of the targets to fade at the same rate no matter where they were in the string of targets. It was not possible to make individual targets "disappear" as the interference power was increased. Therefore, the data taken for radar E reflects whether or not the appearance of all the targets was affected or not at each *I*/*N* level. The data for Radar E are summarized in Table 27.

Table 27. Radar E Responses to Gated CDMA Interference

| ***I*/*N* Ratio** | **WB CDMA** | **CDMA-2000** |
|---|---|---|
| -12 dB | No effect | No effect |
| -10 dB | No effect | No effect |
| -9 dB | No effect | No effect |
| -6 dB | Targets dimmed | Targets dimmed |
| -3 dB | Targets dimmed | Targets dimmed |
| 0 dB | Targets not visible | Targets not visible |
| 3 dB | Targets not visible | Targets not visible |
| 6 dB | Targets not visible | Targets not visible |

The data in Table 27 show that the unwanted CDMA signals affected the visibility of the targets for Radar E on its PPI at an *I*/*N* level of -6 dB. At that level the brightness of the targets on the PPI was noticeably dimmed from their baseline state. At *I*/*N* levels of 0 dB and above, the targets had dimmed so much that they were no longer visible on the PPI.

For Radar E, the gated 2.0 and 1.0 µs pulsed interference with duty cycles of 0.1 and 1.0 percent did not affect the visibility of the targets on the PPI at the highest *I*/*N* level, which was 40 dB.

### 6.7.6 Radar F (9 GHz)

The test results for the maritime radionavigation Radar F are contained in Table 28. The table shows that the radar did not suffer any degradation to its performance with any of the chirped or phase-coded waveforms up to an *I/N* of +40 dB. For the unmodulated pulses the radar did not suffer any degradation at an interference duty cycle of 5 percent and an *I/N* of +40 dB. At the higher duty cycles for the unmodulated radiolocation waveform, the radar produced a strobe on the PPI display at the target azimuth when the *I/N* exceeded +20 dB. At lower *I/N* ratios the strobe on the PPI was transformed into an increase in the amount of false targets or speckle. These effects are shown in photographs of the radar's PPI in Figures 47 and 48. These photographs are representative examples of the PPI condition; there was variation from scan-to-scan in the number of false targets.

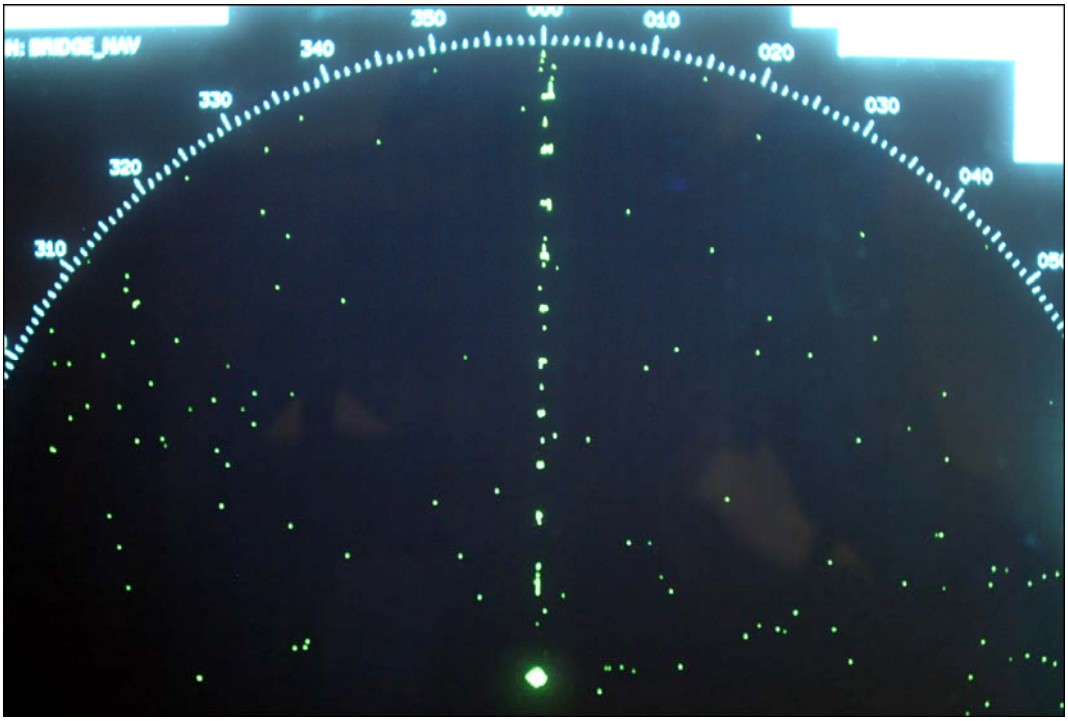


Figure 47. 1-µs pulsed interference at 7.5% duty cycle and *I/N*= +40 dB.

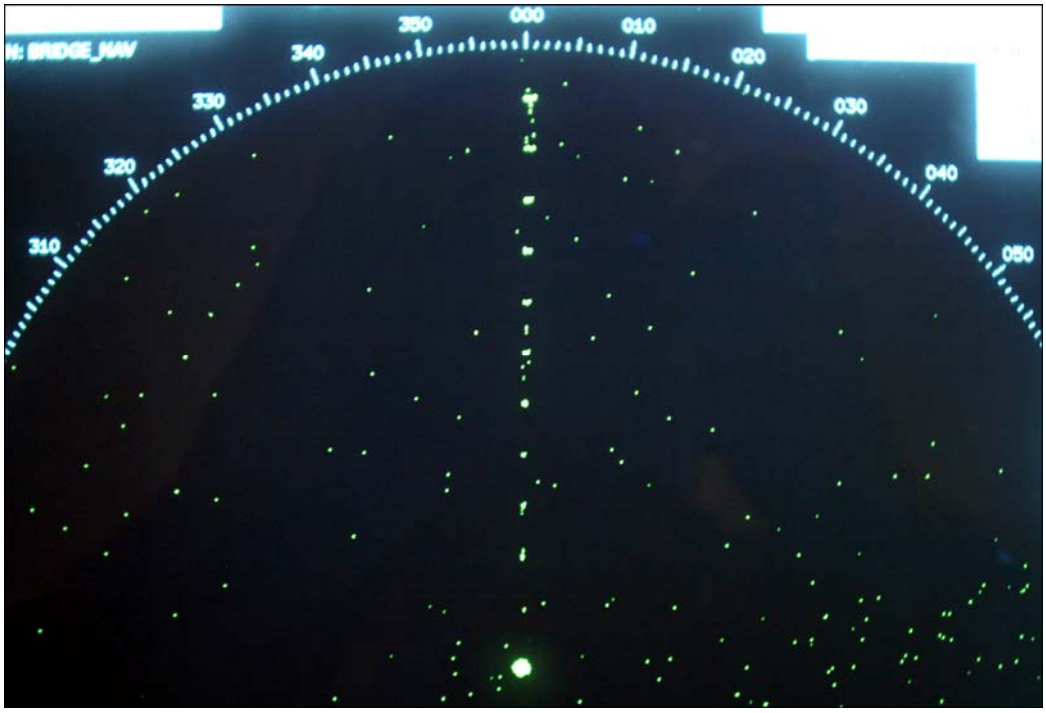


Figure 48. 1-μs pulsed interference at 7.5% duty cycle and *I/N*= +12 dB.

Regarding Figures 47-48, the observers knew in advance where the targets would be displayed and that knowledge made it easier for them to distinguish the targets from interference speckling. Radar operators viewing ordinary targets in an operational environment would not have that condition available to them, making the targets harder to distinguish from background speckle (as seen off the target radial) in these in real-world scenarios. The off-radial speckling is due to random radar receiver noise.

For the OFDM interference (Figures 49-50), the effects on the PPI were noticeable at *I/N* = +3 dB as false targets, and strobes were produced above that *I/N* value. At *I/N* values of 0 dB and -3 dB, the radar's CFAR circuitry performed exactly as it was supposed to, reducing the $P_d$ as the overall noise level increased. (The OFDM signal would appear to the radar as broadband noise.) At *I/N* = 0 dB the $P_d$ was 0.83 and at *I/N* = -3 dB the $P_d$ was 0.85. At *I/N* = -6 dB the radar appeared to have recovered to its baseline state. This response demonstrates that the radar was able to reject most of the pulsed interference, but it did not effectively mitigate the OFDM interference effects.

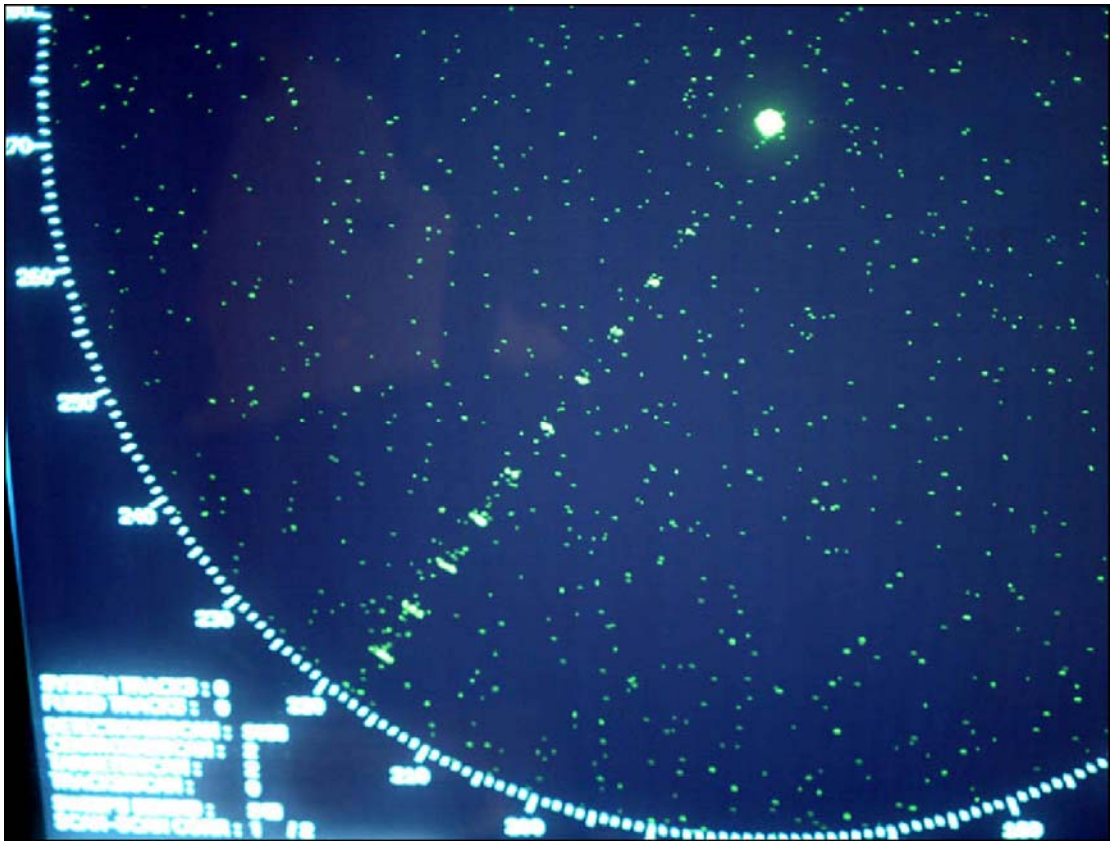

Figure 49. OFDM interference effect at *I/N*= +3 dB.

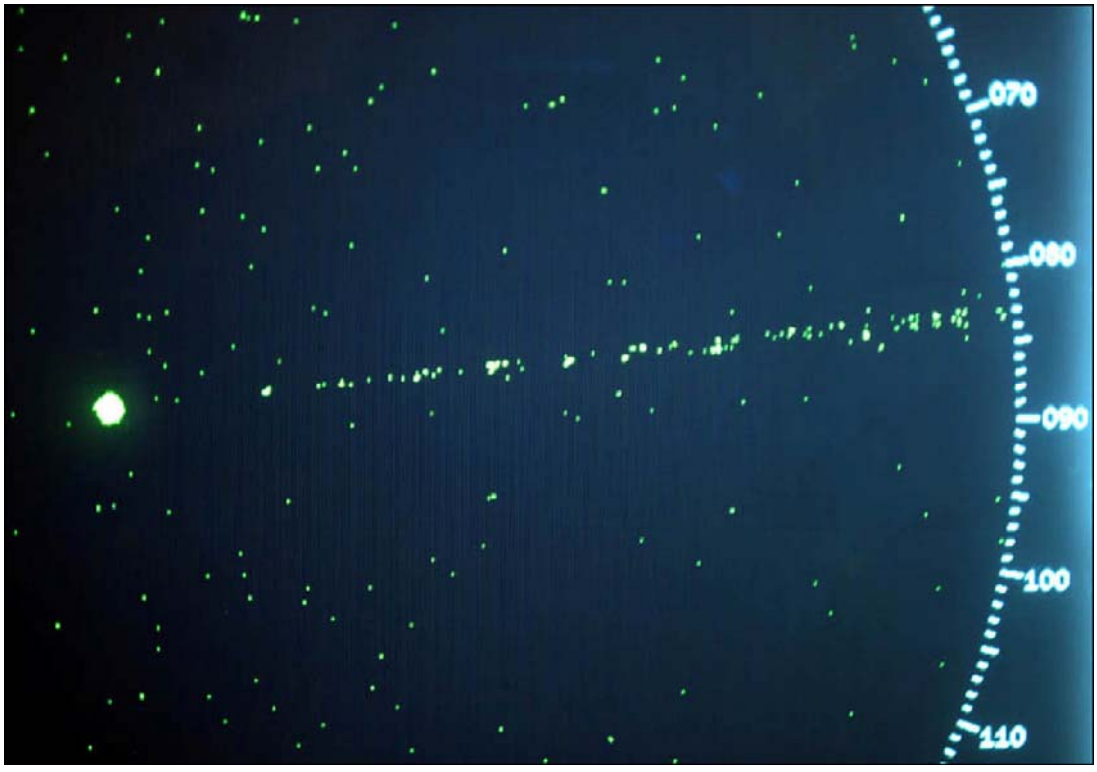


Figure 50. OFDM interference effect at *I/N*= +6 dB.

### *6.7.6.1 Radar F with Fluctuating Targets*

Interference tests were performed with the targets fluctuating in power as described in 2.4.1 of this report using an OFDM interference source. The results showed that there was a small gain in the target $P_d$ at low I/N levels when the target power fluctuated "upwards" (scans 1-5, 9-12, and 14 in Table 21). That is, the target $P_d$ increased because the target power was above the level that produced the $P_d$ of 0.90 percent. However, this effect has limits. When the *I/N* value was around 0 to 3 dB, an increase in target power *did not* further enhance the target $P_d$ even when the target power increased to the higher values in Table 3. This was the effect even when the target power was increased to its maximum Swerling value of 7.3 dB (scan 14 in Table 21) above the baseline power level.

Conversely, when the target power fluctuated "down" from the baseline value that produced the $P_d$ of 0.90 percent, the targets were already weak and the interference made them disappear. In fact, when the target power was only 1.7 dB (scan 7 in Table 21) below the baseline state, the targets were severely degraded without interference. When the interference was injected at low *I/N* levels, the targets disappeared.

Table 28. Radar F Responses to Interference*

| Interference Waveform | Effect at Given *I/N* Ratio (dB) | | | | | | | | | |
|---|---|---|---|---|---|---|---|---|---|---|
| | -9 | -6 | -3 | 0 | +3 | +6 | +9 | +12 | +20 | +40 |
| Chirp 1 | None | none | none | none | none | none | none | none | none | none |
| Chirp 2 | None | None | None | None | None | None | None | None | None | none |
| Chirp 3 | None | None | None | None | None | None | None | None | None | None |
| Chirp 4 | None | None | None | None | None | None | None | None | None | None |
| Chirp 5 | None | None | None | None | None | None | None | None | None | None |
| Chirp 6 | None | None | None | None | None | None | None | None | None | None |
| Chirp 7 | None | None | None | None | None | None | None | None | None | None |
| Phase1 | None | None | None | None | None | None | None | None | None | None |
| Phase2 | None | None | None | None | None | None | None | None | None | None |
| Unmod pulsed 1 | None | None | None | None | None | None | None | None | None | None |
| Unmod pulsed 2 | None | None | None | None | None | None | None | None | None | None |
| Unmod pulsed 3 | None | None | None | None | None | None | None | None | None | None |
| Unmod pulsed 4 | None | None | None | None | None | None | None | None | None | None |
| Unmod pulsed 5 | None | None | None | None | None | None | None | False targets | strobe | strobe |
| Unmod pulsed 6 | None | None | None | None | None | None | None | False targets | strobe | strobe |
| Unmod pulsed 7 | None | None | None | None | None | None | False targets | False targets | strobe | strobe |
| OFDM | $P_d$= 0.93 | $P_d$= 0.90 | $P_d$= 0.85 | $P_d$= 0.83 | False targets | strobe | strobe | strobe | strobe | strobe |

* When no effect is indicated, the interference $P_d$ was within ±3 percent of the baseline $P_d$, and the number of false targets or "speckle" was at the baseline state as well.

The results of these tests with fluctuating targets have demonstrated that:

- Trying to establish interference criteria using fluctuating targets is pointless because changing the *I/N* value while changing the target power only leads to an uncontrolled experiment without a baseline measure or state;

- Adding target power to the radar can only help at low values of *I/N* levels even when the target power is increased to 7.3 dB above the baseline state. Once the interference causes a high increase of false targets and strobing, the radar cannot recover the targets even when the target power increases to its maximum Swerling Case 1 value.

Both of these points are very important and the second one is a key element for radar analyses. There is currently a misconception that by merely increasing the target power, a radar can overcome any level of interference. These test results have disproved that assumption. It *would* be true if target power were adjusted along with detection levels, but that would tantamount to building a new radar with a more powerful transmitter or a bigger antenna.

## 6.8 UWB Interference Tests on a Maritime Radar

This section describes the results of UWB interference susceptibility tests that were performed on maritime radionavigation Radar A. The purpose of the tests was to inject impulse UWB interference into the radar's receiver and observe and document the degradation of the radar's performance as the power level of the UWB signal in the radar receiver was varied. The tests were performed closed-loop, as described above.

### 6.8.1 UWB Interference Test System

The test system and target generator were the same as described for Radar A in Section 6. These tests used UWB signals with prfs of 100 kHz, 1 MHz, and 10 MHz. The UWB transmitter unit that was used for these tests was supplied by the Time Domain Corporation. This UWB device had been used in previous UWB/GPS testing by NTIA. The UWB pulser was connected to an AWG that provided triggering for dithered and non-dithered UWB waveforms. The RF outputs of the target generator and the UWB pulser were combined and connected to a cable-to-waveguide adapter that was then connected to the mixer input of the radar receiver. In effect, this removed the radar antenna from the system but still allowed for normal operation of the radar. The IF output of the radar was monitored with a spectrum analyzer by connecting to a test point on the receiver circuit board.

### 6.8.2 UWB Interference Test Parameters

The RF power output of the target generator system was adjusted so that the target $P_d$ was as close as possible to 0.90 without UWB interference being present. This value was approximately -90 dBm at the waveguide input of the receiver. Figure 42 shows a photograph of the baseline operating state of the radar. The targets appear along a radial, and local clutter returns from buildings are visible on the radar display.

The IR feature of the radar was activated for these tests. The STC and FTC functions were turned off and the auto gain function was selected. This configuration is a normal operating mode for the radar, as confirmed by USCG personnel who are certified to operate the radar on Coast Guard vessels.

### 6.8.3 UWB Test Method

The power of the target generator was held at a constant -90 dBm at the waveguide input. The UWB signal power was varied with an adjustable attenuator and was gated to coincide with the target radial. This simulated the radar's mainbeam sweeping across a UWB device. The radar display was then observed for interference effects. UWB interference effects were documented with digital photographs of the ppi. Between tests, the interference power was reduced until the radar returned to baseline operation.

### 6.8.4 UWB Test Results

The test results for each UWB prf are discussed below. Overall, the results showed that for moderate UWB power levels, the UWB interference caused strobes along the radial of the targets. The targets were impossible to distinguish within the strobes when the UWB interference occurred. As the UWB power was decreased, the strobes become less intense and at some point transformed into numerous false targets. So the effect of the UWB interference at low levels was an increase in the false targets, while at higher levels the desired targets were masked altogether. Figures 51-65 show the PPI display under various interference circumstances. The results showed that for dithered UWB waveforms, independent of the UWB prf, the maximum allowable UWB power in the radar receiver which would let the radar operate at the baseline performance level was about -115 dBm/MHz (root mean square (RMS) average power detected).

### 6.8.5 Effect of UWB Interference on Synthetic Targets

Figures 66-68 show radar PPI displays with synthetic targets in the presence of UWB interference. As shown in those figures, UWB interference was observed to suppress synthetic targets on desired targets while generating false synthetic targets at other locations on the display. Synthetic target generation did not perform well in the presence of UWB interference.

### 6.8.6 Comparison to *I/N* Values

The noise power of the radar receiver for an IF bandwidth of 3 MHz and noise figure of 5.3 dB is -104 dBm. In a 1-MHz bandwidth this is about -109 dBm/MHz. The maximum allowable UWB power was about -115 dBm/MHz, equating to an *I/N* of -6 dB to -7 dB. This value matches the interference threshold used in the UWB analyses in [23].

### 6.8.7 Additional Observations on UWB Interference Effects

Adding more power to the desired targets, i.e., making the targets "stronger," did not help the radar overcome the effects of UWB interference. When the target power was increased by 3 dB the UWB interference still caused false targets to appear. This effect is shown in Figures 66-67. The UWB interference did not resemble clutter returns.

## 6.9 Summary of Interference Effects on Maritime Radars

The results of interference tests on maritime radionavigation radars show that when interference with the characteristics of digital communication signal modulations is coupled into these radars at *I*/*N* levels of -6 dB, some of the radars begin to show degradation effects such as dimmed targets, lost targets, or false targets. For maritime radars with logarithmic IF amplifier/detectors (radars A, C, E, and F), these effects began to be manifested at slightly higher *I/N* levels; the targets were either not visible or dimmed at the *I*/*N* levels of -3 dB and -6 dB, as indicated in Tables 24-27 (and Table 28 for OFDM interference into Radar F). The effects of interference on Radars A, C, and E were maximized (i.e., the targets had disappeared from the PPI and no other effects were visible) at *I*/*N* levels between 0 dB and -10 dB. For Radars B and D (which use a logarithmic amplifier and separate video detector), at the *I*/*N* level of -6 dB, the target $P_d$ values dropped below the baseline 1-sigma error. These test results show that at an *I*/*N* of -10 dB, for Radars A, C, and E, the targets were no longer dimmed and for radars B and D, the target $P_d$ values were slightly below the baseline 1-sigma error. For Radar A the synthetic targets required about 2 dB to 3 dB of additional desired signal power compared to the raw-video targets to obtain the same $P_d$ level when operating at a minimum detectable signal level, but the appearance of the targets was not brighter on the PPI display, as shown in Figure 66.

The test results for Radars B, D, and F show that the maritime radars can withstand low-duty cycle, asynchronous pulsed interference at extremely high (+30 dB to +40 dB) *I*/*N* levels due to the inclusion of radar-to-radar interference mitigating circuitry and/or signal processing. The radar-to-radar interference mitigation techniques of scan-to-scan and pulse-to-pulse correlators and CFAR processing [18, 19] have been shown to work well. But the test results show that the same techniques do not mitigate continuous emissions that appear noise-like or CW-like within the radar receiver.

As most maritime radionavigation radars in the 2900-3100 and 9200-9500 MHz bands are very similar in design and operation, it is expected that these test results should apply equally well to other models of marine radars in these bands.

Determining an exact boundary for acceptable levels of interference effects for these types of radars can be somewhat subjective due to such variables as the eyesight and experience of radar operators, possible fatigue due to staring at PPI displays for long periods, and grading of the brightness and distinguishability of the targets relative to the background noise on the PPI displays. But the design of these radars permits no alternative test techniques, and the tests as run do replicate actual operational conditions.

Experienced, trained radar operators may be better able to discern real targets from false targets, interference and/or clutter than inexperienced ones. But for these tests, the radar manufacturers provided radar design engineers and the UK Maritime and Coast Guard Agency (MCA) provided experienced radar operators and instructors. Those personnel all concurred with the results and conclusions of these tests.

The radar could only marginally process out UWB interference and then only at low power levels such as -115 dBm/MHz for a 1-MHz prf signal. This was probably due to the high prf of the UWB signals.[26] UWB interference did not resemble clutter returns.

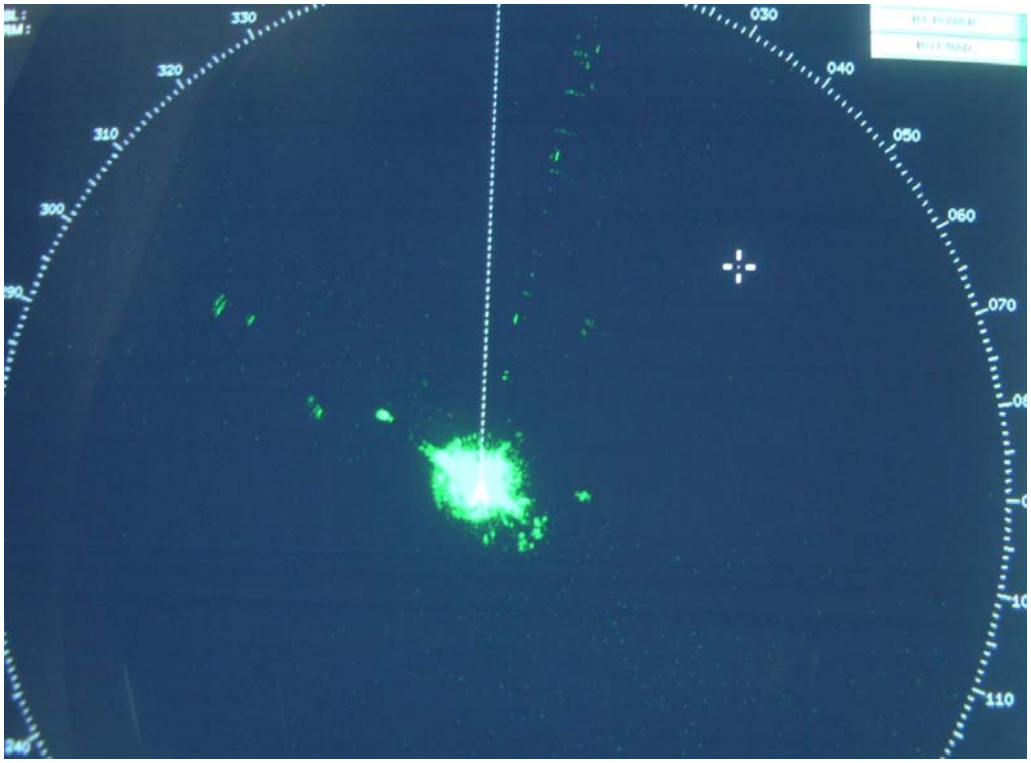


Figure 51. Radar A PPI display with 100-kHz prf gated UWB signal at -85 dBm/MHz (RMS detection).

[26] At high prf values, there is a high probability that a UWB pulse will occur at the beginning of the IR gate and that another UWB pulse will occur at the end of the IR gate.

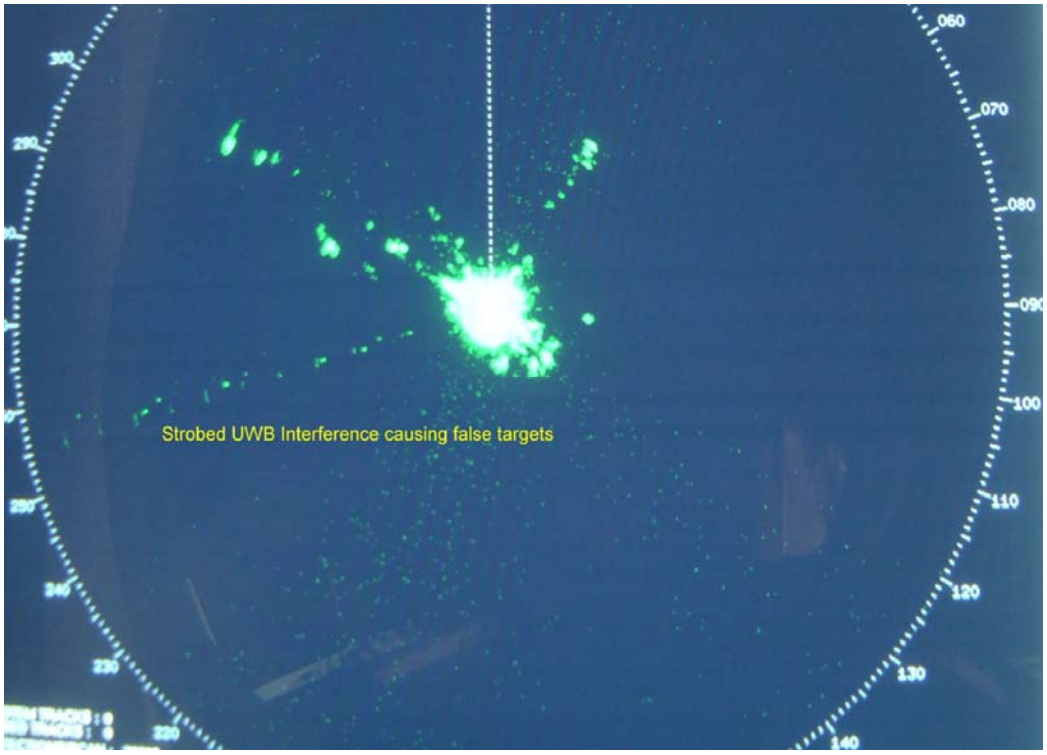


Figure 52. Radar A PPI display with 100-kHz prf gated UWB signal at -95 dBm/MHz (RMS detection).

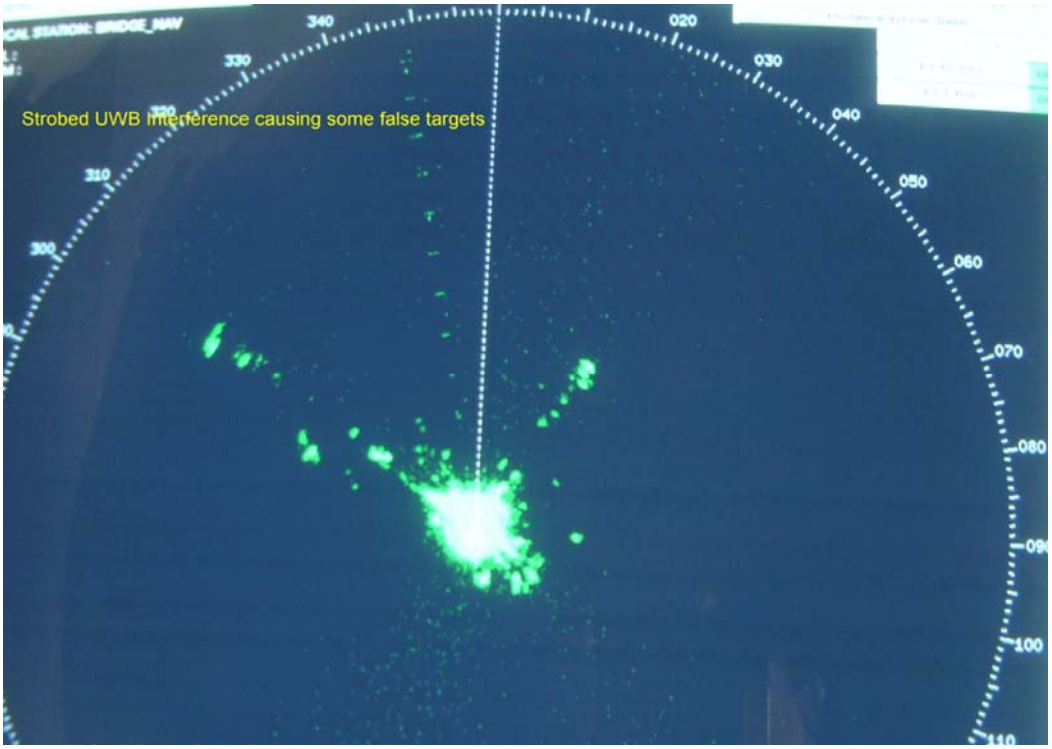


Figure 53. Radar A PPI display with 100-kHz prf UWB signal at -105 dBm/MHz (RMS detection).

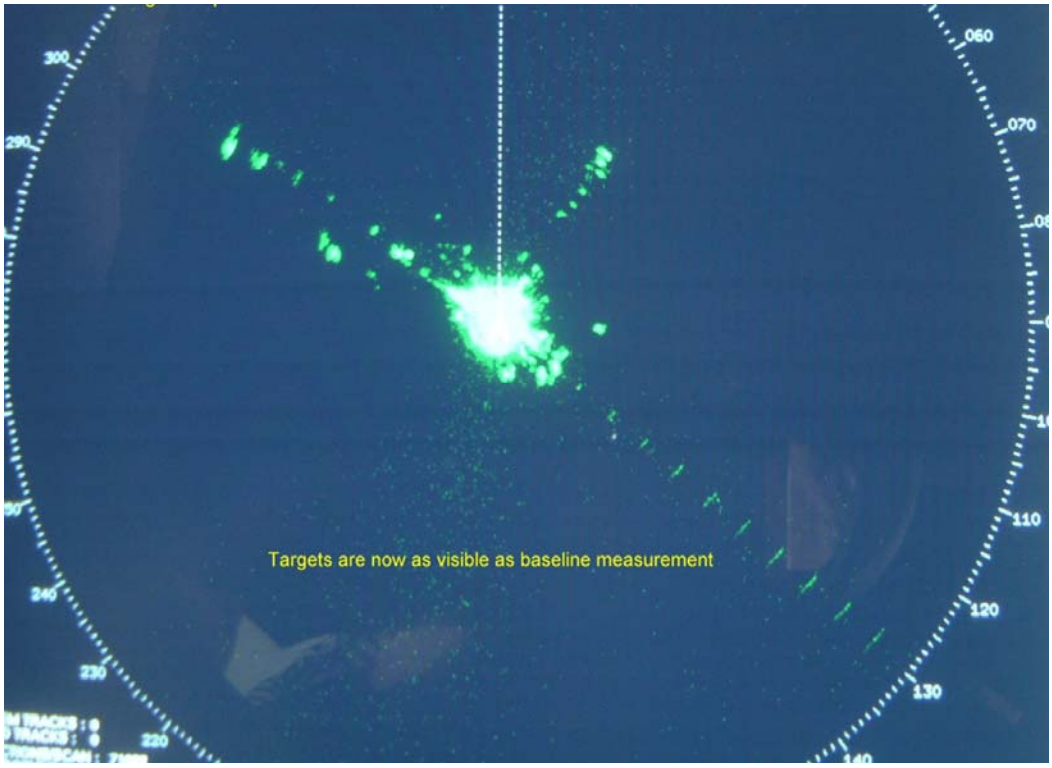


Figure 54. Radar A PPI display with 100-kHz prf UWB signal at -110 dBm/MHz (RMS detection).

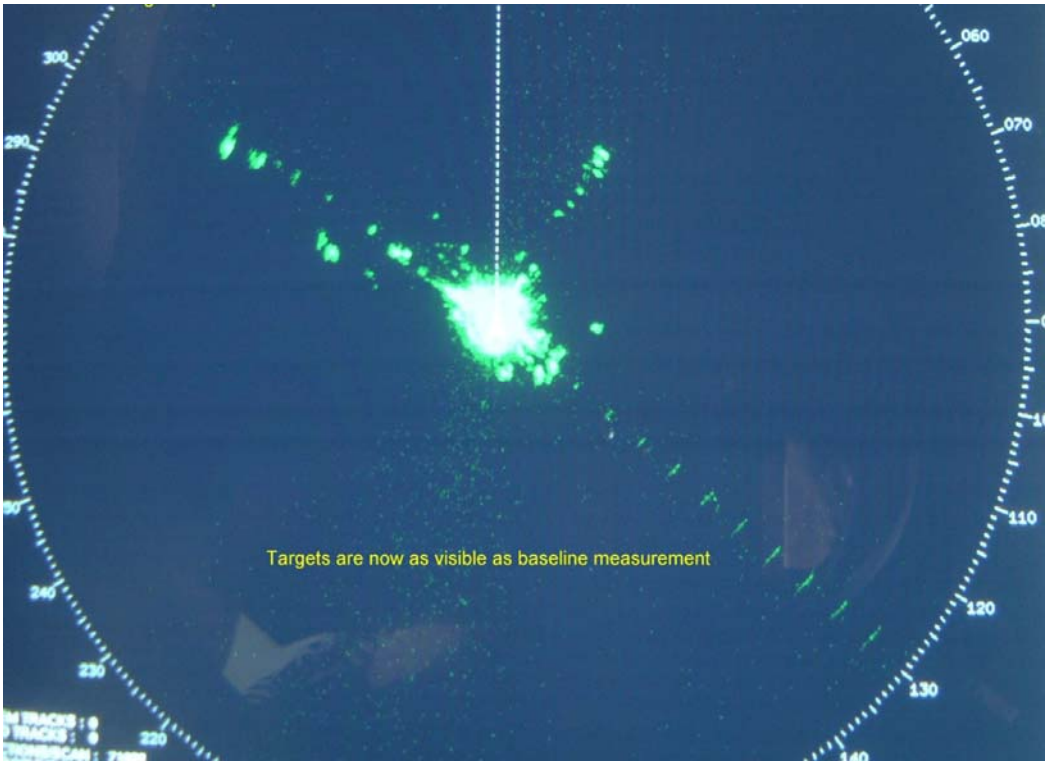


Figure 55. Radar A PPI display with 1-MHz prf UWB signal at -115 dBm/MHz (RMS detection).

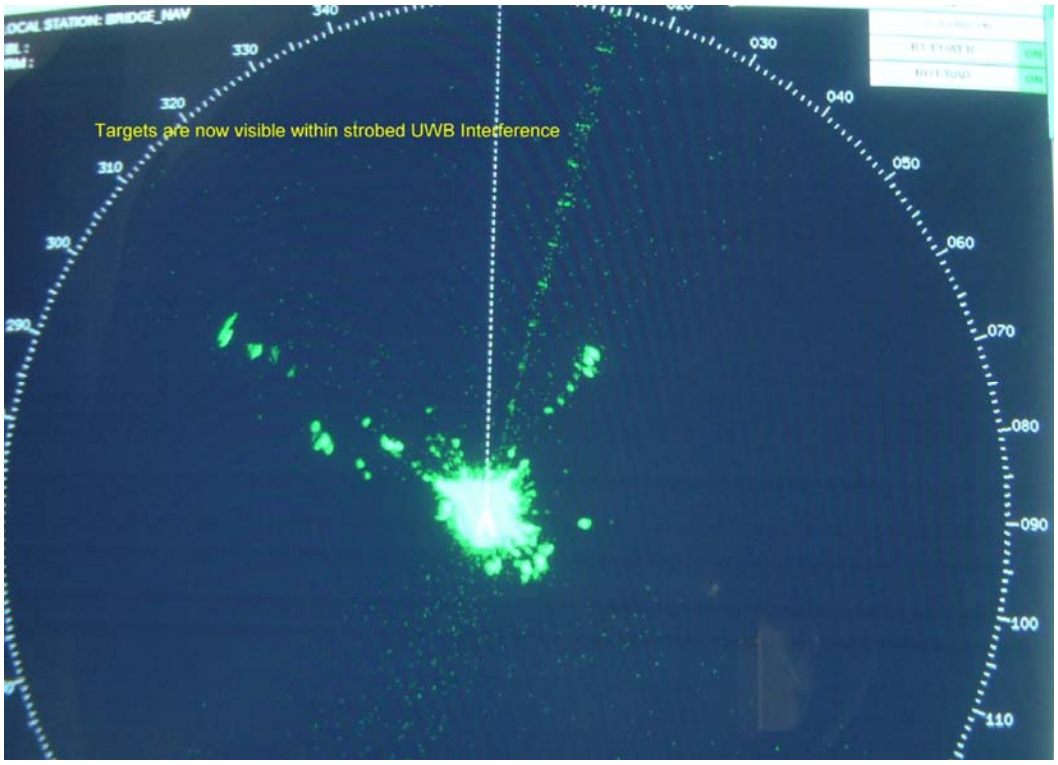


Figure 56. Radar A PPI display with 1-MHz prf UWB signal at -110 dBm/MHz (RMS detection).

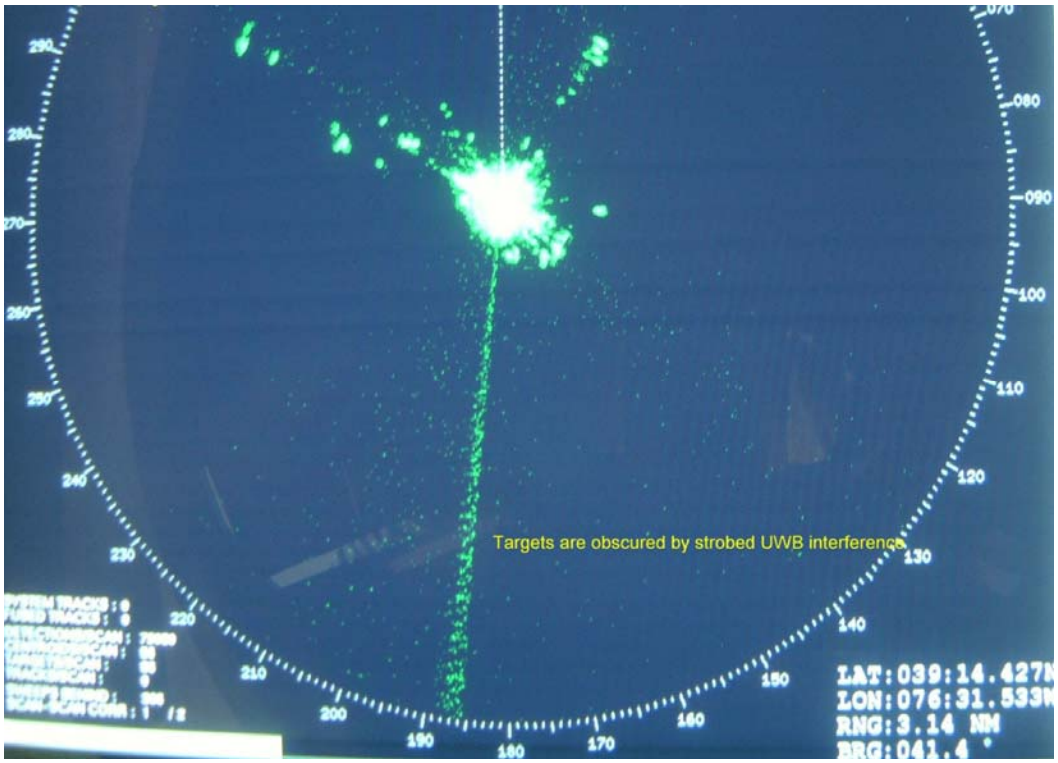


Figure 57. Radar A PPI display with 1-MHz prf UWB signal at -105 dBm/MHz (RMS detection).

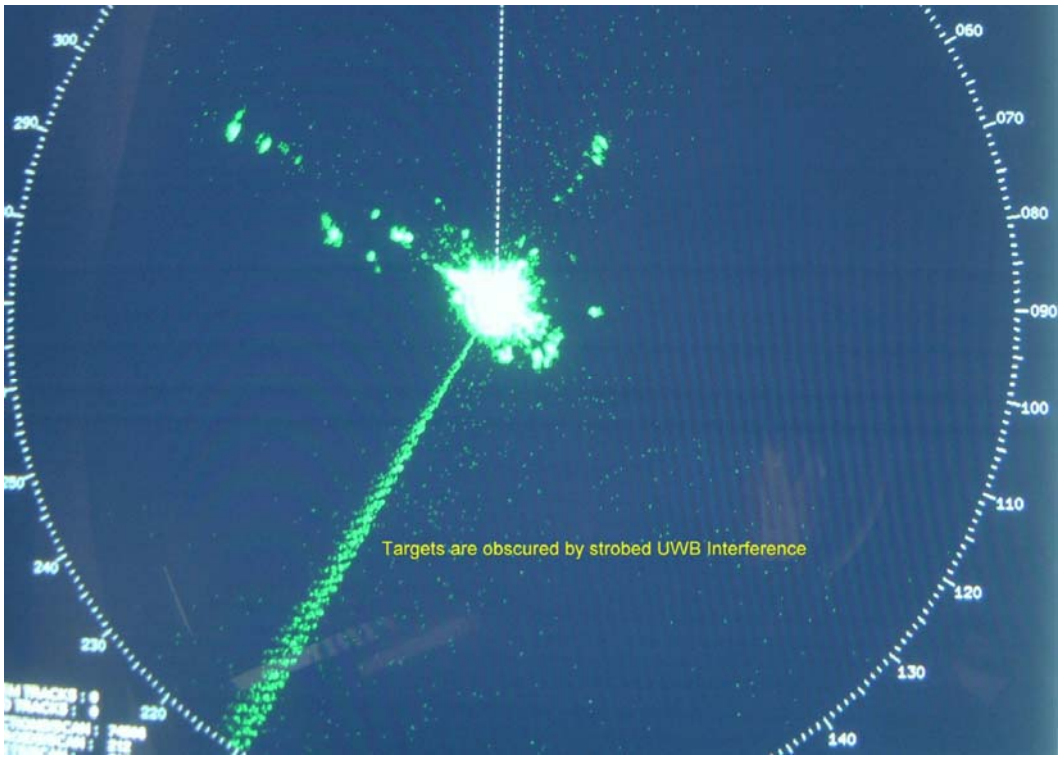


Figure 58. Radar A PPI display with 1-MHz prf UWB signal at -95 dBm/MHz (RMS detection).

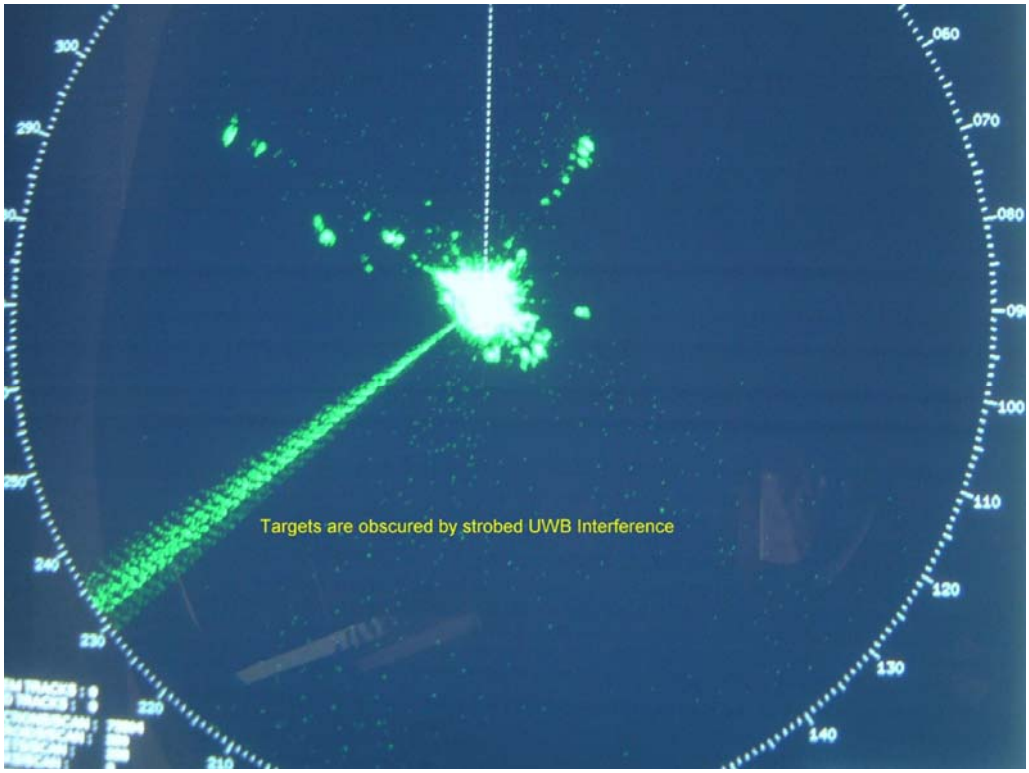


Figure 59. Radar A PPI display with 1-MHz prf UWB signal at -85 dBm/MHz (RMS detection).

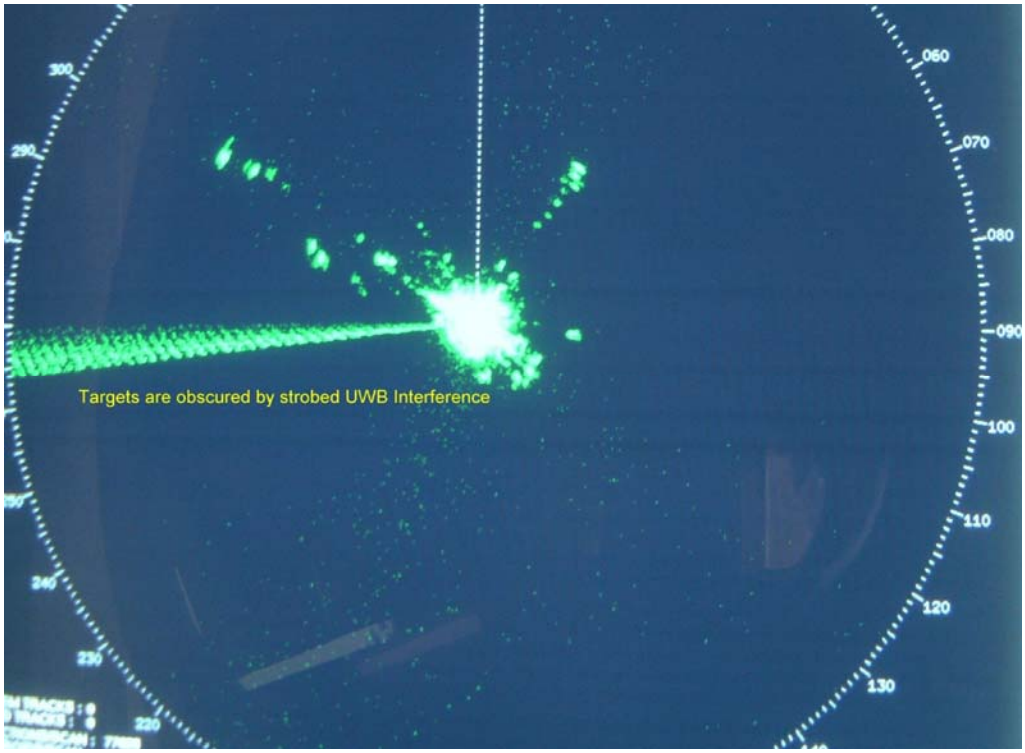


Figure 60. Radar A PPI display with 1-MHz prf UWB signal at -75 dBm/MHz (RMS detection).

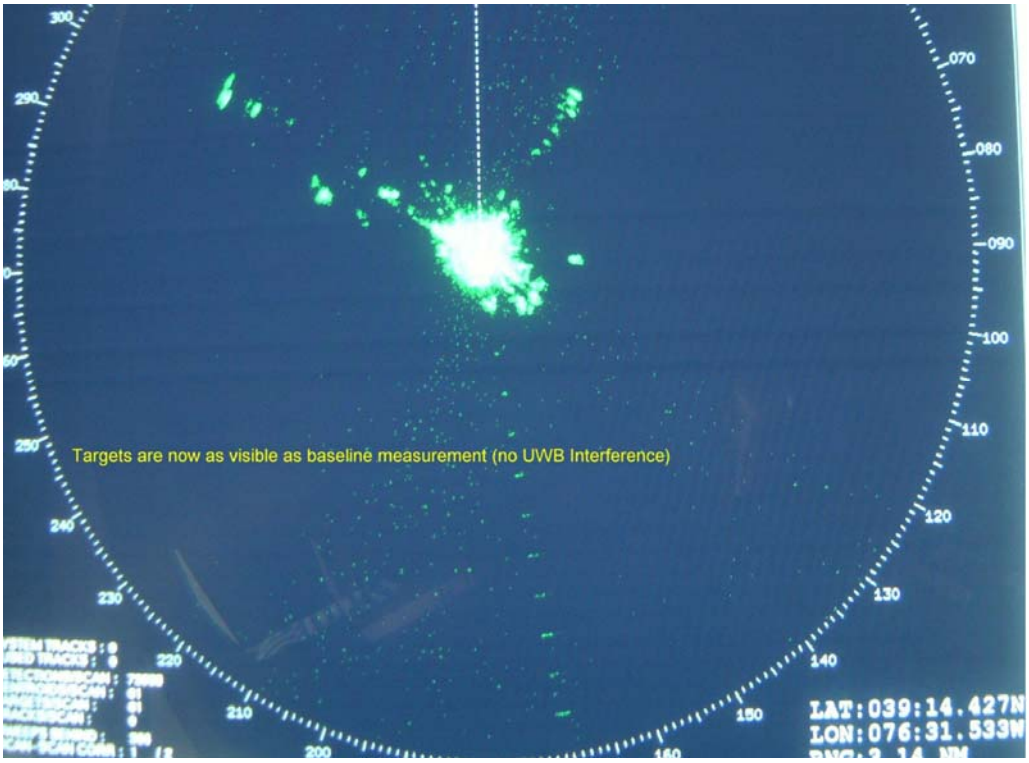


Figure 61. Radar A PPI display with 10-MHz prf UWB signal at -116 dBm/MHz (RMS detection).

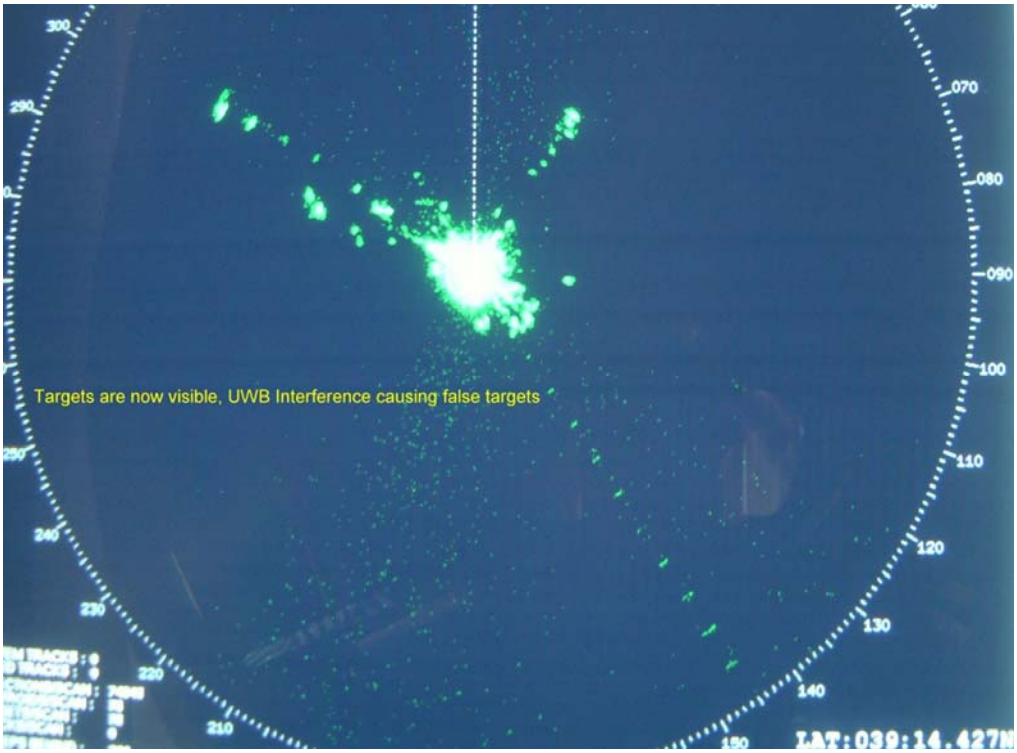


Figure 62. Radar A PPI display with 10-MHz prf UWB signal at -111 dBm/MHz (RMS detection).

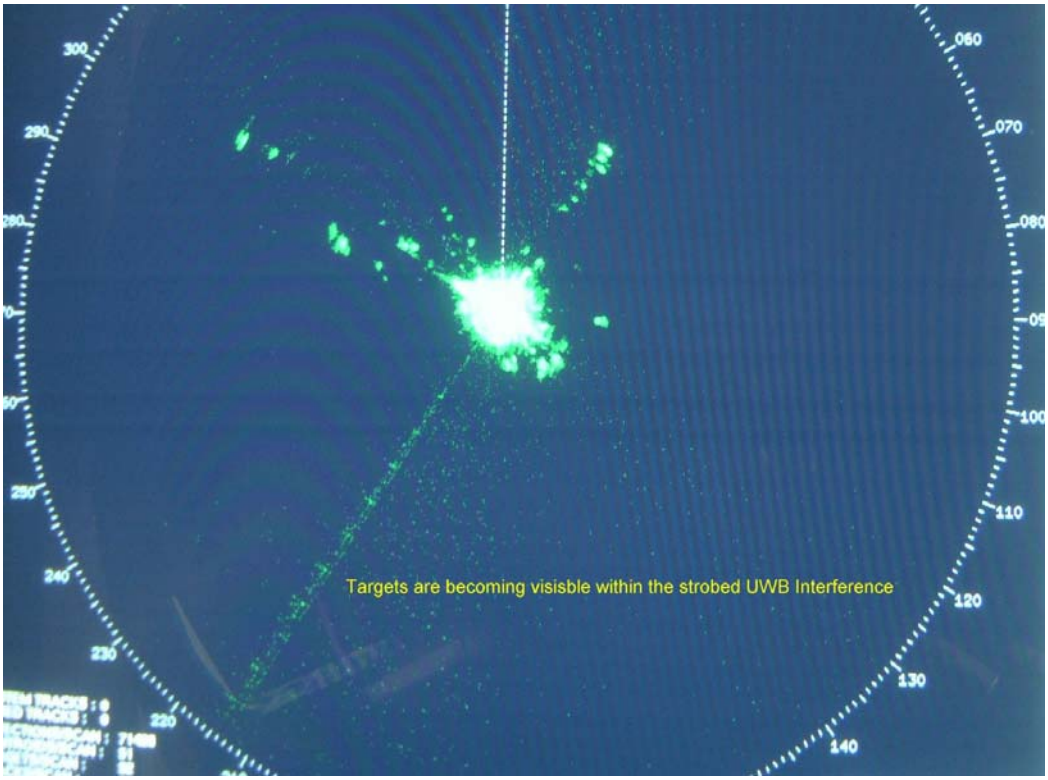


Figure 63. Radar A PPI display with 10-MHz prf UWB signal at -106 dBm/MHz (RMS detection).

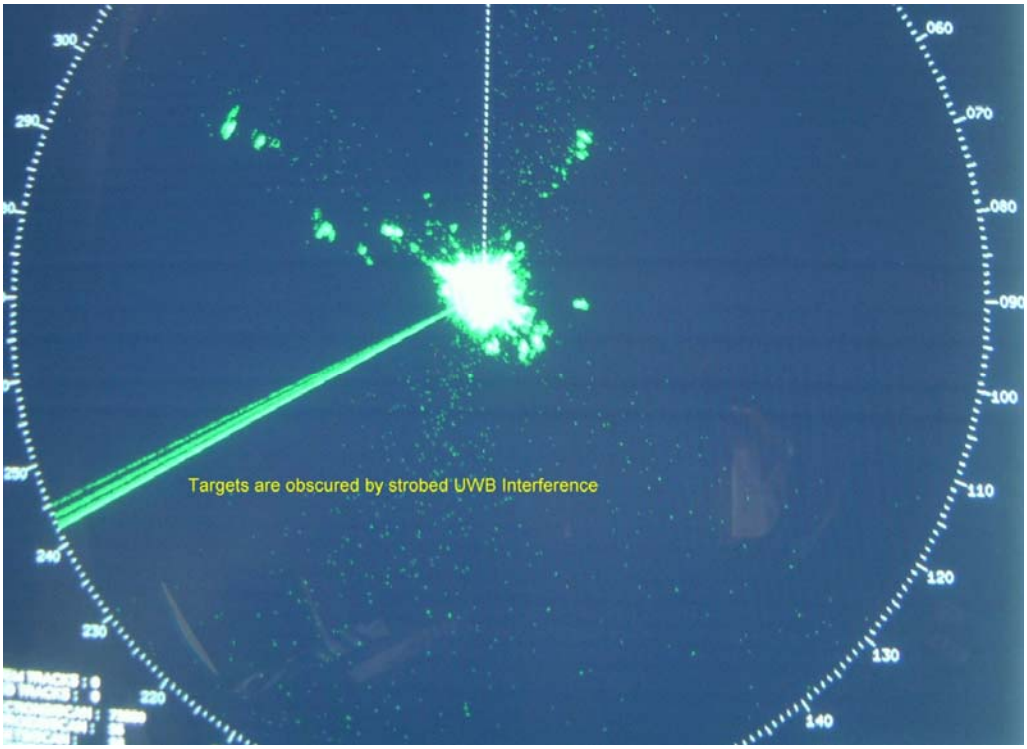


Figure 64. Radar A PPI display with 10-MHz prf UWB signal at -86 dBm/MHz (RMS detection).

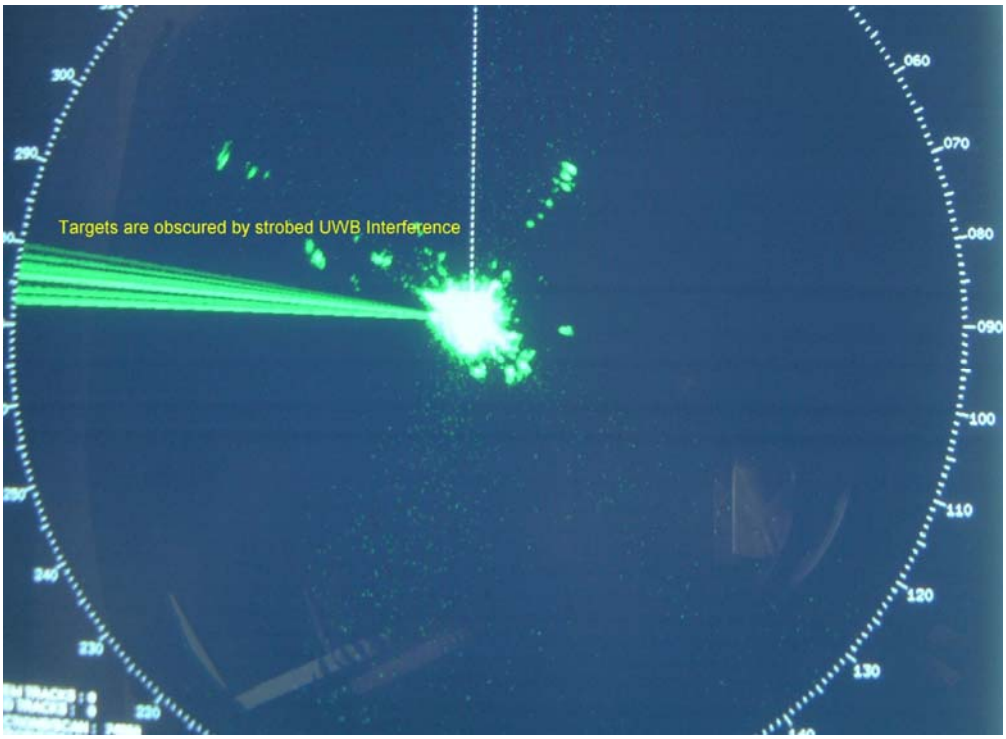


Figure 65. Radar A PPI display with 10-MHz prf UWB signal at -66 dBm/MHz (RMS detection).

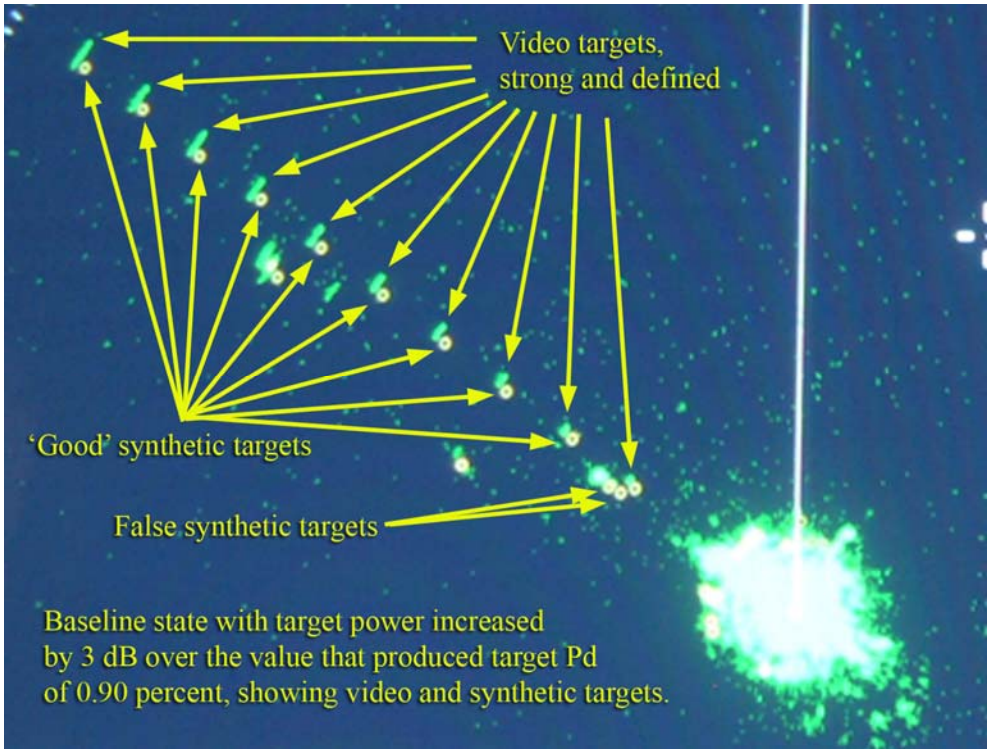


Figure 66. Radar A PPI display with high power video targets and synthetic targets, baseline state (no interference). Compare to Figure 67, which shows more false targets when UWB interference was injected.

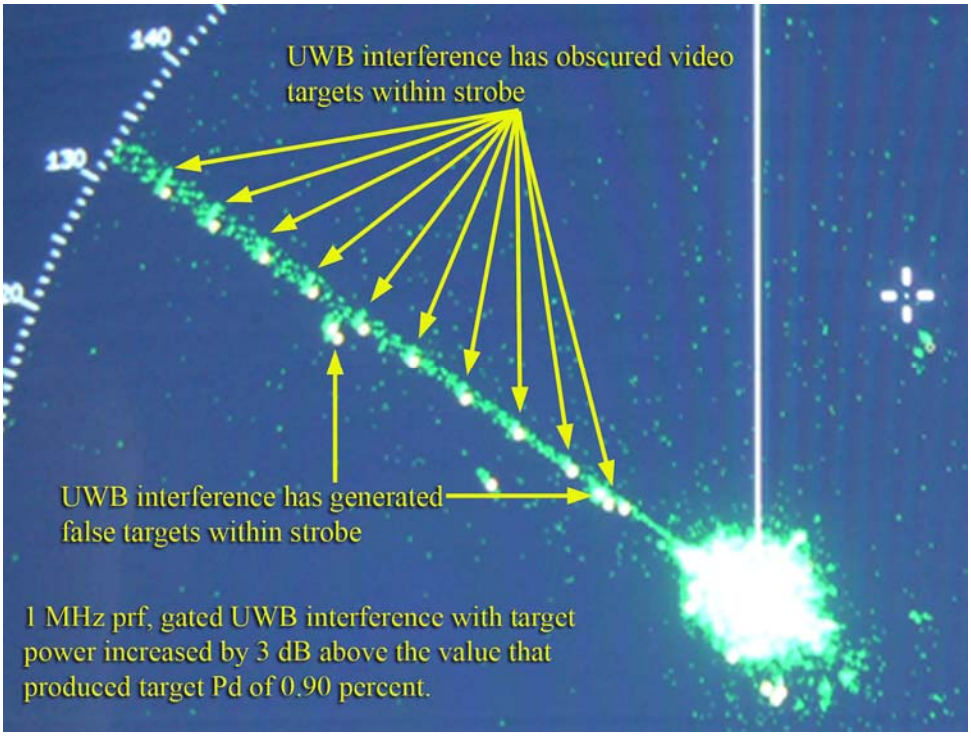


Figure 67. Radar A PPI display with 1 MHz UWB interference suppressing desired raw video targets and synthetic targets while generating false synthetic targets. (Compare to the baseline state of Figure 66.)

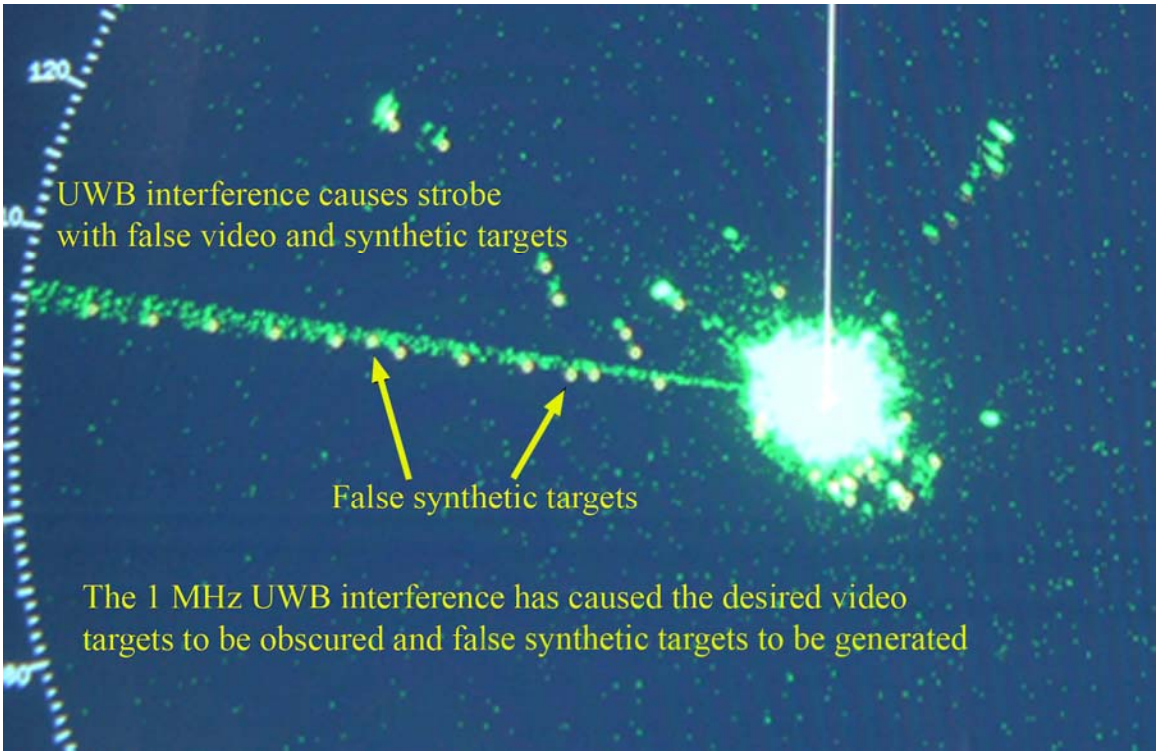


Figure 68. Radar A PPI display showing a loss of video targets and generation of false synthetic targets due to 1-MHz UWB interference.

# 7 INTERFERENCE MEASUREMENTS ON AN AIRBORNE METEOROLOGICAL RADAR

## 7.1 Introduction

This report describes the methodology and results of interference tests on a 9-GHz airborne weather radar. Interference waveforms were injected into the radar at its RF frequency and the effects of the interference were recorded as a function of *I/N* ratio in the radar receiver IF stage. Interference waveforms that were tested included: OFDM, unmodulated pulsed, chirped pulsed, phase-coded pulsed, and BPSK.

## 7.2 Characteristics of the Airborne Weather Radar

The pertinent technical characteristics of the airborne radar are shown in Table 29. The radar is widely utilized on large-capacity, multi-engine turboprop transport aircraft, and it may operate on large jet aircraft in the future. It has functions for identification of active precipitation and identification of wind shear. It has operational modes for short-range, medium-range, and long-range weather surveillance.

Table 29. Characteristics of the Airborne Weather Radar

| Radar Characteristic | Value | |
|---|---|---|
| Radar Modes | Weather surveillance and wind shear alert | |
| Frequency Agility Range | 9310-9410 MHz, spaced every 5 MHz | |
| Frequency Used for Testing | 9335 MHz | |
| Transmitter Type | Solid state | |
| Transmitter Peak Power | 10 kW (?) | |
| Pulse Modulations | Unmodulated pulses (short range)<br>5-Chip Barker Coded (medium range)<br>13-Chip Barker Coded (maximum range) | |
| | Minimum range | Maximum range |
| Pulse Repetition Rates | 2000 pps | 230 pps |
| Pulse Width Range | 0.19 μs | 234 μs |
| IF Bandwidth Range | 5 MHz | 52 kHz |
| Antenna Type | Gimbaled, flat-plate slotted array | |
| Antenna Gain | +32 dBi | |
| Antenna Sector Scan Angular Range | ±15° (minimum), ±135° (maximum) | |
| Antenna Sector Scan Rate | 60°/sec | |
| Antenna Beamwidth | 2.7° horizontal, 4° vertical | |
| Radar Receiver Noise Figure | 5 dB | |
| Radar Output | Color-coded display, with colors based on the strength of echo returns | |

The radar normally operates with automatic frequency agility, hopping among twenty frequencies across 100 MHz of spectrum between 9310-9410 MHz. Available frequencies are spaced 5 MHz apart. During frequency-agility operations, the radar changes frequency from pulse to pulse. Frequencies are selected pseudo-randomly, with a uniform distribution. The frequency-hopping design is intended to minimize frequency-dependent effects in weather echo returns, as well as to enhance operational effectiveness in multi-radar environments. For the tests, the radar was operated in a single-frequency mode.

The radar transmitter generates RF pulses from a set of solid-state modules. The pulses are unmodulated in short-range operations, 5-chip Barker coded when the radar is operating at medium range, and 13-chip Barker coded when the radar is operating at long range.

The radar antenna is a flat-plate, slotted array that sector-scans on a mechanically gimbaled mount inside a radome on the nose of the aircraft. The elevation angle of the scanning (relative to horizontal) is manually controlled from the cockpit during flight.

The radar receiver is a conventional triple-stage heterodyne design in which the RF front-end LNA noise figure determines the noise figure of the entire receiver. The overall receiver noise figure is 5 dB. RF energy from the LNA is downconverted to the input frequency of the first IF stage, at 870 MHz. That signal is downconverted to the frequency of the second IF stage, at 90 MHz. The 90-MHz signals are processed through a quadrature modulator stage that produces *I-Q* outputs. Final downconversion brings the echo signals to baseband video between 0-50 MHz, where they undergo narrowband filtering to match operational pulse widths. Baseband video is detected and sampled with either an 8- or 11-bit A-D converter, depending upon the selected radar range scale. This radar utilizes a CFAR processor to reduce the effects of noise and clutter. Final IF bandwidths are adjusted automatically to match the radar pulse width (or sub-pulse width, in Barker-coded pulse modes). The portion of the radar IF that is significant for this report is shown schematically in Figure 69.

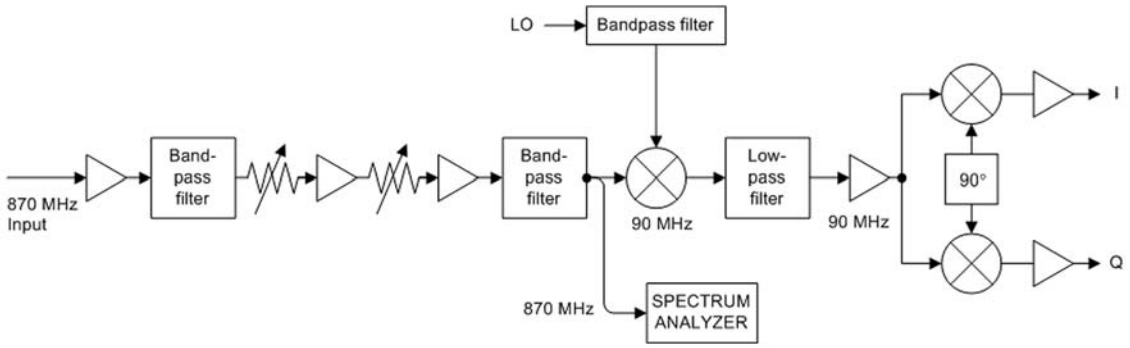


Figure 69. Block diagram of part of the airborne weather radar IF stage.

The radar video output is digitally processed into a color-coded, high resolution cockpit display. Colors correspond to the intensity of precipitation and wind shear ahead of the aircraft. An example of a weather surveillance display when the radar was operated in a receive-only mode, in which it was processing against only its internal noise, is shown in Figure 70. In this figure, as in the interference tests, the radar was operating in its 40 nm maximum range weather surveillance mode; the range rings are 10 nm apart.

The weather radar used in this study represents the current state-of-the art for this technology. Its hardware is highly integrated and modular, and its signal-processing software for echo returns is highly sophisticated. Its capabilities are believed to represent the best hardware and signal processing that are currently available in airborne platforms performing weather surveillance and wind shear detection missions.

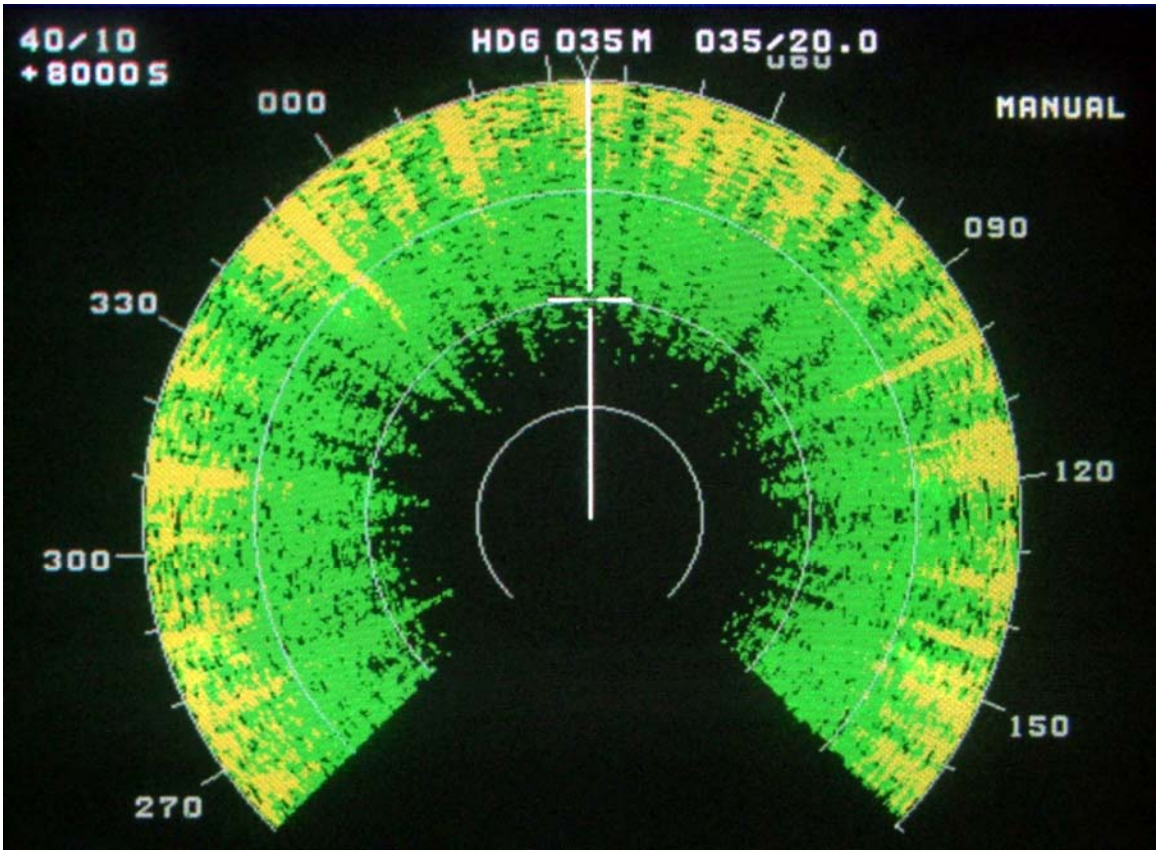


Figure 70. Example of the airborne weather radar display in the weather surveillance mode. There is no interference and the radar is running as receive-only. Green and yellow colors indicate that the receiver is processing only its internal noise.

### 7.3 Interference Measurement Protocol for the Airborne Weather Radar

The goal of the interference tests was to observe the effects of interference on a radar operational frequency as a function of both the type of interference and the interference-to-noise (*I/N*) ratio of the interference in the radar IF stage. Characteristics of the interference waveforms are listed in Table 30.

Table 30. Characteristics of Interference Waveforms for Airborne Weather Radar Tests

| Interference waveform | Pulse width (μs) | Sub-pulse or scaled width (μs) | Pulse repetition rate (pps) | Bandwidth or chirp width (MHz) | Duty cycle (%) |
|---|---|---|---|---|---|
| Chirped 1 | 10 | n/a | 750 | 10 | 0.8 |
| Chirped 2 | 10 | n/a | 750 | 50 | 0.8 |
| Chirped 3 | 13.6/1.65 | n/a | 750 | 660/80 | 0.8 |
| Phase coded 1 | 0.64 | 0.049 | 1600 | 1.56 | 0.1 |
| Phase coded 2 | 20 | 1.54 | 1600 | 0.05 | 3.2 |
| Unmod pulse 1 | 1 | n/a | 8000 | 1 | 0.8 |
| Unmod pulse 2 | 1 | n/a | 19000 | 1 | 1.9 |
| Unmod pulse 3 | 1 | n/a | 35000 | 1 | 3.5 |
| BPSK 1 | 10 | 2 | 2000 | 400/80 | 0.4 |
| BPSK 2 | 80 | 16 | 4500 | 400/80 | 7.2 |
| BPSK 3 | 10 | 17.7 | 515 | 45/80 | 0.91 |
| BPSK 4 | 10 | 1.7 | 5150 | 460/80 | 0.88 |
| OFDM | Continuous* | n/a | n/a | 20 | 100* |

*The OFDM interference was continuous within the 45-ms beam-scanning interval of the radar antenna.

Since most airborne weather radars operate on single frequencies, the primary goal of the tests on this radar was to observe the effects of interference when it was likewise operated on a single frequency. Some additional interference tests were also performed when the radar was operating in its wideband, frequency-agility mode. For both of the radar modes (single-frequency and frequency agility), the protocol for injecting interference and observing its effects was the same. The interference injection arrangement is shown as a block diagram in Figure 71.

The entire radar transmitter/receiver system (including the antenna and all of the radar hardware except for the cockpit monitor display) was mounted at the top of a 20-meter high tower, the tower itself being located on the summit of the highest hill in the area. The radar transmitter was turned off, so that the radar operated in a receive-only mode. The maximum range was set to 40 nmi to eliminate the effect of STC. Processed data were displayed on a cockpit monitor. When no interference was injected, the radar showed only the effects of its internal noise on the cockpit display, as shown in Figure 70.

Interference waveforms were generated with a vector signal generator (VSG)[27] that had been programmed for the waveform characteristics of Table 30. The RF output of the VSG was routed via a hardline from the radar control room to a directional coupler at the radar antenna. Thus the interference energy was injected into the radar ahead of the first RF front-end LNA. The interference energy passed through the radar receiver RF front end, was mixed down and passed through the multi-stage IF (as described above), was quadrature-demodulated to generate *I-Q* outputs, and then passed through a digital signal processor. The processor output was routed to the cockpit display in the radar control room.

[27] A programmable Agilent VSG, model 8267C.

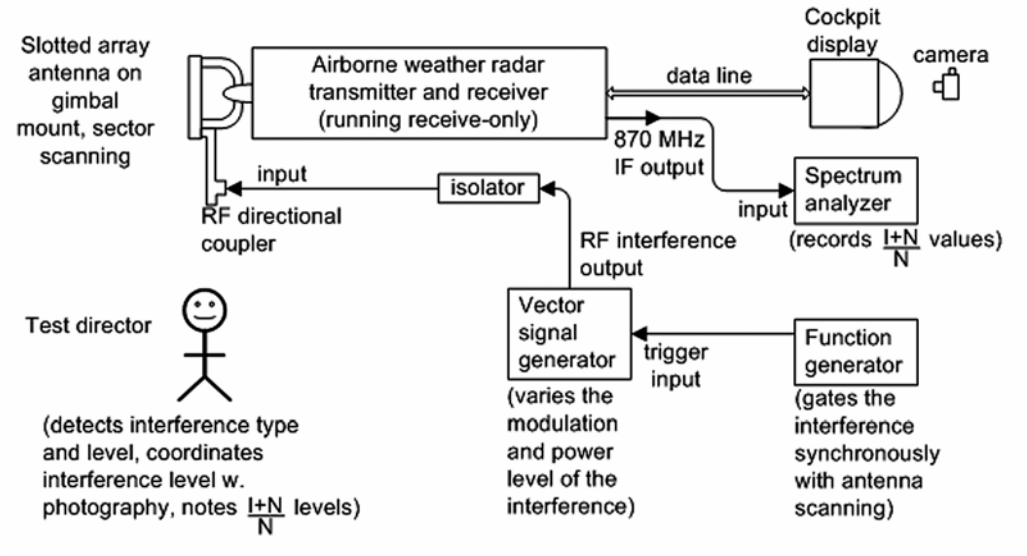


Figure 71. Block diagram of the airborne weather radar interference test setup.

Simultaneously with the observation of interference effects on the cockpit display, the *(I+N)/N* level was monitored on a spectrum analyzer connected to the first stage of the IF (tapped internally as depicted in Figure 1). Thus the effect of interference could be correlated directly with its measured *(I+N)/N* level.[28] An example of the spectrum analyzer data derived from the tap point in the radar IF stage is shown in Figure 72. The interference was gated on for 45-ms intervals, equal to the time required for the radar antenna beam to scan a single azimuth. This made the interference interval equal to the interval it would occupy if it were emitted by a point source in the antenna's far field.

During normal operations, the radar receiver gain automatically decreased from one complete sector scan (that is, a left-right plus a right-left antenna scan) to the next. Each change in receiver gain caused the *I/N* level to change by an equal number of decibels. The decrease from scan to scan was from one to two decibels. Thus, if the initial *I/N* level for an interference waveform was, e.g., +20 dB, that level would normally decrease from scan to scan to levels that would successively look like, e.g., +19 dB, +18 dB, +16 dB, +15 dB, +13 dB, etc. After a succession of about 12 of these decreases, (i.e., after about 12 complete sector scans), the radar automatically performed a complete recalibration of the receiver, the gain level reverted to its original, highest value, and the entire gain sequence was repeated.

[28] Subsequent to the tests, the measured *(I+N)/N* values were converted to the *I/N* values that are reported here.

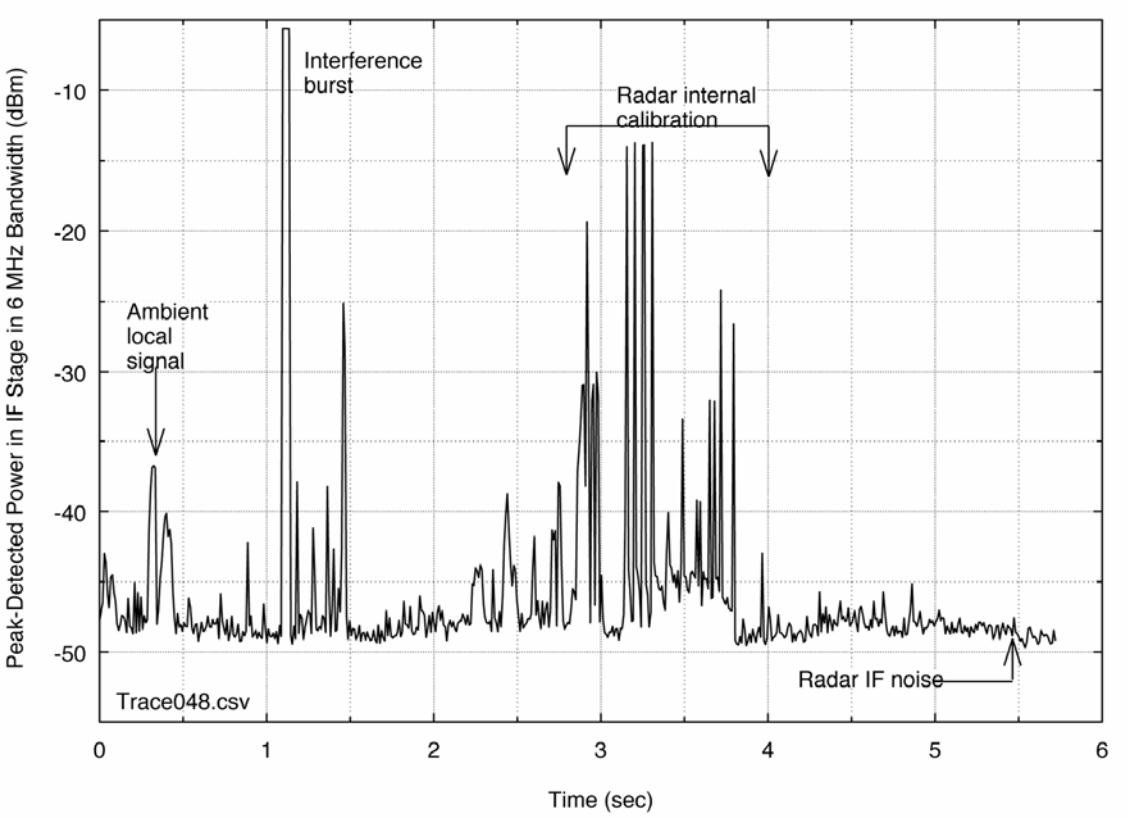


Figure 72. Interference burst as observed in the airborne radar IF stage. The trace is peak-detected, so the RMS level of the radar noise is 10 dB lower (relative to the amplitude of the interference burst) than shown here.

The test personnel used this built-in, gain-varying behavior of the radar to their advantage by generating a high *I/N* level from the VSG at the beginning of each radar gain sequence and then watching the decreasing effect of the interference on the cockpit display as the internal radar gain was automatically decreased from scan to scan. When no interference effects were observed on that display, the corresponding *I/N* level was noted. The VSG power output level was kept constant through each of the gain-variation sequences.

Because this type of radar does not process discrete targets, the criterion of probability of detection of targets is not applicable. Instead, its display was assessed qualitatively as a function of interference. The qualitative levels that were used were: strongly visible; marginally visible; barely visible; and no visible effect. Figures 73-75 show examples of the radar display when an interference effect was strong, marginal, and barely visible, respectively.

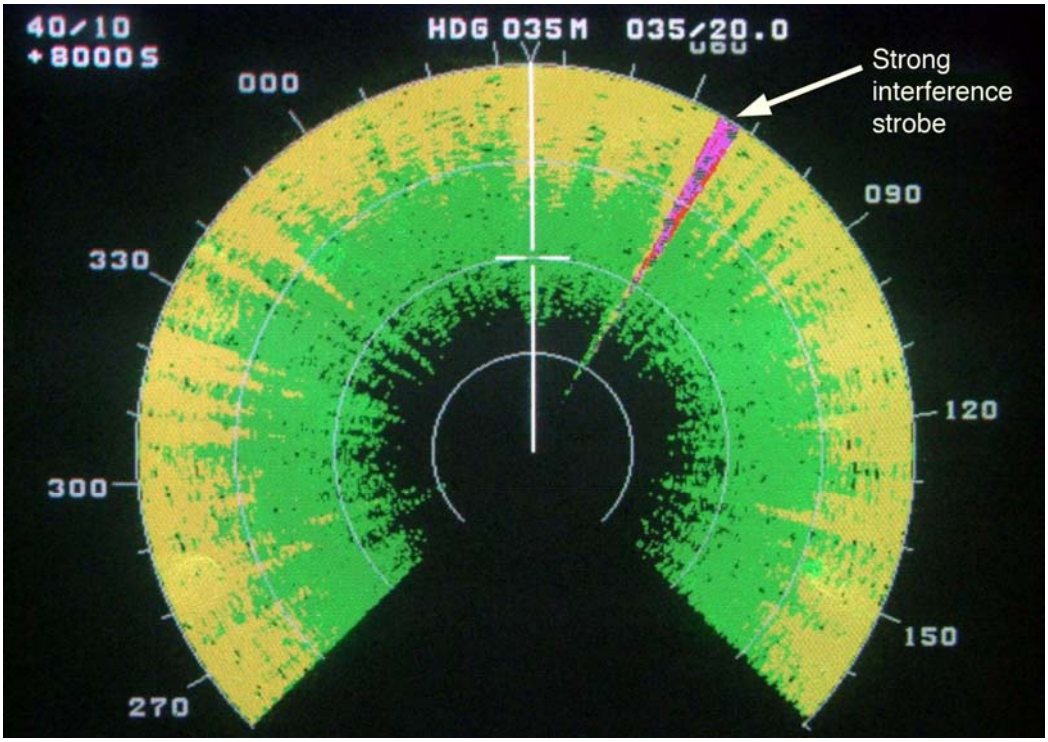


Figure 73. Example of a strongly visible interference strobe (caused by phase-coded waveform 2 at *I/N* = +60 dB).

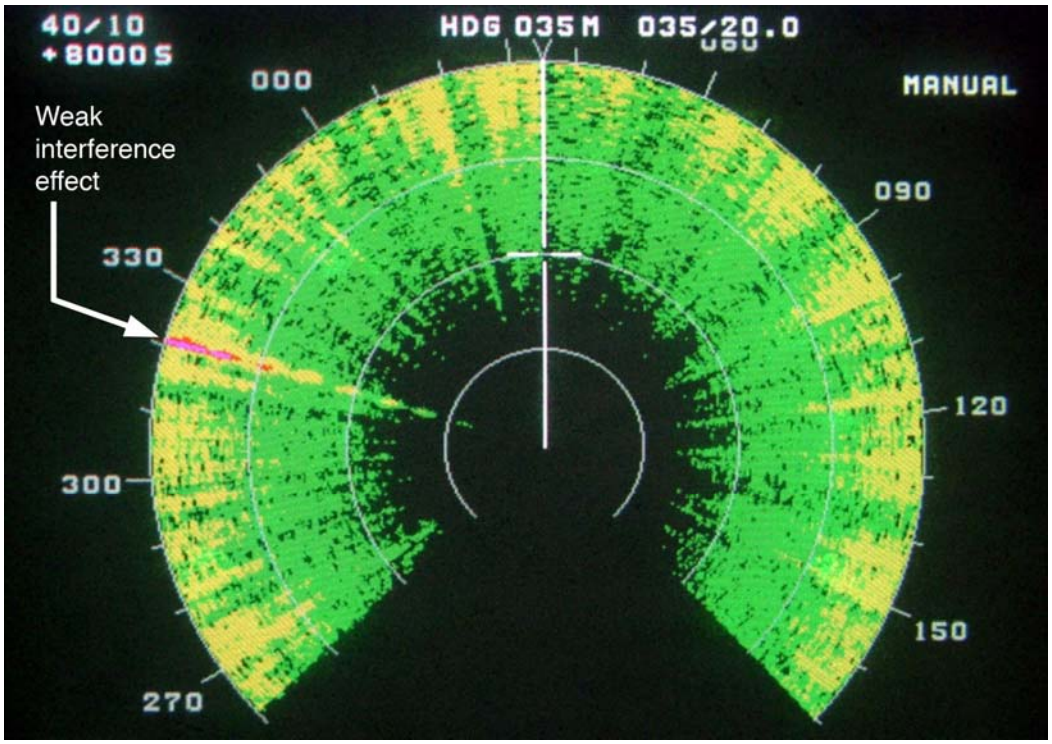


Figure 74. Example of a marginal interference strobe (caused by unmodulated pulse waveform 1 at *I/N* = +24 dB).

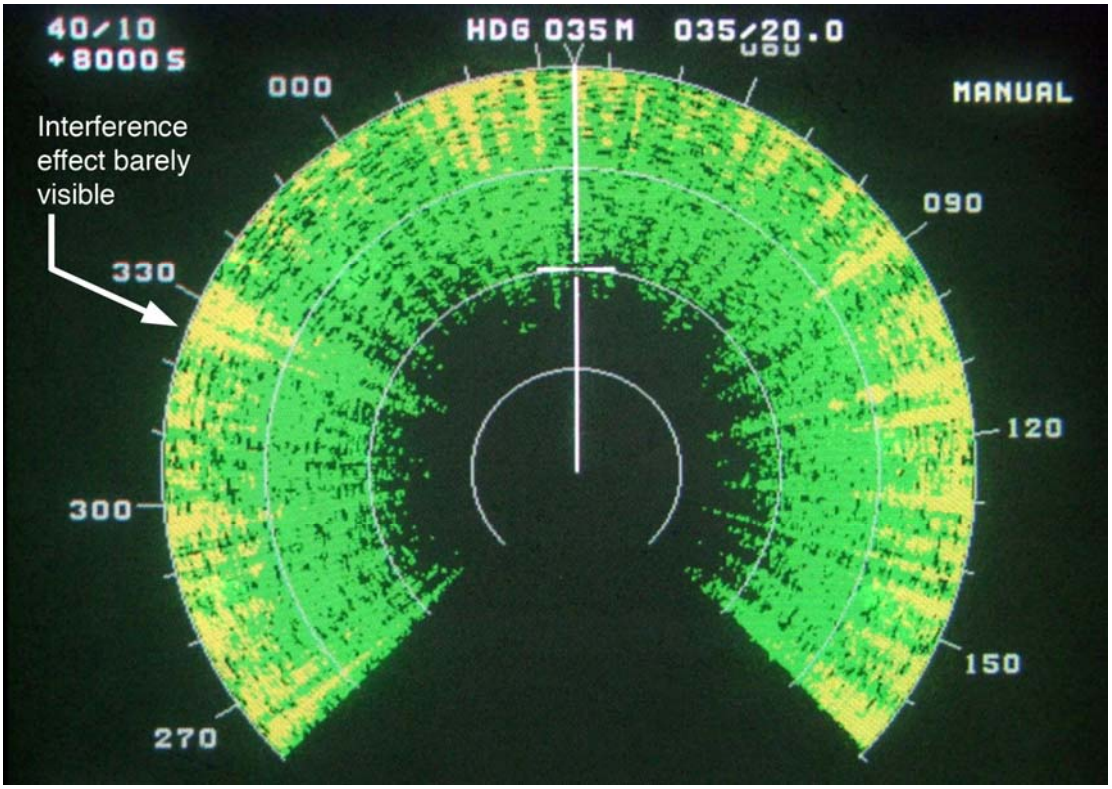


Figure 75. Example of barely visible interference (caused by unmodulated pulse waveform 1 at *I/N* = +20 dB.

### 7.4 Results of Interference Measurements on the Airborne Weather Radar

Results for the airborne weather radar in the single-frequency mode are summarized in Table 31. The results show that the chirp-pulsed waveforms, phase coded waveform 1, BPSK 1, BPSK 3, and BPSK 4 did not cause strobes on the radar's display at *I/N* ratios ranging from +43 to +63 dB. (Those power levels were the maximum that the test equipment could generate, the available maximum depending upon the modulation of each interference waveform.) BPSK 2 caused an effect at an *I/N* of +30 dB. The unmodulated pulsed waveforms 1 and 2 caused effects at *I/N* levels of +18-19 dB, and the unmodulated pulsed waveform 3 caused effects at an *I/N* of +25 dB.

In contrast, the airborne weather radar was affected at relatively low *I/N* levels by the OFDM signal. This result was not surprising due to that signal's high duty cycle. The OFDM signal was 20 MHz wide and continuous throughout a 45-ms dwell time. Therefore, it filled the entire IF filter with energy the entire time the waveform was gated on. The *I/N* had to be below -2 dB before the OFDM signal no longer affected the display.

Table 31. Results of Interference Tests on the Airborne Weather Radar*

| Interference Signal Modulation | Peak-to-RMS *I/N*[29] (dB) | Interference Effect On Radar |
|---|---|---|
| Chirped 1 | +63 | No visible effect on display |
| Chirped 2 | +52 | No visible effect on display |
| Chirped 3 | +43 | No visible effect on display |
| Phase Coded 1 | +47 | No visible effect on display |
| Phase Coded 2 | +60<br>+36<br>+30<br>+28<br>+25 | Strongly visible strobes<br>Strongly visible strobes<br>Marginally visible strobes<br>Barely visible strobes<br>No visible effect on display |
| Unmodulated 1 | +57<br>+22<br>+19 | Visible strobes<br>Marginally visible strobes<br>No visible effect on display |
| Unmodulated 2 | +57<br>+21<br>+18 | Visible strobes<br>Marginally visible strobes<br>No visible effect on display |
| Unmodulated 3 | +32<br>+29<br>+25 | Visible strobes<br>Marginally visible strobes<br>No visible effect on display |
| BPSK 1 | +44 | No visible effect on display |
| BPSK 2 | +52<br>+32<br>+30 | Strongly visible strobes<br>Marginally visible strobes<br>No visible effect on display |
| BPSK 3 | +54 | No visible effect on display |
| BPSK 4 | +43 | No visible effect on display |
| OFDM | +33<br>-2<br>-6 | Strongly visible strobes<br>Marginally visible strobes<br>No visible effect on display |

* Where "no visible effect on display" is indicated, the corresponding *I/N* level indicated is the maximum power level that could be achieved with the test equipment.

Other than for OFDM, the airborne weather radar was affected at some level or another by the following interference waveforms: unmodulated pulsed 1, 2, and 3; BPSK 2; and phase coded 2. The threshold for these waveforms was from +21 dB to +32 dB. (In contrast, the OFDM interference threshold was from *I/N* = -6 dB to -2 dB.) All but one of these waveforms had duty cycles of 1.9% or greater, the sole exception being a duty cycle of 0.8% for unmodulated pulsed 1. This observed relationship between a duty cycle of about 1% or greater and the eventual occurrence of visible interference effects was consistent with the results of tests on other types of radars in this study.

[29] The *I/N* levels in this table have been corrected from measured *(I+N)/N* levels.

Figures 76-77 illustrate the contrast between the relatively robust radar performance at high *I/N* levels for signals with duty cycles of a few percent or less versus the relatively low threshold for the high duty cycle OFDM signal. Figure 76 shows the effect of OFDM interference at *I/N* levels of -2 dB and +16 dB, while Figure 77 shows the effect of the Phase 2 waveform at *I/N* levels of +28 dB and +45 dB. Comparison of these figures shows that the high duty cycle OFDM interference waveform caused effects that were quantitatively similar to those of the low duty cycle (3.2%) phase coded pulsed 2 waveform, but that there is a difference of about 30 dB between the *I/N* levels where the onset of interference effects begins for these two waveforms.

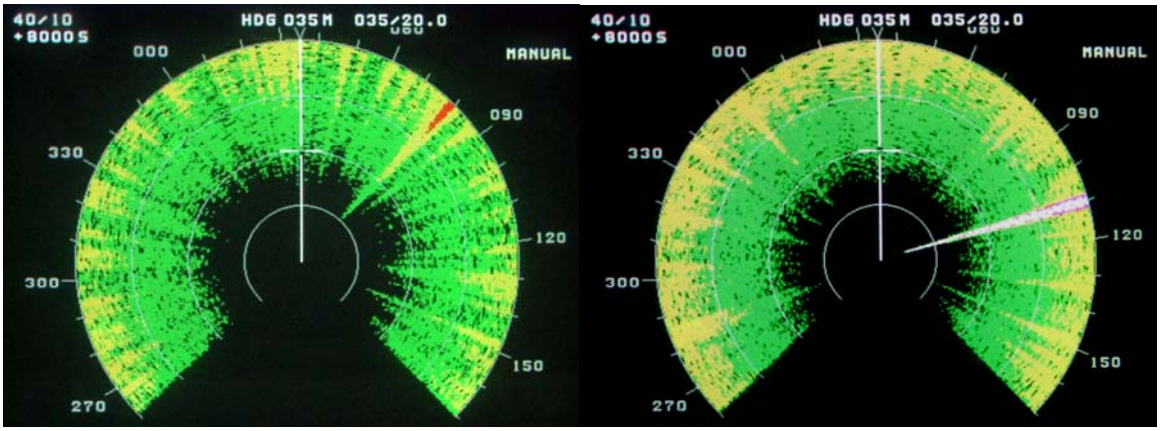


Figure 76. Barely visible (left) and strongly visible (right) strobes due to high duty cycle OFDM interference at *I/N* levels of -2 dB and +16 dB, respectively.

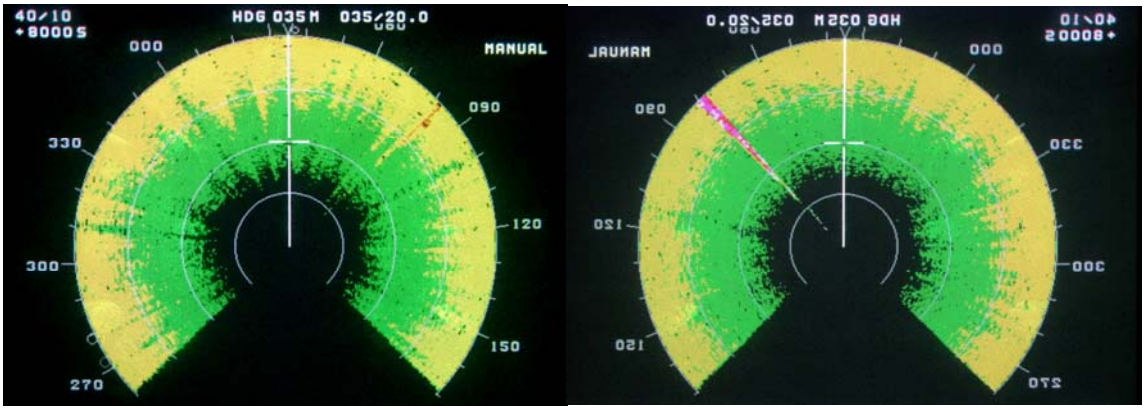


Figure 77. Barely visible (left) and strongly visible (right) strobes due to low duty cycle (3.2%), phase-coded pulsed waveform 2 interference at *I/N* levels of +28 dB and +45 dB, respectively. The effects are similar to those of Figure 76, but occur at *I/N* levels that are about 30 dB higher than the OFDM interference thresholds.

When the radar was operated in its frequency agility mode, all interference was mitigated. This was due to the radar design, in which the radar ceases operations on a frequency on which interference is detected; this behavior was observed during the tests. Interference would appear on the screen as it did for the single frequency case (e.g., the chirp-pulsed waveforms had no

effect at even the highest levels, while the OFDM signal had a strong effect at low levels). But as soon as one full sector-scan was completed, the receiver would stop hopping to the frequency (or frequencies) of the interference and the display would revert to its baseline appearance until the frequency of the interference was changed to match the radar's frequency.

### 7.5 Summary of Interference Effects for the Airborne Weather Radar

The airborne weather radar showed no effects from interference with the lowest duty cycles, on the order of 0.1%, at even the highest *I/N* levels that could be achieved, on the order of +50 dB to +60 dB. Interference waveforms with higher duty cycles, on the order of 1-3% duty cycles, caused effects to occur at *I/N* levels on the order of +21 dB to +32 dB. But for a communication-type signal (OFDM) with a nearly 100% duty cycle (within the 45 ms mainbeam dwell interval of the radar antenna scan), the *I/N* levels where interference effects were manifested for OFDM signals were substantially lower, between -6 dB to -2 dB.

These results are consistent with the results from other radars in this study. In general, radar receivers seem to perform robustly in the presence of signals such as those emitted by other radars (with duty cycles less than 1-3%), but are not robust in the presence of interference with high duty cycles (near 100%) such as are characteristic of communication signals.

# 8 SUMMARY OF INTERFERENCE EFFECTS ON RADARS

This report describes the results of wide-ranging interference measurements that have been performed on many representative radar receivers. The receiver types included long range air search radionavigation radars, a short range air search radionavigation radar, a fixed ground-based weather radar, an airborne weather radar, and several maritime radionavigation radars. Missions performed by these radars include en-route (long range) air traffic control and air defense; airport traffic control; weather surveillance and warning; and maritime navigation and surface search. The radars that have been tested operate in several microwave spectrum bands: 1200-1400 MHz; 2700-2900 MHz; 2900-3100 MHz; and 8500-10500 MHz. Five major results have been observed and documented; they are summarized here.

## 8.1 Radars are Vulnerable to the Effects of Communication Signal Interference

The results of interference tests with communication signal modulations are summarized in Table 32. Interference with communication-type modulations caused degradation in radar performance at *I/N* levels between -9 dB to -2 dB, well below the noise floor of each radar receiver. One radar lost targets at an *I/N* level of -10 dB, and *I/N* = -6 dB caused most of the radars to lose targets. Future improvements to meteorological radars are predicted to render them vulnerable at *I/N* levels as low as -14 dB.

Table 32. *I/N* Levels of Communication Signal Modulations at which Performance Decreased for All Radars Tested

| Radar Tested | *I/N* Threshold for Decreased $P_d$ |
|---|---|
| Long Range Air Search Radiolocation Radar 1 (installation 1) | -9 dB |
| Long Range Air Search Radiolocation Radar 1 (installation 2) | -9 dB |
| Long Range Air Search Radiolocation Radar 2 | -6 dB |
| Short Range Air Search Radionavigation Radar | -9 dB |
| Fixed Ground-Based Meteorological Radar | -9 dB* |
| Maritime Radionavigation Radar A | -7 dB |
| Maritime Radionavigation Radar B | -10 dB |
| Maritime Radionavigation Radar C | -6 dB to -9 dB |
| Maritime Radionavigation Radar D | -9 dB |
| Maritime Radionavigation Radar E | -6 dB |
| Maritime Radionavigation Radar F | -6 dB |
| Airborne Meteorological Radar | Between -6 to -2 dB |

* -14 dB is the predicted threshold for the upgraded version of the fixed meteorological radar.

## 8.2 Radars Perform Robustly in the Presence of Interference from Other Radars

In contrast to the effects of interference from communication signal modulations, pulsed interference at low duty cycles (less than about 1-3%) was tolerated at *I/N* ratios as high as +30 dB to +63 dB. The radar receivers that were tested performed robustly in the presence of signals transmitted by other radars.

## 8.3 Low-Level Interference Effects in Radar Receivers are Insidious

The loss of targets at low interference levels is insidious; there is no overt indication to radar operators or even to sophisticated radar software that losses are occurring. No dramatic indications such as flashing strobes on radar PPI screens are observed. This insidiousness can make low-level interference more dangerous than higher levels that will generate strobes and other obvious warning indications for operators or processing software.

Even when radars experience serious performance degradation due to low-level interference, it is very unlikely that such interference will be identifiable as such. It is therefore unlikely that such interference will ever result in reports to spectrum management authorities even when it causes loss of desired targets. Since low-level interference is not expected to be identified or to generate reports when it occurs, lack of such reports *cannot* be taken to mean that such interference does not occur.

## 8.4 Low-Level Interference Can Cause Loss of Radar Targets at Any Range

Interference can (and will) cause loss of targets at any distance from any radar station; loss of targets due to radio interference is not directly related to distance of targets from radar stations. When radar performance is reduced by some number of decibels, *X*, then all targets that were within *X* decibels of disappearing from coverage will be lost. Range from the radar is not a factor in this equation. Interference can cause loss of desired, large cross section targets (such as commercial airliners, oil tankers, and cargo ships) at long distances, as well as small cross section targets at close distances. Low-observable targets that could be lost include, for example, light aircraft; business jets; incoming missiles; missile warheads; floating debris including partially submerged (and extremely dangerous) shipping containers; life boats; kayaks, canoes, dinghies; periscopes; and swimmers in life jackets.

Because any radar target can potentially be lost at any distance in the presence of radio interference, radio interference does not translate directly into an equivalent radar range reduction. “Range reduction” should therefore *not* be used as a metric in discussions of adverse effects of interference on radars, unless such range reduction is qualified with a reference to a (unrealistic) condition of fixed, constant cross sections for all desired targets.

### 8.5 Radar Interference Waveforms and Test Reporting Should be Standardized

During radar interference measurements, the interference signals should be standardized to include: broadband noise; CW; impulse UWB (dithered and non-dithered); direct sequence UWB; multiband OFDM UWB; CDMA; TDMA; BPSK; QPSK; QAM; GMSK; OFDM; and pulsed signals (both linear FM-modulated (chirped) and unmodulated).

Plots of $P_d$ versus *I/N* are a useful and effective method of displaying interference data and should be adopted as a standard for future radar interference measurements.

For pulsed signals, the parameters of pulse width and prf which comprise the duty cycle should be varied to determine the point at which interference effects transition from pulse-like to noise-like or CW-like. For linear-FM pulsed interference signals, the chirp rate and chirp bandwidth should be varied to observe the onset of the same effects.

# 9 REFERENCES


[1] F.H. Sanders and V.S. Lawrence, "Broadband spectrum survey at Denver, Colorado," NTIA Report 95-321, Sep. 1995.

[2] F.H. Sanders, B.J. Ramsey, and V.S. Lawrence, "Broadband spectrum survey at San Diego, California," NTIA Report 97-334, Dec. 1996.

[3] F.H. Sanders, B.J. Ramsey, and V.S. Lawrence, "Broadband spectrum survey at Los Angeles, California," NTIA Report 97-336, May 1997.

[4] F.H. Sanders, B.J. Ramsey, and V.S. Lawrence, "Broadband spectrum survey at San Francisco, California," NTIA Report 99-367, Jul. 1999.

[5] C.A. Filippi, R.L. Hinkle, K.B. Nebbia, B.J. Ramsey, and F.H. Sanders, "Accommodation of broadcast satellite (sound) and mobile satellite services in the 2300-2450 MHz band," NTIA Technical Memorandum TM-92-154, Jan. 1992.

[6] P.E. Gawthrop, F.H. Sanders, K.B. Nebbia, and J.J. Sell, "Radio spectrum measurements of individual microwave ovens, volume 1," NTIA Report 94-303-1, Mar. 1994.

[7] P.E. Gawthrop, F.H. Sanders, K.B. Nebbia, and J.J. Sell, "Radio spectrum measurements of individual microwave ovens, volume 2," NTIA Report 94-303-2, Mar. 1994.

[8] M.G. Biggs, F.H. Sanders, and B.J. Ramsey, "Measurement to characterize aggregate signal emissions in the 2400-2500 MHz frequency range," NTIA Report 95-323, Aug. 1995.

[9] M.I. Skolnik, *Introduction to Radar Systems*, 2nd ed., New York, NY: McGraw-Hill, 1980.

[10] M.I. Skolnik, ed., *Radar Handbook*, 2nd ed., New York, NY: McGraw-Hill, 1990.

[11] D.K. Barton, *Modern Radar System Analysis*, Norwood, MA: Artech House, 1988.

[12] P.A. Lynn, *Radar Systems*, New York, NY: Van Nostrand Reinhold, 1987.

[13] L.V. Blake, "Recent advancements in basic radar range calculation technique," pp. 49-59, in *Radars Vol. 2: The Radar Equation*, D.K. Barton, ed., Norwood, MA: Artech House, 1974.

[14] L.V. Blake, Summary of "A guide to basic pulse-radar maximum-range calculation," pp. 151-154, in *Radars Vol. 2: The Radar Equation*, D.K. Barton, ed., Norwood, MA: Artech House, 1974.

[15] D. Meyer and H. Mayer, *Radar Target Detection: Handbook of Theory and Practice*, New York: Academic Press, 1973.

[16] A. Paul, G. Hurt, T. Sullivan, G. Patrick, R. Sole, L. Brunson, C-W. Wang, B. Joiner, and E. Drocella, with Contributors S. Williams and G. Saam, "Interference protection criteria, Phase 1: Compilation from existing sources," NTIA Report 05-432, Oct. 2005.

[17] M.I. Skolnik, Editor-in-chief, *Radar Handbook*, 2nd ed., New York: McGraw-Hill, 1990.

[18] ITU-R Recommendation M.1372-1, "Efficient use of the radio spectrum by radar stations in the radiodetermination service," International Telecommunication Union, Radiocommunication Sector, 1998.

[19] S. Kingsley and S. Quegan, *Understanding Radar Systems*, London: McGraw-Hill, 1992.

[20] ITU-R Recommendation M.1464, "Characteristics of and protection criteria for radionavigation and meteorological radars operating in the frequency band 2700-2900 MHz," International Telecommunication Union, Radiocommunication Sector, 1998.

[21] R. Doviak, D. Zrnic, and D. Surmans, "Doppler Weather Radar," *Proceedings of the IEEE*, vol. 67, no. 11, Nov. 1979.

[22] ITU-R Recommendation M.1313, "Technical characteristics of maritime radionavigation radars," International Telecommunication Union, Radiocommunication Sector, 2000.

[23] L.K. Brunson, J.P. Camacho, W.M. Dolan, R.L. Hinkle, G.F. Hurt, M.J. Murray, F.A. Najmy, P.C. Roosa, Jr., and R.L. Sole, "Assessment of compatibility between ultrawideband devices and selected federal systems," NTIA Special Publication SP-01-43, Jan. 2001.